Ablating ATR in mouse meiosis and its consequences for synapsis, recombination and meiotic surveillance mechanisms

Alexander David Widger

University College London

and

The Francis Crick Institute

PhD Supervisor: James Turner

A thesis submitted for the degree of

Doctor of Philosophy

University College London

Dec 2017

Declaration

I Alexander David Widger confirm that the work presented in this thesis is my own. Where information has been derived from other sources, I confirm that this has been indicated.

Abstract

Meiosis is a fundamental part in the life cycle of sexual species. It denotes a specialised cell division that halves chromosome numbers to generate haploid gametes for reproduction. Cells unable to competently progress through meiotic prophase activate cell surveillance mechanisms causing their elimination. Given the importance of DNA damage kinases like ATR in facilitating mitotic cell surveillance mechanisms, I characterized *Atr*-deficient spermatocytes to determine the importance of ATR for mammalian meiosis. I found that ATR ensures efficient chromosome synapsis, and that that is partially independent of meiotic recombination. In addition, ATR has three distinct roles in meiotic recombination. Firstly, during nucleolytic processing, it acts to regulate SPO11-oligonucleotide size when ATM is deleted. Secondly, it is required for accurate RAD51 and DMC1 recruitment to DSBs. Thirdly, it regulates the timing of DNA DSB repair on both unsynapsed and synapsed chromosomes. Finally I found that the loss of ATR is unable to rescue meiotic arrest in multiple meiotic mutants, including mice deficient for the other DNA damage PIKKs ATM and DNA-PK. My findings reveal multiple roles for ATR in male mouse meiosis.

Acknowledgement

I would like to use this space to thank James Turner for giving me this studentship and his endless patience throughout it. It was a decade long ambition to complete a PhD in order to become a geneticist. James has given me “oodles” of help to do this developing my scientific-approach and skills of scientific-communication. Thank you for all the fantastic opportunities you have given to me and also to all the colleagues/friends/collaborators I have met throughout the scientific world, a special mention must be made to Bill Earnshaw, Attila Tóth, Howard Cooke, Paula Cohen and Ian Adams for the antibodies used in the thesis, as well as Simon Lane, Richard Baer, Owen Davies, Jesus Carballo, Johanna Syrianen, Satoshi Namekawa, Anand Swaroop, Daniel Camerini-Otero and Jeremy Wang for resources and advice for other projects.

I would also like to convey my gratitude to close colleagues in the lab, for all their valuable advice. I think that we found an ideal exchange system: my sports coaching in return for their expertise in cloning/molecular biology. I would like to thank the core facilities at both the National Institute for Medical Research (NIMR) and the Francis Crick for the advice and counselling provided; both scientific and otherwise. Thank you to the Medical Research Council and the Francis Crick Institute for the funding. This project would be unrecognisable without the considerable input of multiple members of the Turner lab, my Thesis Committee (Peter Thorpe, Steve Smerdon and Eva Hoffmann), as well as collaborators in New York (Julian Lange and Scott Keeney) and Amsterdam (Dirk de Rooij). Finally and most importantly I thank the mice.

Outside of the lab I would like to thank my friends including Charlie, Jake, Andrew and Louise and family: my parents and my wife Rohini and our little daughter Anna.

Table of Contents

Table of figures

List of tables

Abbreviations

Table 0.1 Abbreviations

Abbreviation	Definition
ACA	Anti-centromere antibody
AE	Axial element
atl-1	ATM-like 1
ATM	Ataxia telangiectasia mutated
ATR	Ataxia telangiectasia mutated and Rad3 related
BAC	Bacteria artificial chromosome
BRCA1	Breast cancer 1
BSA	Bovine serum albumin
CCD	Charged-coupled device
CDK	Cyclin-dependent kinases
CE	Central element
ChIP-Seq	Chromatin Immunoprecipitation-Sequencing
CHK2	Checkpoint Kinase 2
CNTD1	Cyclin N-Terminal Domain Containing 1
CO	Crossover
CSK	Sodium chloride, sucrose and magnesium buffer
CTIP1/BCL11A	B-Cell CLL/Lymphoma 11A (Zinc Finger Protein) Isoform 1
D-loop	Displacement loop
DAPI	4',6-diamidino-2-phenylindole
dCTP	Deoxycytidine triphosphate
DDT	Dichlorodiphenyltrichloroethane
Ddx4	DEAD-Box Helicase 4
dHJ	Double Holliday junction
DIG	Digoxigenin
DMC1	Dosage Suppressor Of Mck1
DNA	deoxyribose nucleic acid
DNA-PK	DNA-protein kinase
dp	Decimal place
d*pc*	Days post coitum
d*pp*	Days post partum
DSB	double strand break
DSBR	Double strand break repair
EGTA	Ethylene glycol-bis(β-aminoethyl ether)-N,N,N',N'-tetraacetic acid
EXO1	Exonuclease 1
FISH	Florescent in-situ hybridisation
G1	Gap 1- phase
G2	Gap 2- phase
GAPDH	Glycerol-3-phosphate dehydrogenase
GE	Gel Electrophoresis
H2AFX	Histone 2A variant FX
H2Aub	Histone 2A ubiqutinlyated
H3K36me3	Histone 3 lysine 36 tri methylation
H3K9me3	Histone 3 lysine 9 tri methylation
HEPES	4-(2-hydroxyethyl)-1-piperazineethanesulfonic acid

Abbreviation	Definition
HOP1	Homolog Pairing 1
HORMAD1	Hop1p, Rev7p and MAD2 domain containing protein 2
HORMAD2	Hop1p, Rev7p and MAD2 domain containing protein 2
HR	Homologous recombination
Hus1	Hydroxyurea-sensitive 1 homolog
IF	Immunoflorescent
IH	Inter-homolog
IHC	Immunohistochemistry
IHO1	interactor of HORMAD1
IP	Immunoprecipitation
IS	Inter-sister
kb	Kilobase (1000 bases) of DNA
kDa	KiloDaltons
KO	Knockout
Lox P	locus of crosing-over from bacteriophage P1
M-phase	Mitosis phase
MDC1	Mediator of DNA damage checkpoint 1
MEC1	Mitosis Entry Checkpoint
Mei-41	Meiotic protein 41
MEI1	Meiotic double-stranded break formation protein 1
MEI4	Meiotic double-stranded break formation protein 4
MER2	Meiotic recombination 2
MI	Metaphase 1
MLH1	Mut L Homolog 1
MLH3	Mut L Homolog 3
mM	Millimolar
MRE11	Meiotic recombination 11
MRN	MRE11-RAD50-NBS1 complex
mRNA	Messenger RNA
MRX	MRE11-RAD50-XRS1 complex
MSCI	Meiotic sex chromsome inactivation
MSH4	Mut S homolog 4
MSH5	Mut S homolog 5
mSPO11	Mouse SPO11
MSUC	Meiotic silencing of unsynapsed chromatin
NaOH	Sodium hydroxide
NBS1	Nibrin
NCO	Non-crossover
Ngn3	Neurogenin3
NHEJ	Non-homologous end joining
nt	Nucleotide
PAR	Pseudo-autosomal region
PBS	Phosphate buffered solution
PCR	Polymerase chain reaction

Abbreviation	Definition
PGC	Primodial germ cell
PIKK	Phosphatidylinositol 3-kinase-related kinases
PIPES	iperazine-N,N′-bis(2-ethanesulfonic acid)
PMSF	phenylmethylsulfonyl fluoride
PRDM9	PR domain zinc finger protein 9
Rad21L	RAD21 like homolog
RAD50	Radation sensitive protein 50
RAD51	Radation sensitive protein 51
RAD9A	RAD9 Homolog A
REC114	Recombination 114
REC8	Recombination-Deficient protein 8
RECA	Recombination protein A
RNA	Ribose nucleic acid
RNA-FISH	Ribose nucleic acid-florescent in-situ hybridisation
RNF212	Ring Finger Protein 212
RPA	Replication protein A
RPMI media	Roswell Park Memorial Institute media
RT	Room temperature
S-phase	Synthesis-phase
S/T-Q	Serine/Theonine-Glutamic acid
SC	Synaptonemal complex
SCD	Serine/Theonine cluster domain
SCID	Severe combined immunodeficiency
SDS	Sodium dodecyl sulfate
SDS-PAGE	SDS-poly acrylamide gel electrophroresis
SEM	Standard error of the mean
SMC	Structural maintainence of chromosomes
SMC1β	Structural maintainence of chromosome 3
SMC1β	Structural maintainence of chromosome 1 beta
SPO11	Sporulation protein 11
Spo11β	Major SPO11-isoform
Sry	Sex-determining region Y
SSDA	Single end
ssDNA	Single stranded DNA
Stra8	Stimulated by retinoic acid 8
SYCE1	Synaptonemal complex central element 1
SYCE2	Synaptonemal complex central element 2
SYCE3	Synaptonemal complex central element 3
SYCP1	Synaptonemal complex protein 1
SYCP2	Synaptonemal complex protein 2
SYCP3	Synaptonemal complex protein 3
TEL1	Telomere Length 1
TEX12	Testis-expressed protein 12
TF	Transverse filament

Abbreviation	Definition
TRIP13	Thyroid hormone receptor interacting protein 13
Trip13^{mod}	Thyroid hormone receptor interacting protein 13$^{moderate\ phenotype\ allele}$
Wt	Wildtype
XRS1	X-ray sensitive 1
γH2AFX	Phosphorylated H2AFX
µg	Microgram
µL	Microlitre
µM	Micromolar

Chapter 1. Introduction

Infertility is defined as the inability of a couple to conceive naturally within 12 months. This medical condition is common, affecting ~15% of French (Slama et al., 2012) and ~24% of American couples (Thoma et al., 2013). The primary goal of my thesis is to elucidate the meiotic roles of a protein, ATR, in mammals by characterising the phenotypes I observed in ATR-deficient mouse models. ATR is essential for male fertility (Royo et al., 2010, Royo et al., 2013) and hypothesised to play fundamental roles throughout meiosis (Carballo and Cha, 2007). Whilst the causes of human infertility are complex, a more complete knowledge of the roles of ATR in mouse meiosis will help in the future to further our understanding of the genetic causes of human infertility.

1.1 An overview of gametogenesis

Meiosis is an integral step in gametogenesis, the process that forms mature eggs and sperm for reproduction. The developmental processes are similar across mammals; here I focus on the time points in mouse gametogenesis.

In both sexes the gametes develop from a common precursor cell-type, primordial germ cell (PGCs). Approximately 50 PGCs are specified at 6.25 days *post coitum* (d*pc*) from the epiblast of the mouse embryo (Hackett and Surani, 2013). These PGCs proliferate and migrate and by ~8.5 d*pc* arrive at the genital ridge within an embryonic kidney-like organ called the mesonephros (Sekido and Lovell-Badge, 2009, Hackett and Surani, 2013, Sinclair et al., 1990). At this stage either testes or ovaries could form from the genital ridge, depending on the sex constitution of the organism, either XX or XY (Sekido and Lovell-Badge, 2009). After sex determination, a pronounced temporal and biological sexual dimorphism begins.

In the majority of mammals the expression of the Y-linked gene, *Sry*, approximately halfway through development, causes male sex determination; in mice this occurs at 10.5 d*pc* (Sinclair et al., 1990, Lovell-Badge and Robertson, 1990). The presence or absence of *Sry* triggers a sex determination signalling cascade that

reinforces the genetic sex of the embryo (Sekido and Lovell-Badge, 2009). After sex determination, germ cells in both sexes undergo multiple rounds of mitotic division. In females, germ cells subsequently enter meiosis, while in males they enter a quiescent state (Adams and McLaren, 2002).

Oocytes enter meiotic S-phase at 11.5 d*pc.* Cells proceed semi-synchronously through the four stages of prophase I and reach the end of prophase I shortly after birth, at approximately 1-2 days *post partum* (d*pp*). After this, oocytes enter dictyate, a stage of prolonged arrest (Barchi et al., 2005). Once females are sexually mature at 6-8 weeks, a small number of oocytes resume meiosis as mice begin their first estrus cycle (Byers et al., 2012). Ovulated oocytes undergo the first meiotic division, segregating a full complement of homologous chromosomes to the first polar body, then arrest again. Upon fertilization, oocytes resume the second meiotic division and complete meiosis, segregating a full complement of sister chromatids to a daughter ovum and the second polar body.

Several days after birth, male germ cells leave their quiescent state and then, after a series of spermatogonial divisions, male meiotic S-phase begins at 10 d*pp.* Prophase I proceeds synchronously through the first meiotic wave reaching pachynema at approximately 14.5 d*pp* (Adams and McLaren, 2002, Vergouwen et al., 1991). By approximately 30 d*pp*, the first wave of cells has completed both meiotic divisions without pause and the subsequent newly differentiated spermatocytes have entered meiosis.

In summary, there are key biological differences between male and female meiosis. Firstly, female meiosis produces only one haploid gamete per primary oocyte, whereas male meiosis produces four haploid sperm per primary spermatocyte (Brooker and Berkowitz, 2014). Secondly, a single cohort of female meiotic cells develops embryonically. In males, spermatogonial stem cells divide asymmetrically every few days and newly differentiated spermatocytes enter meiosis in waves throughout the adult life of the male (Morelli and Cohen, 2005). Thirdly, female meiosis contains two periods of cell-cycle arrest, the first at the end of prophase I and the second prior to fertilization, in contrast to the continuous development of male gametes (Morelli and Cohen, 2005).

1.1.1 Staging the seminiferous tubules of the testis

Male germ cells mature in the seminiferous tubules of the testis (Fig 1.1 A-C). Seminiferous tubules are highly organised structures. Because of their use as a model of stem cell proliferation and differentiation, the organisation of the seminiferous tubules has been extensively studied in mouse and rat (Oakberg, 1956, Hess, 1990). Within each seminiferous tubule, the germ cells have well-characterised periodicity and the different combinations of associated germ cell types are known, enabling stages to be defined. Within each tubule it is possible to see nursing somatic cells, called Sertoli cells that exist in close association with the germ cells. Sertoli cells serve to provide structural, immunological and nourishing functions to the three different cell types present during spermatogenesis: spermatogonia, spermatocytes and spermatids (Fig 1.1 C; Oakberg, 1956).

The stem cells of spermatogenesis are called “A-single“ spermatogonia. To reach meiosis, daughter cells of an “A-single” spermatogonium go through approximately ten mitotic divisions (de Rooij, 1973, de Rooij, 2001). The resulting daughter cells are called “A” spermatogonia and can be identified as they lack the heterochromatic staining nuclei of the “A-single” spermatogonia (Ahmed and de Rooij, 2009). As spermatogonia process through spermatogenesis they accumulate heterochromatin, a hallmark of less-differentiated cell types. Therefore based on the extent of heterochromatin within their nuclei, daughter spermatogonia can be identified as either ‘‘intermediate’’ or ‘‘B’’ types (Ahmed and de Rooij, 2009).

It is the division of the ‘‘B’’ spermatogonia that produces the spermatocytes, which undergo meiosis after completing G1 and S-phase (an overview of mammalian meiotic prophase I is provided in the Section 1.2). After prophase I, the spermatocytes complete the two meiotic divisions and give rise to haploid round spermatids, which then undergo spermiogenesis before transforming into elongated spermatids and leaving the seminiferous tubules (Ahmed and de Rooij, 2009).

In the mouse, there are 12 repeatedly associated germ cell types, or stages that cover all of spermatogenesis (shown schematically in Figure 1.1 D). The epithelial

stages are most easily identifiable based upon changes in the nuclear morphology of the younger generation of spermatids after being counterstained with haematoxylin and eosin, which stain nuclei and acidophilic structures, respectively. Alternatively, periodic acid Schiff (P-AS) staining may be used which stains polysaccharides present in the developing acrosome (an enzyme containing organelle present from round spermatids onwards), enabling the precise identification of tubule stage.

There are many known genetic causes of defects in spermatogenesis that result in a spermatogonial arrest. The absence of spermatids prevents the straightforward staging of tubules, however in these instances, it is often still possible to pinpoint the stage that cells arrest using combinations of characteristics displayed by earlier unaffected cells (Ahmed and de Rooij, 2009, Meistrich and Hess, 2013). In this thesis it is important to understand the organisation of the testis in mice with problems either prior to the onset of meiosis in stages VI-VII, or at mid-pachynema at the beginning at Stage IV. A more comprehensive description is provided below:

Stages VI-VII: In stage VI, A-aligned spermatogonia divide into new A_1 spermatogonia. Then, in stage VII, daughter cells of previous generations of B-spermatogonia undergo meiotic S-phase. In mutant cells that block in the spermatogonial proliferations, some earlier generations of spermatogonia are still present. These spermatogonia are able to grow in size during G1, but are unable to divide successfully and undergo elimination. The eliminated cells stain densely for eosin and P-AS, and are said to be hyperpigmented. This ultimately results in the absence of any spermatocytes in all 12 stages.

Stage IV: In wildtype mice there are two generations of spermatids in this stage; notably in the younger generation of spermatids, the round acrosomal granule that is present in earlier stages now moves towards the nuclear membrane of the spermatids and flattens as it touches the nuclear membrane. Some spermatocytes have started to migrate away from the basal membrane of the tubule, these cells are in mid-pachynema and they exhibit a densely staining sex body that contains the X and Y chromosome. Another defining criterion of this stage is the presence of three types of spermatogonia: A, Intermediate and B. Moreover, some intermediate

spermatogonia divide during this tubule stage. Therefore within stage IV tubules one of three scenarios occurs: before the division, it is possible to see large intermediate spermatogonia in G2 phase; during the division, it is possible to see intermediate spermatogonia undergoing mitosis; after the division, the daughter cells, relatively small B spermatogonia, appear. B spermatogonia are discernable from intermediate spermatogonia as they have more heterochromatin. In mutant mice with a stage IV block, the mid-pachytene spermatocytes begin to show signs of apoptosis, and many are already hyperpigmented. Therefore, the presence of dividing intermediate spermatogonia (See Inm, Figure 1.1) and hyperpigmented cells are good criteria for staging mutant stage IV tubules.

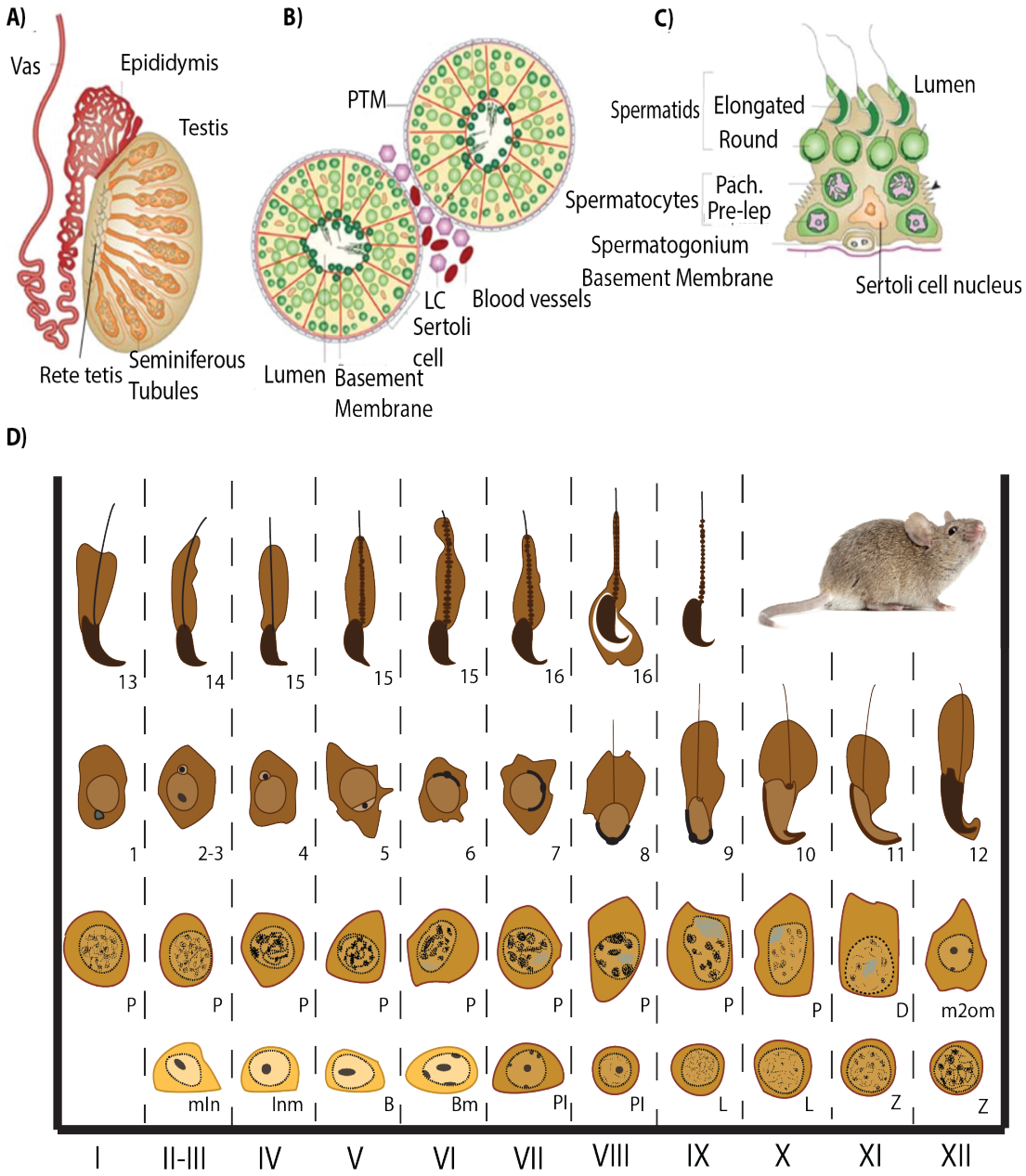

Figure 1.1. Organisation of mammalian testis and the mouse seminiferous stages

Schematic of **(A)** a cross-section through the testis: the locations of the seminiferous tubules, *vas deferens* and epididymis are indicated. (**B**) A cross-section through a testicular tubule showing: the different staged germ cells (green); and supporting blood vessels, somatic Sertoli cells (red); and Leydig cells (LC; purple) present in the interstitium. Maturing sperm are shown in the lumen of the tubules. (**C**) Associated germ cells within a single Sertoli cell: pre-meiotic cells (spermatogonia) are found on one side of the junction; meiotic (spermatocytes); and post-meiotic (round and elongating spermatids) cells are found organised in strict order of maturation moving towards the lumen. (**D**) Diagram to enable staging the twelve (I-XII) stages in mouse spermatogenesis from the mitosis of the intermediate spermatogonia to the release of elongated spermatids. .To follow the development of a single wave of spermatogenesis the diagram is read the from bottom left to top right, row-by-row,. A given tubules will only contain cell types within one column of the diagram i.e. relevant to that stage Key: m, mitosis; In, Intermediate; B, B spermatogonia; Pl, preleptonema; L, leptonema; Z, zygonema; P, pachynema; D, Diplonema; m2om MI and MII divisions; 1-16, the 16 stages of spermatid (round and elongated) development. (A-C) Adapted from (Cooke and Saunders, 2002). (D) Adapted from Russell et al., 1990 and redrawn by colleague Fanny DeCarpentrie edited with permission.

1.2 An overview of mammalian meiosis

Meiosis is characterized by one round of DNA replication and two successive cell divisions. The maternal and paternal chromatids are replicated in meiotic S-phase and bound together by the ring-like structure of newly synthesized cohesin complexes (Brooker and Berkowitz, 2014). The prophase of the first meiotic cell division, called meiotic prophase I, contains four sub-stages: *lepto*nema, *zygo*nema, *pachy*nema, and *diplo*nema. The Greek prefix describes the physical characteristic or behaviour of the meiotic chromosomes during each sub-stage: *thin*, *pairing*, *thick* and *double*, respectively. Specific molecular events must be completed in each sub-stage that are unique to meiosis and essential for the production of viable gametes, summarised in Figure 1.2.

During leptonema, DNA double strand breaks (DSBs) are deliberately introduced throughout the genome by the enzyme SPO11 (Keeney et al., 1997); this results in the pan-nucleus phosphorylation of damage variant histone H2AX by DNA-kinase ATM (Mahadevaiah et al., 2001). Normally individual DSBs are toxic to most cell types, however hundreds of programmed meiotic DSBs are essential for fertility in mammals (Cole et al., 2012). DSBs are an essential substrate on which the repair machinery functions in subsequent steps in prophase I. The machinery that makes and repairs meiotic DSBs is carefully controlled. DSBs are predominately repaired using one of three intact homologous sequences that act as a template to allow accurate repair of the DNA damage (Zhang et al., 2011).

During zygonema, homologous chromosomes physically pair, in a process termed homologous synapsis. Synapsis requires the formation of a large protein complex called the synaptonemal complex (SC). There is an intricate interdependent relationship between homologous synapsis and DSB repair, such that DSBs are required for the initiation of synapsis and synapsis is generally required for the complete repair of meiotic DSBs (Zickler and Kleckner, 2015, Page and Hawley, 2004).

Early during pachynema all the homologous chromosomes have paired and the majority of DSBs have been repaired (Ashley et al., 2004). In this stage meiotic

crossovers (CO) develop and mature, allowing the reshuffling of maternal and paternal chromatids. COs are an essential subset of meiotic DSB repair intermediates, which create novel non-parental chromatids (Zickler and Kleckner, 2015). Each chromosome pair must receive at least a single CO. Together with sister chromatid cohesion, COs promote accurate chromosome segregation in metaphase I (MI) (Barchi et al., 2008).

Even in fertile organisms there are defective meiotic cells. These cells may fail to synapse chromosomes and/or repair DSBs correctly (Kauppi et al., 2013). Defective cells are eliminated towards the end of meiotic prophase, through quality control mechanisms called meiotic checkpoints. Therefore to enter diplonema and exit meiotic prophase, cells must satisfy the requirements of pachytene meiotic checkpoints (See Section 1.5).

During diplonema, having achieved homologous synapsis and DSB repair, the SC is disassembled and chromosomes desynapse. The homologous chromosomes separate except at centromeres. At this stage, it is thought that the SC proteins at centromere establish and/or regulate the assembly of the kinetochores that permits accurate chromosome segregation.in MI. Genetic evidence lead to this hypothesis as homologous centromeres fail to associate in spermatocytes without SYCP1, that are artificially made to enter diplonema and subsequently diakinesis by okadaic acid treatment (Bisig et al., 2012).

Scientists investigating meiosis have utilised many different model organisms, each with its own strengths and weaknesses. Fungal genetics has been used extensively for decades to understand meiotic recombination (Lindegren, 1955). The ability to synchronously large cultures of meiotic cells enables the direct detection of DSB repair intermediates (Murakami and Keeney, 2008). Practical and ethical reasons traditionally restricted the ability to transfer such techniques to mammalian model organisms. The sensitivity of next-generation genomics and proteomics is dispelling these traditional restrictions. Mice have been used traditionally to study meiosis, as their karyotype and cell biology produce excellent cytology as a mammalian model organism widely used as a model of research into human diseases. Meiotic cells from this organism are easily spread onto

microscopy slides so that chromosomes-scale meiotic events like homologous synapsis and meiotic recombination are made “visible” through the use of immunofluorescence (IF) using antibodies raised against different meiotic components (Barlow et al., 1997) (Figure 1.2A).

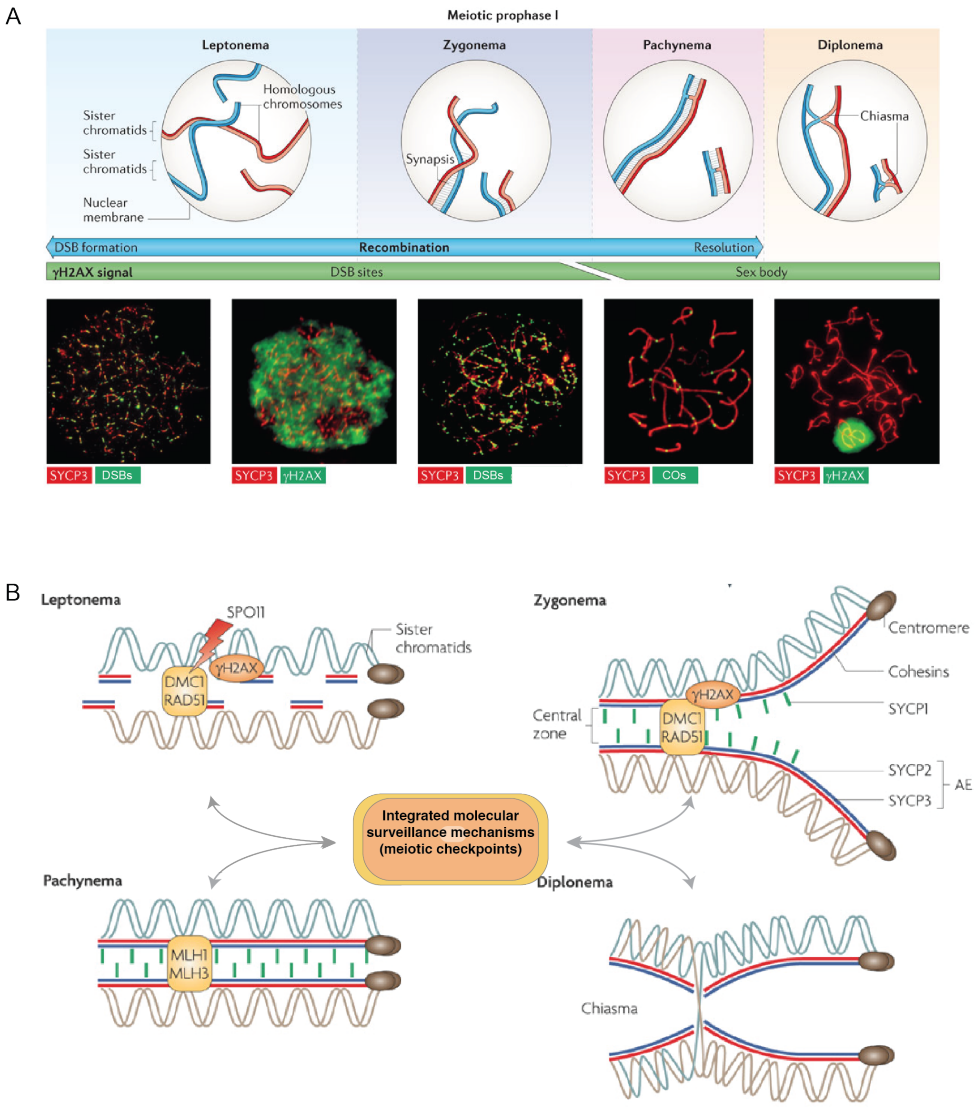

Figure 1.2 Overview of chromosome organisation, events and cytology during meiosis

(**A**) Cartoon of chromosome dynamics during the stages of meiotic prophase I and representative IF images. (**B**) cartoon of axes structure in prophase: in leptonema SPO11 (lightening bolt) induces genome-wide programmed DSBs; causing the recruitment of repair proteins including DMC1, RAD51, RPA and phosphorylated form of histone mark H2AX (γH2AX) to emanate globally from the DSBs; on the recently formed SYCP2 and SYCP3 positive axes. In zygonema, the maternal and paternal homologous chromosomes have found each other and SC formation or synapsis is initiated and SYCP1 is deposited. In pachynema all chromosomes have completed homolgous synapsis and have a full SC, also containing SYCE1-3 and TEX12. Pachynema lasts 9 days and includes the maturation of a subset (<10%) of DSBs into COs which recruit MLH1 and MLH3; in males the X and Y chromosomes are subject to silencing via MSCI. In diplonema; chromosomes undergo desynapsis and homologs are held together by the COs. Finally it is crucial to acknowledge that there are meiotic checkpoints integrated into meiosis that sense, detect and respond to cells unable to completed meioitc events. (**A**) Adapted from (Baudat et al., 2013). (**B**) Adapted from (Handel and Schimenti, 2010).

1.3 Meiotic DSB formation and repair

1.3.1 Repair of meiotic DSBs by homologous recombination (HR)

DSBs are predominately repaired via two distinct methods. DSB ends can be ligated together with minimal processing via non-homologous end-joining (NHEJ). In mammals, the major mechanism for repair in somatic cells is NHEJ, which can be mutagenic as it is error-prone (Kim et al., 2016). Alternatively, a homologous sequence can be used as a template for accurate DSB repair, which is called homologous recombination (HR). The generalised HR pathway begins with the 5'-3' processing of the DSB ends known as DNA end resection. It is known that the resectioning drives the DNA damage response (DDR) into HR rather than NHEJ (Greene, 2016). In meiosis, HR repairs the majority of DSBs.

1.3.2 An overview of meiotic recombination

Meiotic recombination beings with the creation of meiotic DSBs by SPO11 (Keeney et al., 1997, Baudat et al., 2000) and ends the successful repair of DSBs and CO maturation (Figure 1.3). Discovered SPO11 orthologs are highly conserved at the sequence and amino acid, unlike other components in meiotic recombination (Keeney et al., 1997, Kumar et al., 2010). The conservation of *Spo11* is strongly correlated with sexual reproduction and is widely accepted as such. The currently evolutionary hypotheses are that at least multiple paralogs Spo11 existed prior to the last common ancestor of extant eukaryotes. As a type-IV topoisomerase-like transesterase (Bergerat et al., 1997), SPO11 cleaves and forms a covalent bond with the DNA producing a SPO11–DNA complex intermediates called Spo11-oligos (Neale et al., 2005).

As well as SPO11, additional factors are required to create DNA DSBs. The archaeal topoisomerase VI consists of two subunits; biochemically SPO11 resembles the A subunit of archaeal topoisomerase VI (Bergerat et al., 1997). The eukaryotic second subunit, TOPOVIBL, was recently identified in *Arabidopsis thaliana* and in mammals. Like SPO11, TOPOVIBL is widely conserved (Vrielynck et al., 2016), and is required in mice to form meiotic DSBs (Robert et al., 2016).

Furthermore, DSB formation requires a "pre-DSB complex" (Keeney, 2001). Some pre-DSB components have characterized mouse orthologs, including MEI1 (Libby et al., 2003), MEI4 (Kumar et al., 2010), HORMAD1 (Wojtasz et al., 2009, Daniel et al., 2011) and the mammalian MER2 ortholog IHO1 (Stanzione et al., 2016). Reverse genetics analysis has found that deletion of these factors significantly impairs DSB formation. In the next sections I introduce meiotic phenomena that promote regulated spatial distribution (Section 1.3.3) and numerical control (Section 1.3.4) of meiotic DSBs.

The next step of recombination requires the resectioning of the DSB to generate a tract of homolog with which to find a donor sequence (Figure 1.3). How meiotic resection differs to mitotic resection is currently unclear. An obvious initial difference is that yeast SPO11 creates a DSB containing a two-nucleotide overhang (Liu et al., 1995), and then remains covalently attached to the 5' ends. To liberate SPO11 and its attached oligonucleotide, nucleases must nick and resect the SPO11-bound DNA. Studies suggest that DSB resection is similar in both budding yeast and mouse. The nick is carried out by the MRE11 component of the MRX complex (Borde, 2007), which in mammals is comprised of MRE11, RAD50 and NBS1. After removal of the Spo11-oligo, further resection is likely to occur by exonucleases CTIP/BCL11A and EXO1, which creates an extended 3' single-stranded DNA (ssDNA) overhang, as occurs in budding yeast (Garcia et al., 2011).

Next, the resulting 3' ssDNA tails recruit the heterotrimeric protein complex RPA and then the recombinases RAD51 and DMC1 (Greene, 2016, Brown et al., 2015). These recombinases form a nucleoprotein filament around the ssDNA that is used to search for a homologous donor sequence (Greene, 2016). In mitotic cells the recruitment of RPA to ssDNA activates an ATR-dependent checkpoint (Villa et al., 2016). It is unknown whether there is an equivalent checkpoint requiring ATR operating during meiosis.

The recombinases RAD51 and DMC1 enable single end invasion (SEI), which creates an asymmetric strand exchange intermediate (Hunter, 2015). The next steps require DNA synthesis of the invading 3' end, second DSB capture and

further DNA synthesis. Evidence from budding yeast suggests that it is this stage, after the resynthesis of the resected DNA strand (Allers and Lichten, 2001), that the decision to resolve the heteroduplex as either a CO or non-crossover (NCO) is made. The CO-promoting pathway generates the majority of COs, requiring a MutLγ complex comprised of mismatch repair proteins MLH1 and MLH3 (Edelmann et al., 1996, Lipkin et al., 2002, Holloway et al., 2008). To occur successfully double Holliday junctions (dHJ) must form requiring the second end of the original DSB to be captured and ligated. dHJ resolution yields a CO when the adjacent Holliday junctions are resolved, and an NCO if the opposing Holliday junctions are dissolved. NCOs also occur if second end capture and ligation is unsuccessful, perhaps due to insufficient DNA synthesis. By dissolving the D-loop, the strand re-anneals with its original homolog, in a process known as synthesis-dependent strand annealing (SSDA), which also occurs in mitotic DSB repair (Hunter, 2015, Phadnis et al., 2011). In SSDA, the newly synthesised DNA anneals to the complementary ssDNA on the other side of the break, and further DNA synthesis and ligation produces a mature NCO product (Hunter, 2015).

Recently, important advances have been made to increase our understanding of how some proteins help to stabilise heteroduplexes; and couple this process to homologous chromosome synapsis. First identified in budding yeast, the ZMM proteins includes seven functionally collaborating yet structurally diverse proteins: ZIP1-4 and the MutSγ DNA mismatch-repair proteins MSH4-5 and MER3 (Lynn et al., 2007). The roles of mammalian proteins with functional homology to these ZMMs have been characterized by reverse genetics: examples include the E3 ligase ZIP3-like proteins HEI10 (Qiao et al., 2014) and RNF212 (Reynolds et al., 2013), and CNTD1 (Holloway et al., 2014), the ortholog to *C. elgans* COSA-1. Therefore it seems that post-translational modifications: ubiquitylation, SUMOylation and phosphorylation via these proteins all stabilise heteroduplexes, promote homologous synapsis and affect crossover regulation; how this is all genetically integrated into establishing the normal NCO:CO bias has yet to be determined (Hunter, 2015).

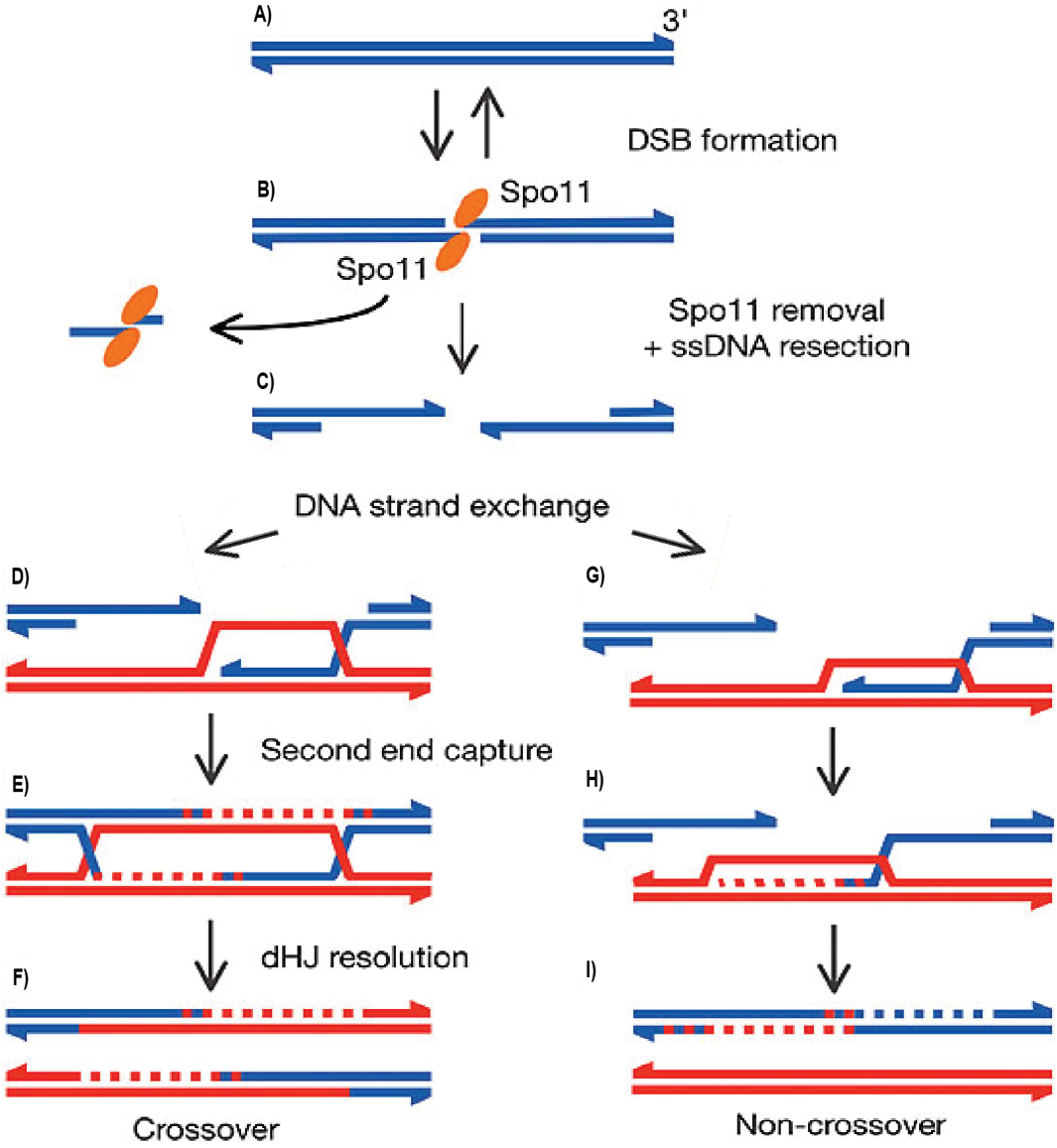

Figure 1.3 Overview of meiotic recombination

(A) The pre-DSB complex (not shown) primes the DNA prior to SPO11 activity. **(B)** SPO11 (orange ellipses) cleaves dsDNA to produce a covalently bound Spo11–DNA complex intermediate (Spo11-Oligo). **(C)** Endonucleases release Spo11-oligos, the degradation of 5' DNA strands yield 3' ssDNA tails, which are then bound by RPA before recombinases RAD51 and DMC1 are recruited (proteins not shown). **(D-F)** Crossover promoting pathway, requiring MLH1 and MLH3. **(D)**, Single end invasion forms an asymmetric strand exchange intermediate. **(E)**, DNA synthesis (red dashed line) is primed from the invading 3' end, next the second DSB end is captured and primes DNA synthesis (red dashed line), then ligation yields a pair of Holliday junctions, or double Holliday junction (dHJ). **(F)** Asymmetrical dHJ resolution yields non-parental chromatids. **(G-I)** Non-crossover pathway/strand displacement dependent synthesis. **(G)** The invading strand is displaced by the action of DNA helicases and **(H)** The newly synthesised DNA anneals to complementary ssDNA on the other side of the break **(I)**. Further DNA synthesis and ligation produces a mature non-crossover (NCO) product. Adapted from (Neale and Keeney, 2006).

1.3.3 Distribution of meiotic DNA DSBs

The distribution of meiotic DNA DSBs around the genome is non-random. Deterministic factors lead to areas of high and low incidences of DSBs which are referred to as “hot” and “cold” spots throughout genomes (Jeffreys et al., 2004, Kong et al., 2010, de Boer et al., 2015). The factors vary between organisms and can be subject to complex regulation (Cooper et al., 2016, Choi and Henderson, 2015).

In mammals, hot spots occur in regions with high levels of the histone marks H3 lysine 4 trimethylation (H3K4me3) and H3 lysine 36 trimethylation (H3K36me3), while cold spots occur in gene promoters and enhancers (Brick et al., 2012, Baker et al., 2014, Powers et al., 2016). Initially discovered whilst examining hybrid male sterility between wild and laboratory mouse strains (Forejt and Ivanyi, 1974), in the last two decades, the zinc-finger methyltransferase, PDRM9 has been identified (Parvanov et al., 2010, Baudat et al., 2010) and subsequently shown in reverse genetics by reverse genetics using mouse models that it is the principal enzyme that methylates histone H3, causing DSB formation at meiotic recombination hotspots (Powers et al., 2016, Baker et al., 2014, Brick et al., 2012).

Of relevance to my thesis, studies in budding yeast have found that the orthologs of ATR and related kinase ATM play a part in the homeostatic spatial regulation of DSBs via two potentially distinct mechanisms: firstly *cis*-inhibition, that prevents localized clusters of DSBs occurring on the same chromatid (Cooper et al., 2016) and secondly *trans*-inhibition, that prevents syntenic allelic DSBs on intact sister chromatids or homologous chromosomes. Therefore trans-inhibition would ensure to preserve donor repair sequence (Zhang et al., 2011).

Mechanistically, how ATR and ATM constrain the spatial distribution of where meiotic DSBs can form is a fundamental question in DNA damage repair. Studies of budding yeast mitosis suggest that ATR ortholog MEC1 promotes an efficient nucleus-wide search for homologous sequence to permit the repair of a single induced DSB (Dion et al., 2012, Seeber et al., 2013, Mine-Hattab and Rothstein,

2012). Therefore it is possible that ATR and ATM regulate repair machinery signalling and modulate the accessibility of different repair templates.

1.3.4 Numerical regulation of meiotic DSB formation

DSBs are required to prevent asynapsis and create at least one CO per chromosome (Kauppi et al., 2013). Different model organisms have different average numbers of DSBs induced in meiosis, e.g. *S. cerevisiae* ~150-200, *A. thaliana* ~200-300 and mice 220-300 (Plug et al., 1998) based upon counts of RPA foci. These DSB numbers do not scale with genome size, for example the lily plant, *Lilium longiflorum*, receives approximately ten times more breaks, 2000 DSBs (Terasawa et al., 1995), whilst the genome is >30-fold larger than both mice and human. The ability of species to control the extent of DSB formation suggests that cells are able to employ a species-specific numerical regulation of DSB formation (Kauppi et al., 2013). Evolving numerical control of meiotic DSB formation would be a logical method to balance potentially lethal DSBs against sufficient and evenly distributed DSBs per chromosome. Early IF studies found that the number of meiotic DNA DSBs formed in late leptonema in mouse is typically 200-300 (Plug et al., 1998).

Simple stochastic models of DSB formation cannot account for the rarity of asynapsis observed *in vivo*, as parameters show that far greater than 0.5% of cells would contain chromosomes without any DSBs under these conditions (Keeney et al., 2014). Thus, some regulation of DSB placement and number must occur (Keeney et al., 2014). Empirically, numerical feedback homeostasis has been observed by the “reining in”, or reduction in the variation of recombination protein foci that decreases sub-stage by sub-stage, over the duration of meiotic prophase in mouse spermatocytes (Cole et al., 2012). This would serve to ensure that chromosomes receive sufficient DSBs to synapse and form obligate COs.

ATR and ATM are known to contribute to the regulation of DSB homeostasis in meiosis. The removal of ATM orthologs in budding yeast, fly and mouse leads to an increased DSB formation in meiosis (Garcia et al., 2015, Lange et al., 2011, Joyce

et al., 2011). Using hypomorphic *Spo11* and DNA damage recombination (DDR) defective alleles, ATR ortholog MEC1 was found to promote DSB formation in budding yeast, (Gray et al., 2013).

REC114 is an ATM/ATR phosphotarget and an essential component of the pre DSB-complex (Carballo JA, 2013). The levels of REC114 diminish as SPO11 activity increases and chromosomes synapse. In addition TEL1/MEC1-dependent phosphorylation of REC114 prevents further DSB formation (Carballo JA, 2013). Therefore, the molecular machinery that provides DSB-homeostasis is able to sense the status of DSB formation and on going repair at several stages during meiotic prophase.

1.4 Meiotic homologous chromosome synapsis

1.4.1 An overview of homologous chromosome synapsis

Homologous synapsis, the pairing of maternal and paternal homologs, is an essential and highly conserved aspect of meiotic prophase (Page and Hawley, 2004, Zickler and Kleckner, 1999, Zickler and Kleckner, 2015). Synapsis is achieved through the formation of the SC, a large protein complex. The SC is thought to act as chromosome-scale scaffolding that enables homologous chromosomes to dock collinearly. The 100nm juxtaposition of homologous chromosomes by the SC is presumed to bring IH donor sequences into closer proximity to the DSB ends, reducing the nuclear search space required for repair between homologous chromosomes to occur (Zickler and Kleckner, 2015).

1.4.2 The SC

The mammalian SC consists of at least seven known proteins, which form a tripartite structure (Zickler and Kleckner, 2015). Two components, SYCP2 and SYCP3, can be seen as early as leptonema via cytology and electron microscopy, before synapsis occurs (Yuan et al., 2000, Yang et al., 2006). This is because SYCP2 and SYCP3 contribute to form the outer layer of the SC, the axial element (AE). During zygonema, the remaining five components are deposited between the AE homologous chromosomes in two layers as the chromosomes synapse, zipping the homologs together. The transverse filament (TF) consists of arrays of SYCP1-dimers in an arranged head-to-head conformation (Liu et al., 1996). It is the TF that joins the AE to the central element (CE), which is comprised of SYCE1, SYCE2, SYCE3 and TEX12. By pachynema, homologous chromosomes have a full SC along the entire length. The majority of DSBs have been repaired on each chromosome and COs have began to mature, when the homologous chromosomes begin to desynapse at diplonema, losing the TF and CE layers of the SC (Page and Hawley, 2004). The AEs are however retained, allowing the chiasmata to be seen.

As cells enter diakinesis, SC proteins are only present at centromeres (Bisig et al., 2012).

Mutant mice have been generated for each of the seven known mammalian SC proteins: SYCP2 (Yang et al., 2006), SYCP3 (Yuan et al., 2000), SYCP1 (de Vries et al., 2005), SYCE1 (Bolcun-Filas et al., 2009), SYCE2 (Bolcun-Filas et al., 2007), SYCE3 (Schramm et al., 2011) and TEX12 (Hamer et al., 2008). Mutants for each of these seven SC proteins have problems with SC formation and homologous synapsis. DSB repair and homologous synapsis are mutually interdependent (Schramm et al., 2011), interestingly, whilst DSB formation is proficient in all SC mutant animals, DSB repair is delayed and/or deficient (Kouznetsova et al., 2011). All seven mutant males are sterile, whereas only female mutants of the CE are sterile. The female mutants of the TF and AE proteins are sub-fertile, and *Sycp3 -/-* females have been shown to produce aneuploid oocytes and embryos (Yuan et al., 2002). In summary, the SC is essential for homologous synapsis and fertility.

1.4.3 Other meiotic chromosome components

The cohesin complex is another key component of meiotic chromosomes, which maintains sister-chromatid cohesion (Zickler and Kleckner, 2015). The complex consists of two different SMC proteins, an α-kleisin protein and a stromal antigen (Brooker and Berkowitz, 2014). The disruption of cohesin components alters the length of chromosomes axes, impairs homologous synapsis, which leads to precocious loss of sister-cohesion and aneuploidy (Hopkins 2015). DSB formation appears normal in cohesin complex mutants: *Smc1β* (Biswas et al., 2013), *Rad21l -/-* (Herran et al., 2011), *Rec8 -/-* (Bannister et al., 2004, Xu et al., 2005) and *Stag3 -/-* (Winters et al., 2014, Fukuda et al., 2014, Hopkins et al., 2014). However DSB repair is impaired and/or delayed and the recruitment of specific DDR factors is compromised (Llano et al., 2012). Finally, disruption of these cohesin sub-units impairs fertility, with male mutants being sterile (Ward et al., 2016); there is less information regarding the fertility of female cohesin mutants, however it has been suggested that based on the infertility of *Rec8 -/-* females (Bannister et al., 2004, Xu et al., 2005) that it is likely that the phenotype results in sterility for both sexes

(Hopkins et al. 2014). There are further examples of the cross talk between the SC and cohesin, as indicated by additional phenotypes of cohesion mutants: in *Rec8 -/-* meiotic cells, CE components of the SC are deposited between sister chromatids (Xu et al., 2005), and SMC1β is required for synapsis between non-homologs (Biswas et al., 2013).

In addition to these two major complexes, there are many other proteins that interact with the SC and/or cohesin complex (Berkowitz et al., 2012, Holloway et al., 2011). Three especially important components are HORMAD1, HORMAD2 and TRIP13, which are conserved meiotic proteins that sense and monitor asynapsis.

HORMAD1 and HORMAD2 are both found on regions of unsynapsed chromatin. As such they are present on all pre-synaptic axes during leptonema and become progressively evicted as regions synapse in zygonema. During pachynema they are absent from synapsed chromosomes. During diplonema, the behaviour of HORMAD1 and HORMAD2 differs: HORMAD1 is re-recruited to desynapsed axes, whereas HORMAD2 is not (Wojtasz et al., 2009). The phenotypes of *Hormad1 -/-* and *Hormad2 -/-* mice differ. *Hormad1 -/-* mice of both sexes are sterile (Shin et al., 2010, Kogo et al., 2012b, Daniel et al., 2011), whereas *Hormad2 -/-* females are fully fertile while the males are sterile (Wojtasz et al., 2012, Kogo et al., 2012b, Shin et al., 2010, Daniel et al., 2011). The phenotypes of *Hormad1 -/-* meiotic cells suggest that HORMAD1 is fundamental to meiotic DSB formation and homologous synapsis. Furthermore, immunoprecipitation (IP) and IF experiments have illustrated that HORMAD1 is required for HORMAD2 recruitment (Wojtasz et al., 2012, Kogo et al., 2012a). Therefore, in addition to its role in DSB formation, it is conceivable that HORMAD1 acts as an adaptor-protein to recruit HORMAD2 to asynaptic regions.

The functions of AAA+ ATPase TRIP13 in mouse are less clear, as it is an essential gene (Li and Schimenti, 2007). Nonetheless two hypomorphic alleles have been generated. Roig et al., (2010) used these alleles to demonstrate that TRIP13 is required to repair meiotic DSBs and to remove HORMAD1 and HORMAD2 from synapsed axes (Roig et al., 2010). Interestingly however, *Trip13*$^{mod/mod}$ mice are able to achieve homologous synapsis, and generate

crossovers, despite persistent DNA DSBs in pachynema (Wojtasz et al., 2009). TRIP13 orthologs in budding yeast and *C. elgans* suggest this protein is required for meiotic checkpoints of meiotic chromosomes organization and for regulating meiotic DSB repair (Bhalla and Dernburg, 2005, Zanders et al., 2011), for example by preventing the accumulation of HOP1 recombination at rDNA in budding yeast .

1.5 Meiotic prophase I checkpoints

Cell cycle checkpoints serve to monitor the progress and fidelity of cell cycle progression (Hartwell and Weinert, 1989). Activated checkpoints can cause cell cycle delay to enable corrective mechanisms, or lead to the activation of cell elimination pathways (Elledge, 1996). For the last two decades it has been thought meiosis has two main molecular checkpoints (Barchi et al., 2005, Di Giacomo et al., 2005, Burgoyne et al., 2009, Burgoyne et al., 2007), modifications of the mitotic DNA damage checkpoint, that sense defective DSB repair and chromosome synapsis respectively.

1.5.1 Cell-cycle checkpoints

The mitotic cell cycle in eukaryotic organisms consists of four stages: gap phase 1 (G1), S phase, gap phase 2 (G2), and mitosis (M). There are checkpoints that monitor entry into G1, DNA damage in in G1/S and G2/M, and spindle-assembly in metaphase of mitosis (Poon, 2016, Shaltiel et al., 2015). During G1, organelles replicate, cells grow and activate genes that will be required in S phase. Entry into S phase is delayed until cells reach a sufficient size and remove any DNA damage detected by the DNA damage network. During S phase DNA is replicated. In G2, the cell prepares for division, by growing and synthesizing the required proteins. The G2 phase ends with the onset of prophase, when cells enter into mitosis. Entry into mitosis is prevented if DNA damage is detected. Progression through the phases is coordinated by the spatial and temporal activity of cyclins and cyclin dependent kinase (CDK) proteins (Risal et al., 2016). Activated checkpoints function by blocking the actions of cyclins and CDKs (Shaltiel et al., 2015).

1.5.2 The DDR Network: ATM and ATR

In somatic cells, the DDR network preserves eukaryotic genomic integrity through life's inevitable intrinsic and extrinsic DNA damage (Jackson and Bartek, 2009). *Atm*, *Atr* and *Dna-pk* are key to this network they encode three sensor DNA damage kinases that respond to DNA damage in eukaryotes. These large kinases are part of the phosphatidylinositol-3-kinase-like kinase (PIKK) protein family (Marechal and Zou, 2013). All six sub-families of the PIKKs are large proteins important for cell signalling in response to intracellular and extracellular stresses.

The large size of these proteins has traditionally prevented a clear understanding of the relationship between the structure and function of these proteins. Recently, a high-resolution crystal structure of the kinase domain of DNA-PK was published {Sibanda, 2010 #26403} which provided mechanistic insight how the kinase domain and adjacent flanking regions provide substrate specificity. In the last twelve months cryo-EM structures of ATM have been published in two independent studies and found the existence of active and inactive states, with support the biochemical evidence of dimers of ATM is autophosphoryated to become active {Wang, 2016 #26405}{Baretic, 2017 #26404}. This is a distinct from ATR, which is reliant on other co-factors to become fully active to trigger a checkpoint response. Co-factors are recruited by non-kinase regions, including the sequence of certain HEAT repeat units are preserved within PIKK sub-families, this may account for the specificity some known protein-protein interactions such as the between ATR and its activating co-factor ATRIP (Cortez et al., 2001).

Prior to these structural studies, bioinformatics analysis found across PIKKs the C-terminal kinase domain accounts for between 5-10% of protein length (Perry and Kleckner, 2003). The majority of the N-termini of ATRs and ATMs orthologs comprise up to ~50 repeated units of alpha-helical of Huntington-elongation factor 3-protein phosphatase 2A-TOR1 (HEAT) domains (Perry and Kleckner, 2003).

The bioinformatics suggests that ATR and ATM sequences have diverged by modular additions, subtractions or translocations of small regions/domain. These changes underlie how the different functions they have in both mitosis and meiosis.

Early in response to DNA damage, ATM and ATR phosphorylate hundreds of proteins at S/T-Q motifs, initiating the signalling cascade (Olsen et al., 2010, Matsuoka et al., 2007). DNA-PK also phosphorylates some targets containing this motif (Tomimatsu et al., 2009), however its primary role is in NHEJ (Davis et al., 2014). In addition, ATM and ATR trigger subsequent waves of phosphorylation in the cascade by activating downstream effector kinases, for example CHK1 (Liu et al., 2000) and CHK2 (Matsuoka et al., 1998). ATM and ATR have been termed the master controllers of the DNA damage network (Shiloh, 2001). There are examples when they function in concert to regulate DSB repair; or when ATM and ATR have separate functions e.g. ATM and Double strand break Induced Silencing in *Cis* (DISC) (Shanbhag et al., 2010).

Much less is known about the meiotic DNA damage network. The meiotic roles of ATM and ATR are slowly being revealed, first from observational studies and subsequently forward and reverse genetics analysis using model organisms. To date, mammalian studies have found that ATM is required for DSB homeostasis, homologous synapsis, meiotic recombination and prophase checkpoints. The evidence surrounding the functionality of mammalian ATR is less clear due to the lethality of ATR-deficient embryos (Brown and Baltimore, 2000). Below is a summary of the previously described meiotic roles of ATM and ATR in model organisms.

1.5.3 ATM

Model organisms deficient for *Atm* have reduced meiotic chromosome axis integrity and chromosome fragmentation in both *Arabidopsis thaliana* (Culligan and Britt, 2008, Garcia et al., 2003) and *Mus musculus* (Barlow et al., 1998, Xu et al., 1996, Elson et al., 1996, Barchi et al., 2008). In *A. thaliana* the absence of ATM also impairs chromosome synapsis, and increases SPO11-dependent non-homologous synapsis (Culligan and Britt, 2008); In *Caenorhabditis elgans* ATM is required for the re-establishment of synapsis in pachynema post-irradiation (Couteau and Zetka, 2011).

ATM is also important for early recombination in prophase I in mouse (Bellani et al., 2005) (Lange et al., 2011), budding yeast (Cheng et al., 2013) and *Drosophila melanogaster*. Via the phosphorylation of pre-DSB complex component REC114, ATM/ATR are important for controlling total levels of DSB in budding yeast meiosis (Carballo JA, 2013). In budding yeast, *TEL1*, the ortholog of mammalian *Atm*, also negatively regulates DSB formation (Murakami and Keeney, 2008) and is required to establish the IH-bias in meiosis (Ho and Burgess, 2011). In mouse, ATM also plays important roles later in recombination, controlling crossover placement (Barchi et al., 2008).

1.5.4 ATR

In both budding yeast (Lydall et al., 1996) (Weinert et al., 1994) and *D. melanogaster* (Abdu et al., 2002) ATR orthologs are required for meiotic checkpoints. In this way ATR ensures that meiotic DNA replication is controlled and coordinated with meiotic recombination (Blitzblau and Hochwagen, 2013) and centromere pairing (Falk et al., 2010). Consistent with a coordinating role ATR orthologs have been found to ac during multiple steps in meiotic recombination; firstly, in budding yeast MEC1 has been shown to positively regulate DSB formation (Gray et al., 2013). Secondly suggestive of multiple roles in modulating early steps in meiotic recombination, ATR regulates RAD51/DMC1 stoichiometry in *A. thaliana* (Kurzbauer et al., 2012); and controls the activity of key factors in DNA DSB resection in budding yeast (Joshi et al., 2015); and is known to phosphorylate the RPA complex in budding yeast (Brush et al., 2001). Phosphorylation of the RPA complex is conserved between budding yeast (Brush et al., 2001) and mouse (Fedoriw et al., 2015), although its functional consequences are unclear. At later stages in meiotic recombination ATR was shown to promote interhomolog repair directly (Grushcow et al., 1999) and indirectly via the phosphorylation of meiotic chromosome associated protein HOP1 (Carballo et al., 2008, Penedos et al., 2015); finally one of the principal characteristics of ATR-defective *D. melanogaster Mei-41* mutants was defective CO regulation (Carpenter, 1979). It has been suggested that ATM and ATR are activated sequentially in meiotic prophase to restrict their activities, which have distinct sensitivities to DSBs within the cell (Joshi

et al., 2015); which fits the data and model of the ATM/ATR-dependent DSB-distribution presented in (Zhang et al., 2011).

1.5.5 Meiotic checkpoints

DNA is replicated in meiotic S phase. After replication, cells enter meiotic prophase I. This has been viewed as the meiotic equivalent of the G2/M phase (Burgoyne et al., 2007). In vertebrates, ATM, ATR and DNA-PK trigger checkpoint signalling in somatic cells at G1/S and G2/M (Durocher and Jackson, 2001). Once activated, these kinases activate downstream effector kinases like CHK1 and CHK2, which mediate further protein-protein interactions to arrest the cell cycle. Considering the large number of potential mutagenic DSBs inherent to meiosis, it is intuitive to hypothesize that the mitotic cell cycle checkpoint and its proteins have been adapted to control this process (MacQueen and Hochwagen, 2011). Indeed, this hypothesis does have credence in a number of model organisms examined (MacQueen and Hochwagen, 2011). Previous work suggests that two distinct meiotic checkpoints operate in mammalian meiosis: one that is DNA-damage dependent, and the other that is DNA-damage independent (Di Giacomo et al., 2005, Barchi et al., 2005).

In the DNA-damage dependent checkpoint, it is known that persistent DSBs present in pachynema cause apoptosis. These are abundant in mutant mice lacking proteins essential for meiotic recombination e.g. *Dmc1 -/-, Msh5 -/- and Atm -/-* (Barlow et al., 1998, Pittman et al., 1998, Edelmann et al., 1999). It was recently shown that CHK2 functions in the DNA-damage dependent checkpoint (Bolcun-Filas et al., 2014). Inactivation of *Chk2* partially prevents the oocyte losses observed in meiotic recombination defective mutants including *Atm -/-*.

Chromosomes unable to complete homologous synapsis in pachynema activate the DNA-damage independent checkpoint. This checkpoint has been demonstrated extensively in the past using chromosomal translocation models (Burgoyne et al., 2009), as well as sex chromosome aneuploid models like 39, XO mice (Phillips et al., 1973) and XYY mice (Rodriguez and Burgoyne, 2001). The DNA-damage

independent checkpoint also causes arrest in targeted mutants that do not initiate recombination, including *Spo11-/-* (Romanienko and Camerini-Otero, 2000) and *Mei4-/-* (Kumar et al., 2010).

1.5.6 MSCI

As already introduced, during prophase I the DNA and chromosomes undergo dynamic changes to permit homologous synapsis coupled to DSB repair. These interactions depend upon the high degree of sequence similarity between maternal and paternal homologues. However, whilst this is not an issue for the homogametic XX this creates a problem for the heterogametic XY.

In mice, the X and Y chromosomes are unique in the chromosome complement in that they are largely heteromorphic except at the pseudoautosomal region (PAR), an approximately 700kb region of genetic homology (Perry et al., 2001). Despite having such limited homology, the PAR receives DSBs, synapses and goes on to form an obligate CO that is necessary for proper segregation of the XY pair (Barchi et al., 2008). The non-homologous regions of the X and Y chromosome remain asynapsed during pachynema. Any DSBs that form in the non-homologous XY regions therefore cannot be repaired via HR using a homologous chromosome.

Over 50 years ago, a dense chromosome-containing structure was observed during pachynema in both testis histology and cytology (Solari, 1964). Later, this was found to be the chromatin of the X and Y chromosome, and was therefore termed the sex body (Solari, 1974). Studies analysing RNA expression of X and Y linked genes using *in situ* tritiated uridine labelling (Kierszenbaum and Tres, 1974, Henderson, 1963, Monesi, 1965a, Monesi, 1965b) and later, reverse-transcription PCR for X and Y encoded genes (McCarrey et al., 1992), revealed that the sex body was transcriptionally inactive at pachynema}(Henderson, 1963, Monesi, 1965a, Monesi, 1965b).

Therefore during male meiosis there is a considerable region of the genome that is kept inactive. For decades scientists tried to elucidate why, were there toxic genes

that needs to be supressed (Lifschytz and Lindsley, 1972)? It was not until work of Paul Burgoyne and his contemporaries that demonstrated that this process was important for a meiotic surveillance mechanism, or checkpoint that monitored the synapsis of the sec chromosomes (Odorisio et al., 1998, Turner et al., 2004, Turner et al., 2005, Turner et al., 2006, Burgoyne et al., 2007, Mahadevaiah et al., 2008).

This epigenetic process later called meiotic sex chromosome inactivation or MSCI (McKee and Handel, 1993), is required to permit progression into diplonema in male meiosis (Turner et al., 2004, Royo et al., 2010); where the X and Y-chromosomes accumulate repressive epigenetic marks like H2Aub, H3K9me3 and DNA-damage marker γH2AX (Baarends et al., 2005, Turner et al., 2004).

MSCI is present in both eutherian (Turner et al., 2004, Turner et al., 2005, Baarends et al., 2005) and metatherian mammals like the marsupial *Monodelphis domestica* (Mahadevaiah et al., 2009), but is absent in prototherian mammals e.g. Platypus (Daish et al., 2015) or in birds (Guioli et al., 2012). It is therefore likely MSCI / MSUC evolved prior to the eutherian-metatherian divergence, some 180 million years ago.

After the success of a pair of studies in 2004 and 2005, it was observed that the chromatin of asynapsed regions of autosomes are transcriptionally silenced in both male and female meiosis, in a process termed Meiotic Silencing of Unsynapsed Chromatin (MSUC) (Baarends et al., 2005, Turner et al., 2004). Collectively, both MSCI and MSUC are now referred to as meiotic silencing (Turner, 2015). While MSCI is required to complete meiotic prophase in males (Royo et al., 2010), MSUC can lead to germ cell elimination in males and females.

Around the same time meiotic studies using *neurospora crassa* and C. elgans found that these organisms were supressing the expression of regions of their genomes. Mechanistically distinct in N. crassa, DNA sequences that remain unpaired during meiosis are silenced (Shiu et al., 2001, Shiu and Metzenberg, 2002). In the nematode worm, it was described that just like on the hetromorphic regions of the mouse sex chromosomes, unpaired chromosomes, unsynapsed nematode chromosomes acquire repressive chromatin marks (Bean et al., 2004).

The same molecular pathway mediates both MSCI and MSUC. Firstly, SYCP3, HORMAD1 and HORMAD2 recruit the DNA-damage protein BRCA1 to chromosomal axes experiencing asynapsis during late zygonema (Turner et al., 2004). The kinase ATR then co-localizes with axial-BRCA1, before progressing to spread throughout the unsynapsed chromatin via an MDC1-dependent process (Ichijima et al., 2011). Phosphorylation of serine-139 of histone variant H2AX, mediates the structural changes to the chromatin that leads to transcriptional silencing to all X chromosome genes including miRNAs (Royo et al., 2015) and protein-coding genes, at early pachynema (Turner et al., 2004, Royo et al., 2010).

1.5.7 Sexual dimorphism in the fidelity of the meiotic checkpoints

It is well known that aneuploidies are more frequently derived from oocytes than spermatocytes in both mice and humans (Nagaoka et al., 2012). This has been correlated with molecular differences with both SC formation and abundance of DSB repair proteins in mouse and human gametogenesis (Gruhn et al., 2016).

Studies have looked at the meiotic silencing response in spermatocytes and oocytes and found key differences. Some epigenetic marks are sex-specific for example, they found that chromatin mark H3K9me3, is absent in oocytes, but present in spermatocytes (Cloutier et al., 2016;(Taketo and Naumova, 2013) Cloutier et al., (2016) also demonstrated that meiotic silencing of X-linked RNAs is likely inefficient or stochastic within oocytes, since mosaic expression of 3 X-linked genes was observed; the equivalent analysis of male spermatocytes found that these X-linked genes were efficiently silenced (Cloutier et al., 2016).

Whether MSCI and meiotic silencing are a phenomena important for human fertility is yet to be shown unequivocally. A study investigating MSCI in human spermatocytes suggests that MSCI is less strictly enforced than in male mice (de Vries et al., 2012). However, the data: reduced RNA polymerase II and *Cot-1* staining, which mark regions of active transcription and nascent RNA transcripts do not prove inefficacy *per se*. To compare the fidelity of the human meiotic silencing

checkpoint in future studies, it will be necessary to perform RNA-FISH for sex-linked genes to observe the de-repression of genes from asynapsed chromosomes in human spermatocytes. Analysis of meiotic silencing in human oocytes and spermatocytes may have important ramifications for human fertility.

1.6 Conclusion

It is likely that ATR is important for fundamental roles in meiosis as well as meiotic surveillance mechanisms. Therefore a basic understanding of the roles of ATR will serve to further our knowledge of the molecular genetics of meiotic cell biology, which in the future may have implications for medical interventions to treat aneuploidy and infertility.

1.7 Aims of thesis

The overall goal of this thesis is to determine and characterize the meiotic roles of ATR in mouse meiosis. To achieve this goal, I will address the following aims:

1. **Evaluate the use of *Atr* +/- and *Atr flox* alleles and different *Cre*-driver lines for their suitability to investigate the meiotic roles of ATR in the male germline.**
2. **Determine whether ATR has fundamental roles in meiosis and novel roles in meiotic surveillance mechanisms by examining:**
    a. **Fundamental steps in meiotic chromosome interactions**
    b. **Fundamental steps in meiotic DSB metabolism**
3. **Determine whether ATR is part of the DNA-damage dependent checkpoint**
    a. **Develop and refine models of the roles of ATR in prophase I checkpoints in male meiosis**

Chapter 2. Materials & Methods

2.1 Mice

All mice were maintained according to UK Home Office Regulations at the National Institute for Medical Research (NIMR) and the Francis Crick Institute Mill Hill laboratory. Owing to the integration of multiple mutant strains, the contributing strain backgrounds are MF1, 129S1/SvImJ, FVB/NJ and C57BL/6, unless otherwise noted. C57BL/6 is the largest contributing background strain. Littermate controls were used, where possible, to reduce effects associated with using a mixed genetic background. To generate material at specific developmental stages, female mice were set up in with male mice and checked each morning for vaginal plugs. The day that a vaginal plug was identified, this was considered to be 0.5 d*pc* and litters were typically recorded 19 days later. Alternatively the birth of a litter was recorded and this was considered as 0.5 days *post partum* (d*pp*) for other breeding cages. Mice were sacrificed at 13.5 and ~30.5 d*pp* using UK Home Office Schedule I methods. Testes were dissected from animals then flash frozen in liquid nitrogen, and stored at -80°C until later use. In addition some material was preserved in histological fixatives at room temperature. All of the final crosses used to generate each mouse strain are shown in figure 2.1.

2.1.1 *Atr* conditional (*Atr flox/-*) mice

Atr conditional mice i.e. containing a single *Atr* null allele, a single *Atr flox* allele and a *Cre*-recombinase transgene (see 2.1.2, 2.1.3 and 2.1.4) were produced by mating *Atr +/- Cre tg/+* males with *Atr flox/flox* females. *Atr+/-* and *Atr flox/flox* mutant mice were originally obtained from Eric Brown (University of Pennsylvania, USA). The *Atr* knockout allele contains a neomycin selection cassette that replaces the first three coding exons of *Atr* (Brown and Baltimore, 2000). The *Atr flox* allele contains two lox P sites flanking exon 44 in the essential C-terminal kinase domain of ATR (Brown and Baltimore, 2003). *Cre-lox* mediated recombination of the *Atr flox* allele leads to deletion of these essential kinase-encoding exons and a subsequent frameshift in 3′ exons (Brown and Baltimore, 2003). I will refer to *Atr flox/-* in the presence of a CRE recombinase as *Atr -/-* and *Atr flox/+* in the presence of a CRE recombinase, which are presumed to be equivalent to Atr

heterozygotes as *Atr wt.* The origin of the majority of the *Atr -/- Ngn3-Cre* mice from used extensively in this thesis originated from two F1 brothers, which were *Atr +/- Dmc1 +/+ Ngn3-Cre+.* Given that the *Atr flox/flox* females were similarly generated from intercrosing the initial of suitable heterozygous *Atr* littermates. Eric Brown provided a combined *Atr flox/-* Cre-ERT^2 strain. Therefore all resulting backcrosses analysed material and should be isogenic for *Prdm9.*

2.1.2 *Ddx4-Cre* mice

Ddx4-Cre mice were obtained from the Jackson Laboratory, USA (strain 006954). The *Ddx4-Cre* transgene contains a 5' 5.6 kb mouse *Ddx4-* promoter fragment, including a TATA box and more distant expression control elements controlling its germ cell expression (Gallardo et al., 2007).

2.1.3 *Ngn3-Cre mice*

Ngn3-Cre mice were obtained from the Jackson Laboratory, USA (strain 006333). 81 kb of 5'- sequence *Neurgenin3* (*Ngn3*), was used to generate the *Ngn3-Cre* transgene. It is expressed in endocrine and some non-endocrine stem cell lineages (Schonhoff et al., 2004).

2.1.4 *Stra8-Cre* mice

Stra8-Cre mice were obtained from Paul Burgoyne at the NIMR. The transgene contains a 1.4 kb promoter fragment from the *Stra8* gene and drives germline CRE expression (Sadate-Ngatchou et al., 2008).

2.1.5 *Atr -/- Dmc1 -/-* mice

Atr -/- Dmc1 -/- conditional mice were produced by mating *Atr +/- Dmc1 +/- Cre tg/+* males with *Atr flox/flox Dmc1 +/-* females. The *Dmc1* knockout allele contains a neomycin selection cassette replacing exons 10 and 11, encoding conserved RecA-like DNA binding domains necessary for enzymatic activity (Pittman et al., 1998).

2.1.6 *Atr -/- Msh5 -/-* mice

Atr -/- Msh5 -/- conditional mice were produced by mating *Atr +/- Msh5 +/- Cre tg/+ males* with *Atr flox/flox Msh5 +/-* females. The *Msh5* knockout allele contains a hygromycin selection cassette integrating into exon 18 (Edelmann et al., 1999).

2.1.7 *Atr -/- Spo11 -/-* mice

Atr -/- Spo11 -/- conditional mice were produced by mating *Atr +/- Spo11 +/- Cre tg/+* males and *Atr flox/flox Spo11* +/- females. The *Spo11* knockout allele contains a neomycin resistance cassette that replaces exons four, five and six which contain the catalytic domain including the active tyrosine Y138 (Baudat et al., 2000, Carofiglio et al., 2013).

2.1.8 *Atr -/- Atm -/-* mice

Atr -/- Atm -/- conditional mice were produced by mating *Atr +/- Cre tg/+ Atm +/- Cre tg/+* males and *Atr flox/flox Atm +/-* females. The knockout *Atm* allele contains a neomycin resistance cassette replacing regions within exons 36 and 37 (Barlow et al., 1998).

2.1.9 *Atr -/- Atm* conditional *Dna-pk$^{scid/scid}$* (*PIKK-null*) mice

PIKK-null mice were produced by mating *Atr +/- Atm +/- Dna-pk^{Scid}/+ Cre tg/+* males with *Atr flox/flox Atm* flox/flox *Dna-pk$^{Scid/Scid}$* females. *Atm flox/flox* mice were obtained from the Jackson Laboratory, USA (strain 021444). The *Atm flox* allele contains two lox P sites flanking exons 57 and 58, which contain the core PIKK kinase domain of ATM. CRE-mediated recombination of the *Atm* flox allele leads to the removal of these essential kinase-domain encoding exons (Callen et al., 2009). *Dna-pk$^{Scid/Scid}$* mice were already present at NIMR on a NOD.CB17 background. The severe combined immunodeficiency (*Scid),* mutation was first reported in 1983 at the Fox Chase Cancer Centre, USA (Bosma et al., 1983).

2.1.10 *Chk2 -/-* mice

Frozen *Chk2 -/-* testis material was kindly provided by John Schmenti (Cornell, USA). This strain was first described 2000 (Hirao et al., 2000).

(A)

		Atr flox/flox
		Atr flox
Atr+/- Ddx4-Cre +	*Atr- Ddx4-*	*Atr fl/-Ddx4-*
	Atr+ Ddx4 -	*Atr fl/+ Ddx4-*
	Atr+ Ddx4+	***Atr fl/+ Ddx4+***
	Atr- Ddx4 +	***Atr fl/- Ddx4+***

(B)

		Atr flox/flox
		Atr flox
Atr+/- Stra8-Cre +	*Atr- Stra8-*	*Atr fl/-Stra8-*
	Atr+ Stra8 -	*Atr fl/+ Stra8-*
	Atr+ Stra8+	***Atr fl/+ Stra8+***
	Atr- Stra8 +	***Atr fl/- Stra8+***

(C)

		Atr flox/flox
		Atr flox
Atr+/- Ngn3-Cre +	*Atr- Ngn-*	*Atr fl/-Ngn3-*
	Atr+ Ngn -	*Atr fl/+ Ngn3-*
	Atr+ Ngn+	***Atr fl/+ Ngn3+***
	Atr- Ngn +	***Atr fl/- Ngn3+***

(D)

		Atr flox/flox Dmc1+/-	
		Atr flox Dmc1+	*Atr flox Dmc1-*
Atr+/- Ngn3-Cre + Dmc1+/-	*Atr- Ngn3- Dmc1+*	*Atr fl/- Ngn3- Dmc1+/+*	*Atr fl/- Ngn3- Dmc1+/-*
	Atr+ Ngn3 - Dmc1+	*Atr fl/+ Ngn3- Dmc1+/+*	*Atr fl/+ Ngn3- Dmc1+/-*
	Atr+ Ngn3+ Dmc1+	*Atr fl/+ Ngn3+ Dmc1+/+*	*Atr fl/+ Ngn3+ Dmc1+/-*
	Atr- Ngn3 + Dmc1+	*Atr fl/- Ngn3+ Dmc1+/+*	*Atr fl/- Ngn3+ Dmc1+/-*
	Atr- Ngn3- Dmc1-	*Atr fl/-Ngn3- Dmc1+/-*	*Atr fl/- Ngn3- Dmc1-/-*
	Atr+ Ngn3 - Dmc1-	*Atr fl/- Ngn3- Dmc1+/-*	*Atr fl/+ Ngn3- Dmc1-/-*
	Atr+ Ngn3+ Dmc1-	*Atr fl/- Ngn3+Dmc1+/-*	***Atr fl/+ Ngn3+ Dmc1-/-***
	Atr- Ngn3 + Dmc1-	*Atr fl/- Ngn3+ Dmc1+/-*	***Atr fl/- Ngn3+ Dmc1-/-***

(E)

		Atr flox/flox Msh5+/-	
		Atr flox Msh5+	*Atr flox Msh5-*
Atr+/- Ngn3-Cre + Msh5+/-	*Atr- Ngn3- Msh5+*	*Atr fl/- Ngn3- Msh5+/+*	*Atr fl/- Ngn3- Msh5+/-*
	Atr+ Ngn3 - Msh5+	*Atr fl/+ Ngn3- Msh5+/+*	*Atr fl/+ Ngn3- Msh5+/-*
	Atr+ Ngn3+ Msh5+	*Atr fl/+ Ngn3+ Msh5+/+*	*Atr fl/+ Ngn3+ Msh5+/-*
	Atr- Ngn3 + Msh5+	*Atr fl/- Ngn3+ Msh5+/+*	*Atr fl/- Ngn3+ Msh5+/-*
	Atr- Ngn3- Msh5-	*Atr fl/-Ngn3- Msh5+/-*	*Atr fl/- Ngn3- Msh5-/-*
	Atr+ Ngn3 - Msh5-	*Atr fl/- Ngn3- Msh5+/-*	*Atr fl/+ Ngn3- Msh5-/-*
	Atr+ Ngn3+ Msh5-	*Atr fl/- Ngn3+Msh5+/-*	***Atr fl/+ Ngn3+ Msh5-/-***
	Atr- Ngn3 + Msh5-	*Atr fl/- Ngn3+ Msh5+/-*	***Atr fl/- Ngn3+ Msh5-/-***

(F)

		Atr flox/flox Spo11+/-	
		Atr flox Spo11+	*Atr flox Spo11-*
Atr+/- Ngn3-Cre + Spo11+/-	*Atr- Ngn3- Spo11+*	*Atr fl/- Ngn3- Spo11+/+*	*Atr fl/- Ngn3- Spo11+/-*
	Atr+ Ngn3 - Spo11+	*Atr fl/+ Ngn3- Spo11+/+*	*Atr fl/+ Ngn3- Spo11+/-*
	Atr+ Ngn3+ Spo11+	*Atr fl/+ Ngn3+ Spo11+/+*	*Atr fl/+ Ngn3+ Spo11+/-*
	Atr- Ngn3 + Spo11+	*Atr fl/- Ngn3+ Spo11+/+*	*Atr fl/- Ngn3+ Spo11+/-*
	Atr- Ngn3- Spo11-	*Atr fl/-Ngn3- Spo11+/-*	*Atr fl/- Ngn3- Spo11-/-*
	Atr+ Ngn3 - Spo11-	*Atr fl/- Ngn3- Spo11+/-*	*Atr fl/+ Ngn3- Spo11-/-*
	Atr+ Ngn3+ Spo11-	*Atr fl/- Ngn3+Spo11+/-*	***Atr fl/+ Ngn3+ Spo11-/-***
	Atr- Ngn3 + Spo11-	*Atr fl/- Ngn3+ Spo11+/-*	***Atr fl/- Ngn3+ Spo11-/-***

(G)

		Atr flox/flox Atm+/-	
		Atr flox Atm+	*Atr flox Atm-*
Atr+/- Ngn3-Cre + Atm+/-	*Atr- Ngn3- Atm+*	*Atr fl/- Ngn3- Atm+/+*	*Atr fl/- Ngn3- Atm+/-*
	Atr+ Ngn3 - Atm+	*Atr fl/+ Ngn3- Atm+/+*	*Atr fl/+ Ngn3- Atm+/-*
	Atr+ Ngn3+ Atm+	*Atr fl/+ Ngn3+ Atm+/+*	*Atr fl/+ Ngn3+ Atm+/-*
	Atr- Ngn3 + Atm+	*Atr fl/- Ngn3+ Atm+/+*	*Atr fl/- Ngn3+ Atm+/-*
	Atr- Ngn3- Atm-	*Atr fl/-Ngn3- Atm+/-*	*Atr fl/- Ngn3- Atm-/-*
	Atr+ Ngn3 - Atm-	*Atr fl/- Ngn3- Atm+/-*	*Atr fl/+ Ngn3- Atm-/-*
	Atr+ Ngn3+ Atm-	*Atr fl/- Ngn3+Atm+/-*	***Atr fl/+ Ngn3+ Atm-/-***
	Atr- Ngn3 + Atm-	*Atr fl/- Ngn3+ Atm+/-*	***Atr fl/- Ngn3+ Atm-/-***

(H)

		Atr flox/flox Atm flox/flox Dnapk$^{Scid/Scid}$
		Atr flox Atm flox Dnapk^{Scid}
Atr+/- Ngn3-Cre + Atm+/- Dnapk^{Scid}/+	*Atr- Ngn- Atm+ Dnapk+*	*Atr fl/- Ngn3- Atm fl/+ DnapkScid/+*
	Atr+ Ngn - Atm+ Dnapk+	*Atr fl/+ Ngn3- Atm fl/+ DnapkScid/+*
	Atr+ Ngn+ Atm+ Dnapk+	*Atr fl/+ Ngn3+ Atm fl/+ DnapkScid/+*
	Atr- Ngn + Atm+ Dnapk+	*Atr fl/- Ngn3+ Atm fl/+ DnapkScid/+*
	Atr- Ngn- Atm- Dnapk+	*Atr fl/-Ngn3- Atm fl/- DnapkScid/+*
	Atr+ Ngn - Atm- Dnapk+	*Atr fl/- Ngn3- Atm fl/- DnapkScid/+*
	Atr+ Ngn+ Atm- Dnapk+	*Atr fl/- Ngn3+ Atm fl/- DnapkScid/+*
	Atr- Ngn+ Atm- Dnapk+	*Atr fl/- Ngn3+ Atm fl/- DnapkScid/+*
	Atr- Ngn- Atm+ Dnapk^{Scid}	*Atr fl/- Ngn3- Atm fl/+ DnapkScid/Scid*
	Atr+ Ngn- Atm+Dnapk^{Scid}	*Atr fl/+ Ngn3- Atm fl/+ DnapkScid/Scid*
	Atr+ Ngn+ Atm+ Dnapk^{Scid}	*Atr fl/+ Ngn3+ Atm fl/+ DnapkScid/Scid*
	Atr- Ngn+ Atm+ Dnapk^{Scid}	*Atr fl/- Ngn3+ Atm fl/+ DnapkScid/Scid*
	Atr- Ngn- Atm- Dnapk^{Scid}	*Atr fl/-Ngn3- Atm fl/- DnapkScid/Scid*
	Atr+ Ngn- Atm- Dnapk^{Scid}	*Atr fl/- Ngn3- Atm fl/- DnapkScid/Scid*
	Atr+ Ngn+ Atm- Dnapk^{Scid}	***Atr fl/+ Ngn3+ Atm fl/- DnapkScid/Scid***
	Atr- Ngn + Atm- Dnapk^{Scid}	***Atr fl/- Ngn3+ Atm fl/- DnapkScid/Scid***

Figure 2.1 Summary of final crosses

Punnet squares for the final crosses used to generate each the eight compound *Atr* mutant strains are shown in (A-H). The control and mutant animals are shown in embolden **black** and **red** respectively.

2.2 Genotyping

Mice were genotyped using DNA extracted from a small biopsy of somatic tissue. Biopsy were digested in 250 µl of 50mM NaOH buffer and incubated in a heat block at 95°C for 90 min, before being centrifuged at maximum speed for 5 min before adding 25µl of 25mM Tris-HCl pH 8.0. Each genotyping PCR reaction had the following contents: 2x MyTaq Red mix (Bioline), 10mM genotyping primers, 1ul of DNA template and finally distilled water to bring the total reaction volume to 25ul. Genotyping PCR primers and cycling conditions are listed below (**Table 2.1**).

Table 2.1 Primers for genotyping

Strain/PCR and amplicons	Primers 5' --> 3'	Reference	PCR conditions
Atr ko	Atr-KO	**Brown & Baltimore,** (2000)	1x94ºC, 3 min
	CAG CGC ATC GCC TTC TAT CGC CTT CTT GAC		35x:
***Atr ko* allele 590bp**	ATR-Exon1		94ºC, 30 sec
	TTC CGG GAG GAG AAT TTT GGA C		56ºC, 30 sec
			72ºC, 30 sec
			1x72ºC, 10 min
Atr flox/wt	gATR-I#5	**Brown & Baltimore,** (2003)	1x94ºC, 3 min
	TAC ATT TTA GTC ATA GTT GCA TAA CAC		34x:
***Atr flox* allele 550bp**	gATR-I#15		96ºC, 10 sec
***Atr wt* allele 450bp**	CTT CTA ATC TTC CTC CAG AAT TGT AAA AGG		60ºC, 30 sec
			72ºC, 30 sec
			1x72ºC, 5 min
Atm ko/wt	ATM-A	**Barlow *et al.*,**(1996)	1x94ºC, 3 min
	GAC TTC TGT CAG ATG TTG CTG CC		37x:
***Atm ko* allele 400bp**	ATM-B		96ºC, 10 sec
***Atm wt* allele 165bp**	CGA ATT TGC AGG AGT TGC TGA G		56ºC, 30 sec
	ATM-Neo		72ºC, 30 sec
	GGG TGG GAT TAG ATA AAT GCC TG		1x72ºC, 10 min
Atm flox/wt	F16147	**Callén *et al.*,** (2009)	1x94˚C, 2 min
	CTT TAA TGT GCC TCC CTT CG		10x:
***Atm flox* allele 320bp**	R16148		94˚C, 20sec
***Atm wt* allele 269bp**	GAA GGA TCT TCC CCT GTT CA		65˚C, 15sec [-0.5˚C per cycle]
			68˚C, 10sec
			28x:
			94˚C,15sec
			60˚C,15sec
			72˚C,10sec
			1x72˚C, 2 min
Dmc1 ko/wt	oIMR5332	**Pittman *et al.*,** (1998)	1x 94˚C, 3 min
	GCC AGA GGC CAC TTG TGT AG		25x:
Dmc1 ko* allele *147bp	oIMR9132		94˚C, 20 sec
Dmc1 wt* allele *233bp	CCG GCC AGA TTA CAT TTC TT		54˚C, 30 sec
	oIMR9133		72˚C, 20 sec
	AAA GGG ACT GCT GAG GCA TA		1x: 72˚C, 7 min
Cre	CreF	*Turner Lab*	1x94ºC, 3 min
	GGC GGA TCC GAA AAG AAA A		35x:
***Cre* allele ~400bp**	CreR2		94ºC, 40 sec
	CAG GGC GCG AGT TGA TAG C		63ºC, 40 sec
			72ºC, 40 sec
			1x72ºC, 3 min
H2afx ko/wt	HX5	**Celeste *et al.*,** (2002)	1x: 94˚C, 3 min
	CTC TTC TAC CTC GTA CAC CAT GTC CG		35x:
H2afx ko* allele *424bp	RW		96˚C, 10 sec
H2afx wt* allele *453bp	CTC GGC GCG GGC CCC C		65˚C, 30 sec
	KXR		72˚C, 30 sec
	GTC ACG TCC TGC ACG ACG CGA GC		1x: 72˚C, 10 min

Strain/PCR and amplicons	Primers 5' --> 3'	Reference	PCR conditions
Msh5 ko/wt ***Msh5 ko allele 501bp*** ***Msh5 wt allele 405bp***	Msh5FW GAG GAC AAG CTG CAC TAT CGT AG Msh5Rev CCT GCC ATT CCT GAT TCG TAC TC 2-PGKRev CCG GTG GAT GTG GAA TGT GTG CG	**de Vries *et al*.,** (1999).	1x94ºC, 5 min 30 x: 94ºC, 30 sec 65ºC, 1 min 72ºC, 1 min 1x72ºC, 5 min
Ngn3-Cre ***Ngn3-Cre allele 250bp***	CRE-DS: TTC AAC TTG CAC CAT GCC GCC CAC G Ngn3-Cre-US: GCT GGC ACA CAC ACA CCT TCC AT	**Boiani *et al*,. (2004)**	1x94ºC, 5 min 35 x: 94ºC, 20 sec 54ºC, 30 sec 72ºC, 40 sec 1x72ºC, 5 min
Spo11 ko ***Spo11 ko allele 147bp***	PRSF4 CTG AGC CCA GAA AGC GAA GGA SP16R ATG TTA GTC GGC ACA GCA GTA G	**Baudat *et al*,** (2000)	1x: 94˚C, 5 min 35x: 94˚C,30 sec 58˚C,30 sec 72˚C, 45 sec 1x: 72˚C, 10 min
Spo11 wt ***Spo11 wt allele 233bp***	DelF CAA GGG ATT GAT TGC TGG CA DelR AGT TTG ATC CCA GGA GTG CA	**Turner Lab**	1x: 94˚C, 5 min 35x: 94˚C,30 sec 58˚C,30 sec 72˚C, 45 sec 1x: 72˚C, 10 min
Stra8-Cre ***Stra8-Cre allele 170 bp***	Stra8-F GTG CAA GCT GAA CAA CAG GA Stra8-R AGG GAC ACA GCA TTG GAG TC	**Sadate-Ngatchou *et al*., (2009)**	1x: 94˚C, 5 min 35x: 94˚C,30 sec 58˚C,30 sec 72˚C, 45 sec 1x: 72˚C, 10 min
Scid/wt ***Scid allele 180bp*** ***scid wt allele101bp***	Primer-F GAG AAA AGG AGG ATC ATG GAT TCA AGA AAT AAA TGT AAC G Primer-WR ACG AAT CTC TTT CAA TCG TCC CCG GT Primer-MF TGG TAT CCA CAA AAA ATA CGC TAA Primer-R CCG TGA AGT GAC ACA TTT ACC TCT TTT CAC TGA AAT CC	**Maruyama *et al*., (2002)**	1x94ºC, 2 min 30x: 94ºC, 30 sec 60ºC, 30 sec 72ºC, 20 sec 1x72ºC, 1 min

2.3 Chromosome spreads & immunofluorescence

Chromosome spreads were preformed using a protocol adapted from Barlow and colleagues (Barlow et al., 1998) Briefly, -80°C frozen testes were thawed in small petri dishes containing chilled RPMI medium (plus L-glutamine). Testes were mechanically disrupted using two scalpel blades to liberate meiotic cells from the seminiferous tubules to create a cloudy milky cell suspension. Two drops of cell suspension were added to pre-boiled glass slides. The cells were permeabilized for 10 min in four drops of 0.05% Triton X-100 (Sigma) in distilled water. Next, the cells were fixed for 20 min in eight drops of 2% paraformaldehyde, 0.02% SDS in PBS. The slides were rinsed in distilled water, allowed to air dry for 15 min and then were blocked in PBT (0.15% BSA, 0.10% TWEEN-20 in PBS) for 60 min.

Next, primary antibodies were applied (**Table 2.2**) in PBT and slides were incubated in a humid chamber overnight at 37°C. The next morning, slides were washed three times in PBS for 5 min each. 50µl of secondary antibodies (AlexaFluor 488, 594 and 647, Invitrogen) were applied at a concentration of 1:500 in PBS and slides were incubated in a humid chamber for 1 hr at 37°C. Finally, slides were washed three times in PBS for 5 min each and then mounted in Vectashield with DAPI.

Table 2.2 Primary antibodies

Antibody	Type Source	Dillution
anti-ACA	Hu polyclonal, Gift, Bill Earnshaw	**1 in 1000**
anti-ATR	Rb polyclonal, Cell Signalling, #2790	**1 in 50**
anti-ATR	G polyclonal, SantaCruz, sc-1887	**1 in 100**
anti-DMC1	Rb polyclonal, Santa Cruz (H-100), sc-22768	**1 in 20**
anti-DMC1	G polyclonal, Santa Cruz (C-20), sc-8973	**1 in 20**
anti-GAPDH	Rb polyclonal, Abcam, ab-9485	**1 in 4000**
anti-HORMAD2	Rb polyclonal, Gift,	**1 in 500**
anti-MLH3	Rb polyclonal, Gift, Paula Cohen	**1 in 100**
anti-pCHK1-S317	Rb polyclonal, Cell Signalling, #2344	**1 in 100**
anti-pCHK1-S3435	Rb polyclonal, Cell Signalling, #2348	**1 in 100**
anti-pCHK2-T68	Rb polyclonal, Cell Signalling, #2197	**1 in 100**
anti-pRPA-S33	Rb polyclonal, Bethyl laboratories, A300-246A;	**1 in 100**
anti-pSMC3-S1083	Rb polyclonal, Bethyl laboratories, A304-637A	**1 in 100**
anti-RAD51	Rb polyclonal, Santa Cruz (H92), sc-8349	**1 in 50**
anti-RAD51	Rb polyclonal, Calbiochem, PC130	**1 in 50**
anti-RPA	Rb polyclonal, Abcam, ab-2175	**1 in 33**
anti-SCYP3	Gp polyclonal, Turner Lab (Cambridge Research Biochemicals)	**1 in 500**
anti-SCYP3	Rb polyclonal, Abcam, ab-15092	**1 in 100**
anti-SCYP3	M monoclonal, Abcam, ab-97672	**1 in 100**
anti-SYCE1	Rb polyclonal, Gift, Howard Cooke/Ian Adams	**1 in 500**
anti-SYCE2	Gp polyclonal, Gift, Howard Cooke/Ian Adams	**1 in 800**
anti-γH2AFX	M monoclonal, Millipore, 05-636	**1 in 100**

2.4 RNA fluorescent *in-situ* hybridisation (RNA-FISH) & immunofluorescence (IF)

RNA-FISH & IF were performed using a protocol described in Mahadevaiah et al. (2009). Briefly, -80°C frozen testes were thawed in small petri dishes containing chilled RPMI medium (plus L-glutamine). Testes were mechanically disrupted using two scalpel blades to liberate meiotic cells from the seminiferous tubules, to create a cloudy milky cell suspension. Two drops of cell suspension were added to pre-boiled glass slides. The cells were then permeabilized for 10 min in an excess of ice cold CSK buffer (100 mM NaCl, 300 mM sucrose, 3 mM $MgCl_2$, 10 mM PIPES, 0.5% Triton X-100, 1 mM EGTA and 2 mM vanadyl ribonucleoside (NEB), pH 6.8), and then fixed for 10 min in an excess of ice cold 4% paraformaldehyde (Fischer Scientific), pH 7-7.4. Slides were then washed in PBS, dehydrated in ethanol series twice for two minutes at each stage (2 x 70%, 80%, 95%, 100%) before being air-dried.

Digoxigenin (DIG)-labelled probes were prepared from 1µg of BAC DNA (from CHORI: *Scml2*, RP24-204O18; using the DIG-Nick Translation Kit (Roche), according to manufacturer's instructions. For each probe, 100ng digoxigenin-labelled BAC was prepared in 15µl formamide (Sigma), with 3µg mouse Cot1 DNA (Invitrogen) and 10µg sheared salmon sperm DNA (Ambion). Probes were denatured for 10 min at 80°C and then combined with 15µl pre-warmed (37°C) 2x hybridization buffer (2x SSC, 10% dextran sulphate (Sigma), 1 mg/ml BSA and 2mM vanadyl ribonucleoside) and incubated for 30 min at 37°C. Finally, 30µl pre-hybridized probes were applied to slides and incubated in a humid chamber overnight at 37°C.

The next day, slides were washed at 42°C, three times in 2x SSC and 50% formamide and three times in 2x SSC, for 5 min per wash. Slides were then transferred to 4x SSC and 0.1% TWEEN-20 and then blocked (4x SSC, 4 mg/ml bovine serum albumin and 0.1% TWEEN-20) for 30 min in a humid chamber at 37°C. Probes were detected using 30µl of 1:10 anti-digoxigenin fluorescein, before

being diluted in a detection buffer (4x SSC, 1mg/ml bovine serum albumin and 0.1% TWEEN-20) for 1 hr in a humid chamber at 37°C.

Slides were washed three times for 2 min in 4x SSC and 0.1% TWEEN- 20. For subsequent immunofluorescence, 50µl of primary antibody anti-HORMAD2, diluted 1:100 in 4x SSC and 0.1% TWEEN-20, was added to slides and incubated for 30 min in a humid chamber at room temperature. Slides were washed for 2 min in 4x SSC and 0.1% TWEEN-20. Next, 50µl of secondary antibody (AlexaFluor 594), diluted 1in 4x SSC plus 0.1% TWEEN-20, was added to slides and incubated for 30 min in a humid chamber at room temperature. Finally, slides were washed for 2 min in 4x SSC and 0.1% TWEEN-20 and mounted in Vectashield with DAPI.

2.5 Fixing testis, histology and immunohistochemistry

Testes were fixed overnight in at least ten times a volume of excess of fixative, before being transferred to 70% ethanol. The choice of fixative was dependent on the subsequent analysis: Bouin's solution for histology and 4% paraformaldehyde: PBS for immunohistochemistry (IHC). Transversely halved testes were embedded in paraffin wax after tissue dehydration. Tissue was dehydrated by transferring samples through increasing ethanol concentrations (85%, 90%, 95% and 100%) for 5 min each before incubating in 100% xylene for 5 min. Testes were serially sectioned at 5 μm.

For histology, Bouin's fixed material was stained with heamotoxilyn and counterstained using Periodic-acid Schiff. For IHC, wax was melted and slides were washed twice in xylene to remove residual wax, each for 5 min. Sections were rehydrated by transferring samples through a decreasing ethanol concentrations series (100%, 100%, 95%, 80%, 70%, 50%), each incubated for 1 min before rinsing in PBS and distilled water. Slides were then boiled for 10 min using 1mM tri-sodium citrate pH 6.0 to retrieve antigens. Slides were blocked in PBT (PBT: 100ml PBS, 0.15mg BSA, 1ml 10% Tween -20) for 1 hr at room temperature. This was followed by adding primary antibodies and incubating at 37^{o}C in a humid chamber for at least 2 hr, or overnight.

Slides were washed three times in PBS before adding 100 μl of secondary antibodies (AlexaFluor 488, 594 and 647, Invitrogen) at a concentration of 1:500, diluted in PBS. Slides were incubated in a humid chamber for 1 hr at 37°C. Finally, slides were washed three times in PBS and then mounted in Vectashield with DAPI.

2.6 Imaging

Imaging was performed using an Olympus IX70 inverted microscope with a 100-W mercury arc lamp. For chromosome spread and RNA FISH imaging, an Olympus UPlanApo 100x/1.35 NA oil immersion objective was used. For testis section imaging, an Olympus UPlanApo 40x/0.75 NA objective was used. A Deltavision RT computer-assisted Photometrics CoolsnapHQ CCD camera with an ICX285 Progressive scan CCD image sensor was used for image capture. 8 or 16-bit (512x512 or 1024x1024 pixels) raw images of each channel were captured and later processed using Fiji software.

For chromosome spreads, the cells were first categorized into meiotic stages based upon SYCP3, as described in Figure 3.1 and Results section 3.1. The cells were then assessed for antibody staining and representative images were captured.

For RNA-FISH preparations, cells were first categorized based upon the presence of entirely HORMAD2 positive axes corresponding to the heteromorphic sex chromosomes or univalent chromosomes, as described in Figure 3.5. Next, the FISH signals were examined and representative images were captured. In all experiments the number of cells counted is indicated in figure legends.

2.7 Statistics

Statistical calculations were performed using GraphPad Prism 6.0. For comparisons between two genotypes, Mann-Whitney test or T-tests were performed. P values are reported in graphs and/or figure legends. Median or mean values are indicated within graphs.

2.8 Protein extraction and quantification

Frozen testes (-80°C) were thawed in pre-chilled protein lysis buffer (50mM Tris-HCl pH 8.0, 150mM NaCl, 1mM EGTA, 1mM $MgCl_2$, 0.1% NP40, 1mM PMSF, 1mM DDT) prior to homogenisation on ice. Samples were centrifuged at 4°C, 8000 rpm for 10 min and the supernatant was collected. The concentration of the protein containing supernatant was determined using Pierce BCA Protein Assay Kit (ThermoFisher).

2.9 Western blot

After SDS-PAGE (Laemmli, 1970), gels were transferred to Amersham Hybond nitrocellulose membrane (GE Healthcare) in transfer buffer (500mM Glycine, 50mM Tris-HCl, 0.01% SDS, 20% methanol) at 4°C, ~130mV for 90 min. Membranes were washed in TBST (10mM Tris-HCl pH 7.4, 100 mM NaCl, 0.1% Tween) and blocked with 3% bovine serum albumin extract (Sigma-Aldrich) in TBST for 1 hr. Membranes were incubated with primary antibody (see table 3) in 3% BSA in TBST overnight at 4°C. Membranes were washed with TBST three times for 3 mins, before being incubated with secondary antibodies (Sigma) coupled to horseradish peroxidase (HRP) for 1 hr at room temperature. After washing the membranes three times for 10 min, signals were visualised using SuperSignal West Pico Chemiluminescent Substrate (ThermoFisher) and Hyper ECL film (GE Healthcare).

2.10 Detection of radiolabelled SPO11-oligonucletides

Julian Lange (Scott Keeney laboratory, NY) performed these experiments as part of a scientific collaboration. The technique has been adapted since first described (Pan and Keeney, 2009) and the method used in this study is comparable with that of recent publications (Daniel et al., 2011, Roset et al., 2014, Pacheco et al., 2015). Essentially, the protocol consists of several steps: (i) protein lysis, (ii) two rounds of immunoprecipitation with a SPO11 antibody, (iii) radiolabelling with [α-^{32}P] dCTP, (iv) resolving labelled SPO11-oligo complexes by SDS-PAGE and quantifying signal using a phosphor imaging plate, (v) western blot detection of free SPO11 that is not bound to oligonucleotides (oligos), and finally (vi) deproteinization and resolution of oligos on a sequencing gel. The methodology is outlined below:

(i) Protein lysis:

Decapsulated testes from sacrificed animals were placed in 1.5 ml tubes on ice containing 100µl lysis buffer (1% Triton X-100, 400 mM NaCl, 25 mM HEPES-NaOH pH 7.4, 5 mM EDTA) supplemented immediately before use with a Complete, Mini, EDTA-free protease inhibitor cocktail tablet (Roche). Testes tissue was disrupted using plastic pestles with gradual addition of 700µl lysis buffer. Homogeneous lysate was carefully transferred to 1ml ultracentrifuge tubes. The viscous crude lysates were centrifuged at ~355,040g in a bench-top ultracentrifuge for 15 min at 4°C. The supernatant was carefully transferred into siliconised 1.5ml tubes without disturbing the pellet, using additional 100µl volumes of lysis buffer to wash and transfer residual supernatant. Additional lysis buffer was added to bring each tube up to the same total volume.

(ii) Two rounds of immunoprecipitation:

Per sample, 3µg anti-mSPO11 antibody (Spo11-180) was added to all tubes except the mock immunoprecipitation negative control. Samples were incubated for 1 hr at 4°C on an orbital rotator. Per sample, 40µl of protein A-agarose bead slurry, that had previously been washed in lysis buffer was added. This was then incubated at 4°C for 3 hr on an orbital rotator. Beads were spun down at ~1000g for 1 min in a bench-top centrifuge, incubated on ice for 1 min and the supernatant removed. Washes were performed by adding 500µl cold 1x IP buffer (1% Triton X-100, 150 mM NaCl, 15 mM Tris-HCl, pH 7.4) to each tube, inverting gently 20 times and spinning down for 1 min in a bench-top centrifuge, as well as being incubated on ice for 1 min and supernatant removed. Washes were repeated twice. Beads were spun down for 1 min in a bench-top centrifuge, incubated on ice for 1 min and the remaining supernatant removed. To elute samples, 40µl of 2xSDS sample buffer containing fresh β-mercaptoethanol was added and samples were boiled at 95^{o}C for 3 min before incubation on ice for 1 min. After a quick spin for 10 sec, samples were incubated on ice for 1 min. 40µl supernatant was transferred to a clean siliconised tube. Elution was repeated adding 40µl 0.5xSDS sample buffer and was consolidated with first elution in siliconised tube. Finally 80µl of 2x IP buffer was added, mixed by inverting vigorously for 10 sec and incubated on ice for 1 min.

80µl of supernatant was carefully added to the siliconised tube to bring the total volume to ~160µL. Finally, 750µl of 1x IP buffer was added.

The immunoprecipitation was then repeated. 3µg anti-mSPO11 antibody was added to all tubes except the mock immunoprecipitation negative control. Samples were incubated for 1 hr minimum at 4°C on an orbital rotator. Per sample, 40µl of protein A agarose bead slurry was added, that had been pre-washed in 1x IP buffer. This was incubated at 4°C overnight on an orbital rotator. After spinning down beads at ~1000g for 1 min in a bench-top centrifuge, these were incubated on ice for 1 min and remove was supernatant. To wash, 500µl cold 1x IP buffer was added to each tube, by inverting gently 20 times, then spun down for 1 min in a bench-top centrifuge, incubated on ice for 1 min and the supernatant removed. Washes were repeated twice. Beads were spun down for 1 min in a bench-top centrifuge, incubated on ice for 1 min and the remaining supernatant removed. Beads were washed twice with 500µl cold 1x labelling buffer (2 mM Tris-acetate, pH 7.9, 5 mM potassium acetate, 1 mM magnesium acetate, 0.1 mM DTT, diluted from 10xNEB4 from New England Biolabs). After spinning down for 30 sec and incubation on ice for 30 sec, the remaining supernatant was removed.

(iii) Radiolabelling with [α-^{32}P] dCTP:

Using fresh [α-^{32}P] dCTP to radiolabel SPO11-oligos, 50 μl TdT labelling reaction (5µl 10× labelling buffer, 2 µl [α-32P] dCTP, 1 µl TdT ~20,000 U/ml (Fermentas) and 42µl H_2O) was added to each sample and incubated at 37°C for 1 hr. Reactions were gently mixed every 15 min. Beads were spun down down in a bench-top centrifuge at ~1000g for 30 seconds and the supernatant was removed. Beads were washed three times with 1x IP buffer and all the supernatant was removed after third wash. 40µl 2x SDS buffer was added and samples were boiled at 95°C for 3 min and spun down.

(iv) Resolving SPO11-oligo complexes by SDS-PAGE and quantifying signal using a phosphor imaging plate:

25µl of each sample was loaded on an 8% SDS-PAGE gel and ran at 150 V for 1 hr 10 min. The gel was transferred to a PVDF membrane using a semi-dry transfer-

method (Bio-Rad). The membrane was air-dried for 15 min, wrapped in plastic wrap and exposed to a phosphor imaging plate overnight. Radiolabeled species were quantified using ImageGauge software to determine relative signal in experimental samples after subtracting signal in *Spo11-/-* control sample.

(v) Western blot detection of free SPO11 (not bound to oligos):
Western blot analysis using SPO11-antibody was performed as described in section 2.9, with the following amendments. Antibody Spo11-180 was used as the primary antibody diluted 1: 2000 in PBS-0.1% Tween 20. Anti-protein A-HRP (Abcam; ab7456) was used as the secondary antibody diluted 1: 10000 in PBS-0.1% Tween 20. HRP signal was detected using ECL Prime (GE healthcare).

(6) Deproteinization and resolution of oligos on a sequencing gel:
To the remaining eluate, 200µl of proteinase K buffer (100 mM Tris-HCl, pH 7.4, 0.5% SDS, 1 mM EDTA, 1 mM $CaCl_2$) and 50µg proteinase K was added and incubated overnight at 50^{o}C in Thermomixer shaking at 300 rpm. Samples were transferred to a Spin-X column, spun for 2 min at maximum speed and transferred into siliconised tubes. 0.3 volumes 9 M ammonium acetate, 10µg glycogen, and 2.5 volumes 100% ethanol was added to precipitate the DNA and samples were incubated at -20^{o}C overnight. Centrifugation was performed three times at 13,200*g* at 4°C for 15 min, rotating tubes between spins and then the supernatant was carefully removed without disrupting the pellet. 250µl of cold 70% ethanol was added to each tube and spun at 13,200*g* in a centrifuge for 1 min. Supernatants were removed very carefully and pellets air-dried for 10 min. 20µl of 2x formamide buffer (80% deionized formamide, 10 mM EDTA, pH 8.0, 0.5 mg/ml xylene cyanol FF, 10% saturated bromophenol blue) was added and incubated at 37°C for 20 min with constant mixing to dissolve pellet. After boiling samples for 3 min and incubation on ice, sample were spun down and loaded onto a 15% sequencing gel. After running the gel, it was fixed by incubating it in 10% methanol: 7% acetic acid: 83% distilled water for 10 min, transferred to distilled water and incubated for 10 min. The gel was vacuum-dried onto a piece of cellulose paper backed by a piece of DE81 ion exchange paper (GE healthcare). Finally this was exposed to a phosphor imaging plate overnight and ImageGauge software was used to determine the distribution of oligo lengths

Chapter 3. Conditional meiotic models of ATR-deficiency

ATR is one of three serine/threonine kinases that sense DNA damage and initiate cellular responses via DDR signalling. ATR, ATM and DNA-PK/PRKDC (hereafter PRKDC) belong to the highly conserved PIKK protein family (Perry and Kleckner, 2003). Mutant mice have been generated for both ATM and PRKDC previously. Analyses of *Atm -/-* mice (Barlow et al., 1998) implicate ATM in several meiotic functions including DSB formation, histone H2AX phosphorylation (Bellani et al., 2005) and regulating CO-formation (Barchi et al., 2008). Mice hypomorphic for *Prkdc*, the gene encoding the catalytic domain of PRKDC, are fertile and meiosis is normal (Bellani et al., 2005). ATR is present throughout mammalian meiosis, suggestive of important meiotic functions. Early in prophase I, at leptonema, ATR is found at meiotic DSBs, later in mid-zygonema ATR marks asynaptic chromosomes before transitioning to the chromatin of asynaptic chromosomes in mid-pachynema (Moens et al., 1999, Keegan et al., 1996).

The loss of ATR results in embryonic lethality; *Atr -/-* mutant mouse embryos are unable to develop beyond 3.5 d*pc* as cells within the mutant blastocysts cannot proliferate successfully (Brown and Baltimore, 2000). Therefore, to determine the roles of ATR, it is necessary to overcome the embryonic lethality using conditional alleles. In 2003, *Atr -/-* cells were generated and analysed *ex vivo* using a *loxP/Cre* condition mutant system (Brown and Baltimore, 2003). In 2007, the same *loxP/Cre* system was used *in vivo* (Ruzankina et al., 2007). Relevant to my thesis, these two studies revealed that ATR is required for the proliferation of cells with high turnover, including those in the testis, and that an exogenous DNA damage checkpoint arrest persists in *Atr -/-* and *Atr -/- Atm -/-* cells. Most importantly these studies demonstrated that *loxP/Cre* in combination with *Atr flox* could be used to conditionally delete ATR in the testes.

Another study reported reduced testis size in mice homozygous for a hypomorphic *Atr* allele (Murga et al., 2009). Using the same experimental system as the Ruzankina et al. (2007) study, our lab in 2013 examined the role of ATR in meiotic

sex chromosome inactivation (MSCI). Royo et al. (2013) found that ATR is required for MSCI, having shown previously that MSCI is essential for male fertility (Royo et al., 2010). After tamoxifen treatment, the *Cre-ERT*^{2} functionally expresses CRE-recombinase in all cell types (Matsuda and Cepko, 2007). After optimisation of different tamoxifen treatment regimes, it was found that a five-day tamoxifen treatment led to highly depleted ATR levels and resulted in MSCI failure in the testes of *Atr flox/-, Cre-ERT*^{2} adult males (Royo et al., 2013). This study further demonstrated that ATR is required to recruit other essential MSCI effector proteins including TOPBP1 and MDC1, and to phosphorylate histone H2AX (Royo et al., 2013).

This study demonstrated that the pachynema sub-stage of prophase I was amenable to tamoxifen-mediated recombination of *Atr-flox* and subsequent loss of ATR protein. However, this tamoxifen treatment was unsuccessful at depleting ATR levels in earlier meiosis. Firstly, it was not possible to discriminate potential ATR-dependent phenotypes in earlier sub-stages from secondary damage arising from the apoptotic pachytene cells. This is because in the adult testis within each tubule there are multiple simultaneously developing sub-stages from different waves of meiosis (see Introduction section 1.1.1 for further details). Secondly, since the *Cre-ERT*^{2} transgene is active in all cell types, ATR was being deleted throughout the animal after tamoxifen treatment. Amongst other cofounding effects, this would disrupt the essential Sertoli cell-germ cell relationships in the adult testis. It has been shown previously that genetic disruption of Sertoli cells leads to extensive germ cell loss (Rebourcet et al., 2014). Therefore, it was decided that a germ cell-specific rather than a ubiquitously active and inducible *Cre-line* might be necessary to examine the roles of ATR throughout meiotic prophase I.

Therefore the primary aim of this chapter is to develop and test three *Atr flox/-, Cre-driver* lines for their suitability to model ATR-deficiency in mammalian meiosis. The requirements for ATR in the developing testis are unknown, therefore it is vital that I determine whether a temporally suitable *Cre*-driver line can be found. The *Cre-driver* must be capable of removing a floxed-allele of the *Atr* gene in restricted cell types to prevent confounding phenotypes from ATR loss in non-meiotic cells. The

second aim is to determine the robustness of ATR knockdown in the three models in comparison to the previously published study (Royo et al., 2013).

3.1 *Atr* deletion causes spermatogenic defects

Mammalian spermatogenesis is highly regulated: the germ cell populations migrate and divide along the basal-apical axis of seminiferous tubules with well-characterised timing (Oakberg, 1956). The original spermatogenesis classification system divides seminiferous tubules into twelve distinct stages based upon the development of spermatids (See Introduction 1.1.1.). It has since been adapted so that staging is possible in meiotic mutants that lack spermatids (Meistrich and Hess, 2013, Ahmed and de Rooij, 2009).

The three chosen *Cre*-driver lines would in principle conditionally remove ATR at different stages in germ cell development (Fig 3.1A). *Ddx4-Cre* activity begins embryonically at around 15 d*pc* (Gallardo et al., 2007). Therefore, under this CRE, ATR levels would be reduced prior to the onset of male meiosis. *Stra8-Cre* becomes active later at 3 d*pp* (Sadate-Ngatchou et al., 2008) when germ cells re-enter the cell cycle prior to meiosis (Bellve et al., 1977). This *Cre*-driver line is recommended to examine the function of essential meiotic genes (Smith, 2011). The activation of *Ngn3-Cre* also occurs after birth, at approximately 7 d*pp* in the mitotically dividing spermatogonia, as well as in other stem cell progenitors (Zheng and Wang, 2012, Schonhoff et al., 2004).

In this chapter I use contracted genotypes (Fig 3.1B). I use "*Atr -/-*" to denote the genotype *Atr flox+/-, Cre+.* "*Atr wt*" is the control, with the genotype *Atr flox+/+, Cre+.* Finally, mice without the *Cre* transgene are called wildtype ("*wt"*) and have genotypes *Atr flox+/+, Cre-* and *Atr flox+/-, Cre-.*

Relevant to this chapter, it is generally agreed that defective spermatocytes cells arrest at three stages: during the spermatogonial divisions (pre-meiotic block), during meiosis at either stage IV (corresponds to pachynema in prophase I) or

during stage XII (corresponds to metaphase I). Mice with defects in spermatogenesis experience germ cell death and testis atrophy.

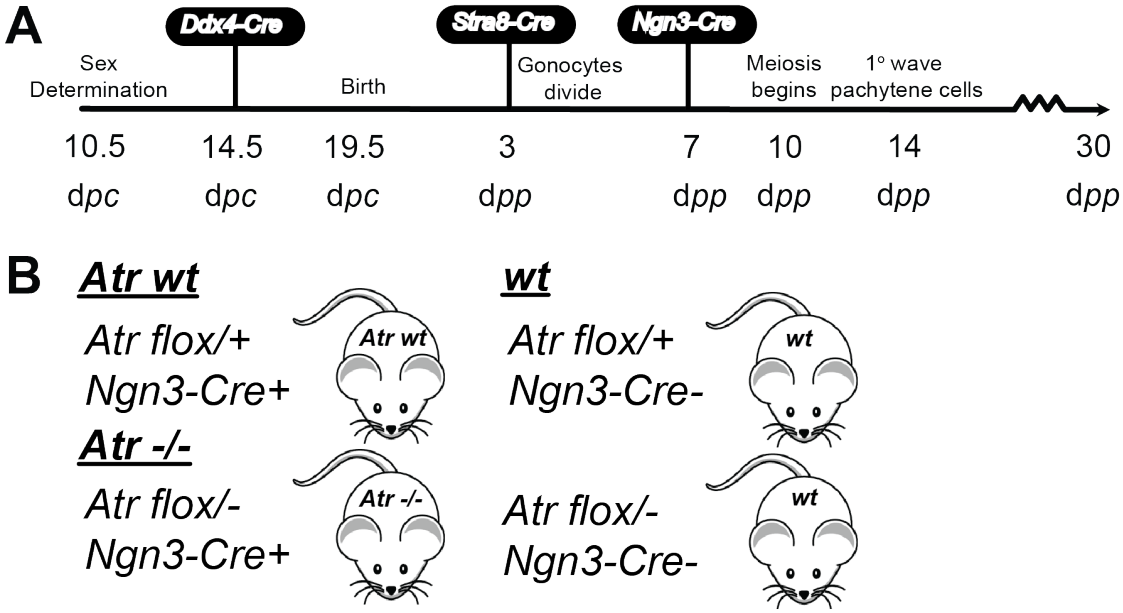

Figure 3.1 Genetic strategy for the conditional ablation of *Atr*

Timeline of male germ cell development. (**A**) Timings and key events are indicated. Black lollipops denote the onset of the expression of each CRE. (**B**) Schematic of the three contracted genotypes in this study *Atr wt*, *Atr -/-* and *wt*.

It was clear whilst harvesting testes at 30 d*pp* that the testes of some genotypes were highly reduced in size relative to other genotypes, independent of mouse body weight. This finding was consistent for all three *Cre*-lines (A) *Ddx4-Cre*, (B) *Stra8-Cre* and (C) *Ngn3-Cre* (Fig 3.2). The testes weights of the *Atr* wt controls were comparable to *wt* mice, indicating that the *Cre* transgenes did not cause a dominant negative effect. I therefore grouped these genotypes together. Most importantly, across (A) *Ddx4-Cre*, (B) *Stra8-Cre* and (C) *Ngn3-Cre* litters, the mice genotyped as *Atr -/-* had statistically significantly reduced testis weights (p-values: (A) 0.0035, (B,C) < 0.0001 respectively; unpaired t-test). Examining the histology of the three *Cre*-lines provided more precise details of the defects in germ cell development.

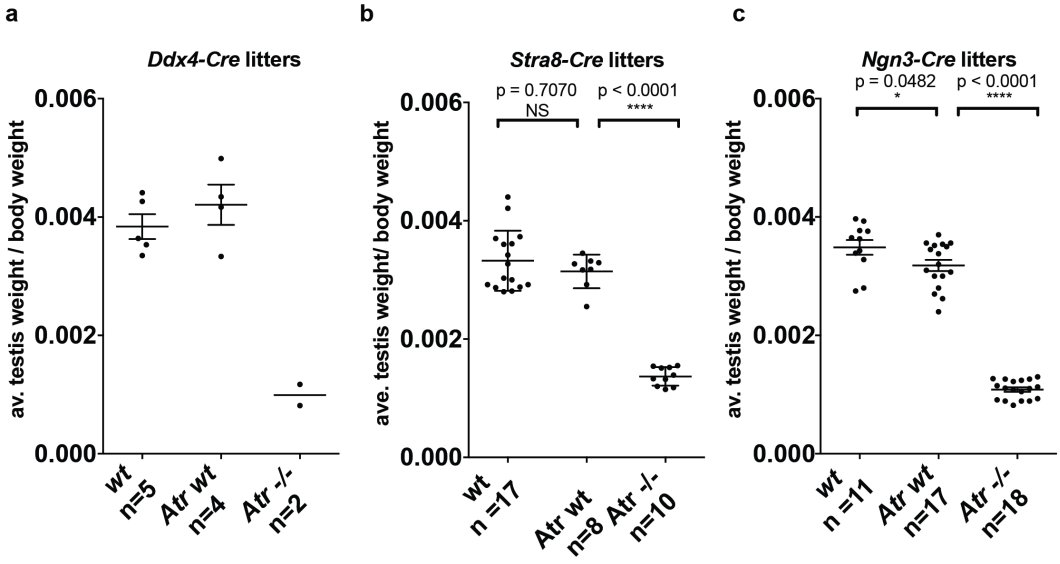

Figure 3.2 *Atr -/-* mice have reduced testis weights relative to other genotypes

To make a normalised comparison testis weight between genotypes and strains, the combined testis weight in grams accurate to 3 decimal places (dp) was mean averaged, then divided by the body weight of mice in grams accurate to 2 dp. Normalised testis weight are presented from **A**) Mice from *Ddx4-Cre* litters aged 30-60dpp. (**B**) Mice aged 30 dpp from *Stra8-Cre* litters. (**C**) Mice aged 30 dpp from *Ngn3-Cre* litters. n = mice of each genotype. Error bars are the standard deviations (SD). P-values in (**B-C**) are from Mann-Whitney test are indicated. N.B. P-vaules were not calculated for (A) as fewer animals were collected, over a larger age window preventing statistical analysis.

Normal spermatogenesis could be seen in histology of *Atr wt* and *wt* samples from the three *Cre*-driver lines: *Atr wt*, *Ddx4-Cre* (n=3; Fig 3.3A), *Atr wt, Stra8-Cre* (n=3; Fig 3.3C), and *Atr wt Ngn3-Cre* (n=3; Fig 3.3E). In contrast, *Atr -/-* samples had visible germ cell defects and overall tubule size was reduced. Seminiferous tubules from *Atr -/-, Ddx4-Cre* males (n=2; Fig 3.3B) contained no meiotic cells. Instead, tubules contained only early active A-type spermatogonial and supporting somatic cells, like Sertoli cells. Therefore, this *Cre*-driver line creates a pre-meiotic block. This clearly shows that ATR has essential roles in germ cells prior to meiotic entry. This block prevented the investigation of meiotic phenotypes; hence this *Cre*-driver was not examined further.

The seminiferous tubules from *Atr -/-, Stra8-Cre* animals (n=4; Fig 3.3D) contained meiotic cells with typical condensed purple thread-like chromosomes. Therefore despite the conditional inactivation of *Atr* from 3 d*pp,* cells are able to enter

subsequent rounds of meiosis. Consistent with ATR having important roles in meiosis, it was evident that there was a problem in prophase I. The majority of meiotic cells failed to progress beyond pachynema; these blocked cells were hyperpigmented, a clear sign of germ cell death. Germ cell elimination is caused by activated checkpoint mechanisms. I found that the elimination began at stage IV. A stage IV block also occurs in other meiotic mutants with activated checkpoint mechanisms like *Dmc1 -/-* and *Spo11 -/-* (Ahmed and de Rooij, 2009, Pittman et al., 1998, Baudat et al., 2000, Romanienko and Camerini-Otero, 2000). Nevertheless, there were some post-meiotic cells, including spermatids, present in *Atr -/-, Stra8-Cre* males. Given that *Atr -/-, Cre-ERT*^{2} males have a robust stage IV block due to MSCI failure (Royo et al., 2013), surviving spermatids in *Atr -/-, Stra8-Cre* males likely retained sufficient ATR to successfully complete MSCI. The testes of *Atr -/-, Ngn3-Cre* (n=6) mice also contained abundant meiotic cells (Fig 3.3F). All pachytene cells in tubules at stages IV-VI had signs of elimination (Fig 3.3F). In contrast to findings in *Atr -/-, Stra8-Cre* males, no more developmentally advanced germ cells were detected. Therefore, conditionally deleting ATR at 7 d*pp* appears sufficient to create *Atr*-deficient meiotic cells.

In summary, the testis weight and histology of *Atr wt* mice were consistent with normal spermatogenesis, whereas *Atr -/-* mice all had testicular atrophy and germ cell defects. These defects occurred either pre-meiosis (*Atr -/-, Ddx4-Cre*) or during pachynema of prophase I (*Atr -/-, Stra8-Cre and Atr -/-, Ngn3-Cre*). Given that the focus of this thesis is to characterise the roles of ATR in meiosis, I decided to proceed with qualitative assessment of *Atr -/-, Stra8-Cre and Atr -/-, Ngn3-Cre* mice.

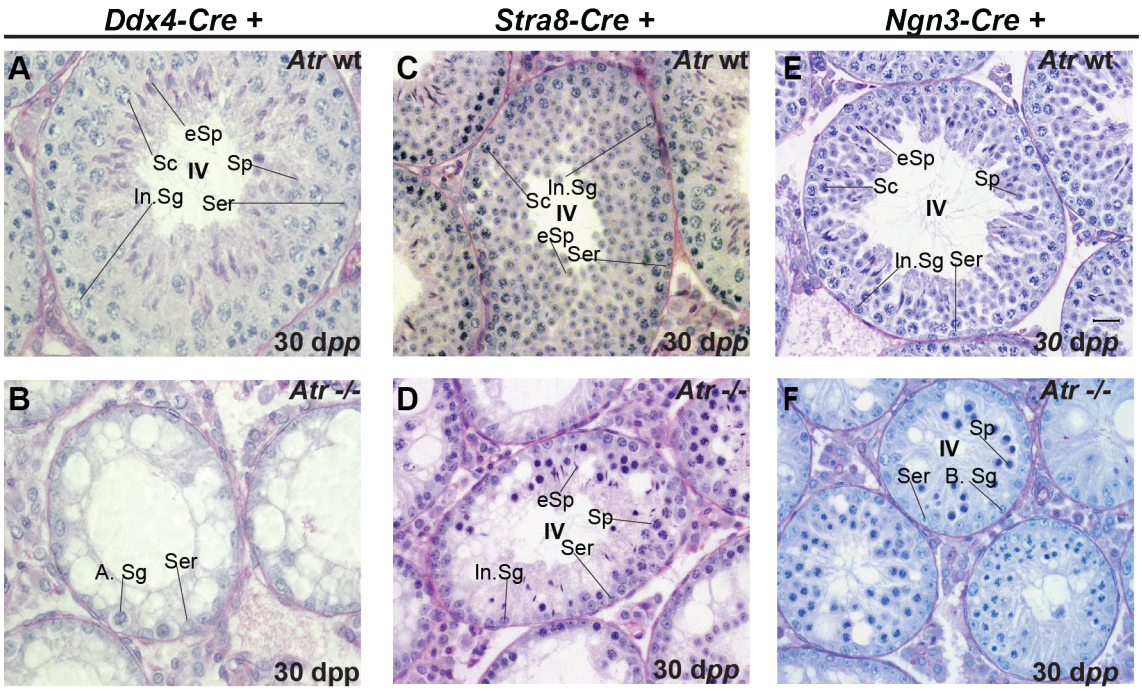

Figure 3.3 Germ cell defects in *Atr*-deficient *Cre*-driver mice

Testis cross-sections of five micron thick were stained with Periodic-acid Schiff to allow accurate staging *N.B.* the incorporation of the dye can vary giving colour variation. In *Atr wt* genotypes (**A**, **C** and **E**) spermatogenesis is normal and very comparable. The indicated stage IV seminiferous tubules have characteristic dividing intermediate spermatogonia (In.Sg) and Periodic-acid Schiff positive staining acrosomes in the round spermatids (Sp). Later elongating spermatids (eSp), normal meiotic cells or primary spermatocytes (Sc) and supporting Sertoli (Ser) cells are also shown. (**B**) *Atr -/-, Ddx4-Cre* tubules lack meiotic cells. Only Sertoli cells and a pre-meiotic A spermatogonium (A. Sg) are present in the labelled tubule. (**D**) *Atr -/-, Stra8-Cre* tubules have a full complement of germ cells prior to stage IV, however the indicated stage IV tubule shows many apoptotic spermatocytes. Not all meiotic cells are apoptotic and therefore later elongating spermatids can be seen. (**F**) In *Atr -/-, Ngn3-Cre* tubules at stage IV, all the spermatocytes appear to undergo apoptosis, with no subsequent cell types present.

3.2 ATR levels are globally reduced in *Atr-/-* testes

To confirm that the testis defects of *Atr -/-* animals arose from reduced ATR levels, I carried out western blots. This enabled a quantitative assessment of the levels of ATR in each *Atr -/-* line relative to the *Atr wt* control, after considering GAPDH loading controls. I first performed western blotting on the *Ddx4-Cre* line, where cells were not entering meiosis (Fig 3.4A). ATR levels were reduced in the *Atr -/-, Ddx4-Cre* relative to *Atr wt, Ddx4-Cre* testes. I conclude that the residual level of ATR was likely to be insufficient for the additional mitotic divisions needed before the onset of meiosis.

Next, I compared ATR levels in the *Stra8-Cre* and *Ngn3-Cre* lines (Fig 3.4B). Notably, less ATR was present in *Atr -/-, Stra8-Cre* than in *Atr wt, Stra8-Cre* testes. However, a clear ATR band was retained in *Atr -/-, Stra8-Cre* males. In the *Atr -/-, Ngn3-Cre* sample there was little or no remaining ATR expression. Levels of ATR in *Atr wt, Ngn3-Cre* appeared similar to other *Atr wt* lines.

In summary, these data demonstrate that *Stra8-Cre* and *Ngn3-Cre* are suitable for depleting ATR in the testis and that the resulting ATR depletion is the likely cause of the observed testis defects. The differences between the *Atr -/-, Stra8-Cre and Atr -/-, Ngn3-Cre* testis phenotypes can be at least partially explained by the residual ATR expression in *Atr -/-, Stra8-Cre* and suggests that in these mutant individuals *Atr* is not being uniformly removed in all spermatocytes. *Stra8-Cre* is commonly used in studies of mouse meiosis (Lyndaker et al., 2013). Since *Atr -/-, Ngn3-Cre* males represent a superior model of meiotic *Atr*-deficiency, I decided to use this model for subsequent sections.

I hypothese that the difference in the amount of residual ATR between *Atr -/-, Ddx4-Cre* + and *Atr -/-, Ngn3-Cre* + could be explained by *Atr -/-, Ddx4-Cre* + accumulating ATR for the spermatogonial stem cell divisions, prior to arrest phenotype at the A-spermtogonia stage seen by histology. Since *Atr -/-, Ngn3-Cre* + cells seems to enter meiosis normally, it seems they negotiated the period of accumulated ATR and consequently no residual ATR band is seen.

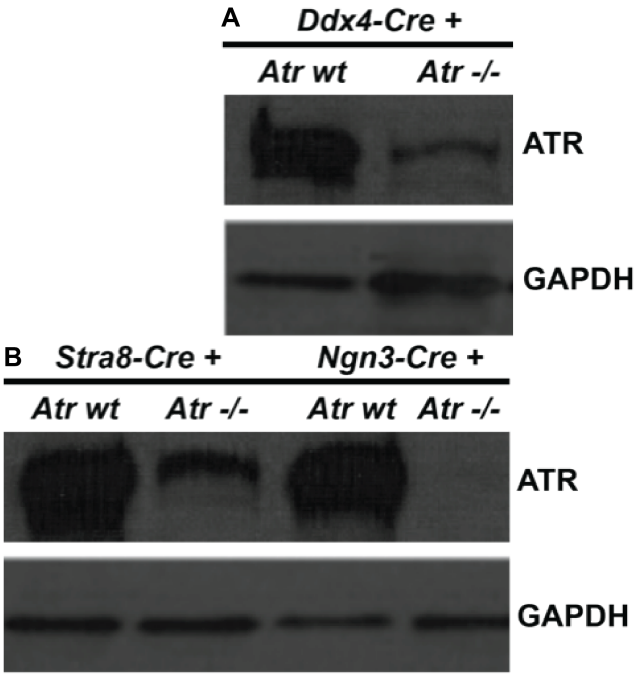

Figure 3.4 Conditional deletion of *Atr* can be seen in anti-ATR western blots

20 µg of whole testis lysate was loaded from mice aged 30 d*pp.* (**A**) In the prenatally active germ cell specific *Cre*-driver, *Ddx4-Cre,* line an ATR band can be seen in both *Atr wt*, *Ddx4-Cre* and *Atr -/-, Ddx4-Cre.* (**B**) Postnatally active *Cre*-driver lines also contain an ATR band for the *Atr wt* samples, however relative abundance of the bands differs between Atr *-/-, Stra8-Cre (*leaky and germ-cell specific*)* and *Atr -/-, Ngn3-Cre* (robust, but also expressed in other stem cell types) samples.

3.3 Verification of ATR depletion in *Atr -/-*, *Ngn3-Cre* by IF

Meiotic prophase is highly dynamic part of gametogenesis, as a result of result of the large-scale chromosome changes. Both the role and location of some molecules change between meiotic sub-stages. This can be seen as changes in their nuclear localisation by using IF to assses protein localisation. Fittingly, anti-SYCP3 staining is commonly used to identify the different prophase I sub-stages as SYCP3 is an essential component of the SC whose staining pattern changes considerable between each meiotic sub-stage (Yuan et al., 2000). The classification system I used to accurately stage prophase cells throughout this thesis was adapted from Barlow et al., (1998) and is described in Table 3.1.

Table 3.1 Classifying meiotic sub-stages based on SYCP3 staining

Stage	Wildtype staining pattern
Leptonema	Nuclei have short SYCP3 positive axes that have started to elongate. These axes are only univalent thickness, having not begun to synapse with homologous chromosomes.
Zygonema	Synapsis between homologous chromosomes is progressively achieved (Bellve et al., 1977). Within a nucleus it is common for the synapsis of bivalents to be asynchronous, visible from the bimodal thickness of SYCP3 staining i.e. synapsed axes are twice the thickness of asynapsed axes.
Pachynema	Nuclei have achieved full synapsis along the entire chromosomal axes of the autosomes by early pachynema; therefore all autosomal axes are twice the thickness of the non-homologous regions of the X and Y chromosomes.
Diplonema	The chromosomal axes of the bivalents begin to desynapse. Beginning at the telomeres, small bulges of SYCP3 appear before desynapsis progresses along the entire length of the axes, except at chiasmata.

Previous studies found that the recruitment of ATR is also dynamic during meiotic prophase I (Barlow et al., 1998, Daniel et al., 2011, Wojtasz et al., 2009, Moens et al., 1999, Keegan et al., 1996). Therefore, I initially examined the localisation of ATR in *Atr wt* using IF with an ATR antibody (Fig 3.5). In *Atr wt* cells during late leptonema (Fig 3.5A) ATR staining was visible as discrete foci in 85.00% of cells (n=20). At this stage, it is marking the recently formed meiotic DSBs (Burgoyne et al., 2007). Later, in zygonema, 82.14% (n=28) of *Atr wt* cells had ATR staining. I found that during this stage, ATR staining transitions from a focal DSB-pattern (Fig 3.5C) to a linear pattern restricted to the unpaired axes until homologous chromosomes synapse in pachynema. I observed that 100.00% (n=30) of *Atr wt* cells had ATR staining on the non-homologous regions of the XY bivalent in pachynema (Fig 3.5E).

I then determined whether ATR was detectable in *Atr -/-, Ngn3-Cre* meiotic cells. In leptotene cells there was no ATR staining (n=21; Fig 3.5B). Similarly, zygotene cells (n=30) lacked detectable ATR staining (Fig 3.5D). Finally, in early pachynema, ATR was not detectable on the XY bivalent in the *Atr -/-* cells (n=32; Fig 3.5F). Early pachynema was the last comparable stage between *Atr -/-* and *Atr wt* due to the complete mid-pachytene stage IV block in *Atr -/-, Ngn3-Cre* cells.

In conclusion, I observed stage-specific ATR staining in *Atr wt,* as has been described previously (Plug et al., 1998, Keegan et al., 1996). ATR is not visible in *Atr -/- , Ngn3-Cre* cells at any of the three examined prophase I sub-stages. Therefore, if any ATR remains it is below the levels of detection by IF. This extent of ATR depletion is better than that achieved using the inducible *Cre-ERT*^{2} approach (Royo et al., 2013). Therefore, I have created a model of *Atr*-deficiency in leptonema, zygonema and early pachynema to allow the elucidation of the meiotic roles of ATR throughout mammalian meiotic prophase.

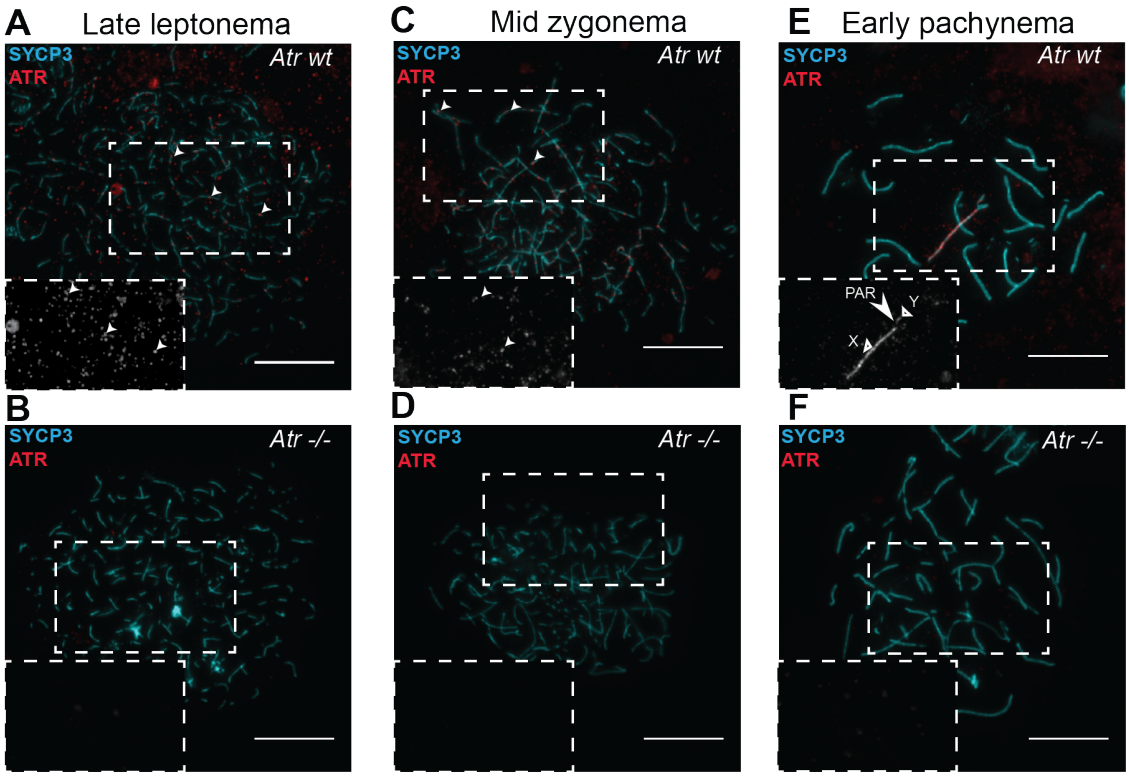

Figure 3.5 *Atr -/- Ngn3-Cre* conditional mice lack sub-stage specific ATR-staining in early prophase

(**A**) ATR is first observed as foci in late leptonema and is thought to be recruited to DSBs as they are formed. I have marked representative DSBs in each panel with filled triangular arrowheads. Inserts contain the regions of interest denoted by the dotted rectangle. Single-channel signal corresponding to ATR is presented in greyscale. (**C**) Simultaneously, DSBs are repaired and homologous chromosomes synapse. ATR staining transits from a focal DSB-like staining to a linear axial staining of unpaired chromosomes in zygonema. (**E**) In early pachynema the constitutively unsynapsed non-homologous regions of the X- and Y-chromosomes have linear ATR staining. In contrast, the paired homologous pseudoautosomal region (PAR) (pointy arrowhead) does not have ATR staining. In all stages (**B**, **D**, **F**), *Atr -/-* cells do not have ATR staining. Scale bar 10 μm.

3.4 Conditional deletion of ATR impairs MSCI

Previously, using *Atr -/-, Cre-ERT*^{2} mice, it was shown that ATR phosphorylates variant histone H2AX at serine-139 (γH2AFX) during pachynema on the non-homologous region of the X and Y chromosomes (Royo et al., 2013). This phosphorylation is required for MSCI (Turner et al., 2004, Turner et al., 2005, Fernandez-Capetillo et al., 2003). The depletion of ATR drastically reduced γH2AFX accumulation on the sex chromosomes and caused MSCI to fail. This subsequently led to a de-repression of X- and Y-linked genes. Experimentally, this de-repression was demonstrated using gene-specific RNA-FISH for the X-linked gene *Scml2* (Royo et al., 2013). *Scml2* expression was observed in 97% of pachytene cells in *Atr -/-, Cre-ERT*^{2} mice (Royo et al., 2013). I therefore used analysis of γH2AX staining and then *Scml2* RNA-FISH to examine consequences of ATR loss on MSCI in *Atr -/-, Ngn3-Cre* and *Atr -/-, Stra8-Cre* mice.

In independent experiments I found that both *Atr wt* strains have normal staining on the XY in pachytene forming a “cloud” coating the chromatid of non-homologous region of the sex chromosomes. In *Atr wt, Stra8-Cre* males 95% of cells (n=45) had anticipated staining (image not shown). Similarly, in *Atr wt*, *Ngn3-Cre* males, 100% of cells (n=29) had abundant γH2AX staining (image not shown). In the absence of ATR, the majority of cells from *Atr -/-, Stra8-Cre* males, (74%; n=78; Fig 3.6A) did not have normal γH2AX associated with the sex chromosomes. Abnormal γH2AX staining ranged from partial coating of the XY, to a complete deficiency of γH2AX; whilst the remaining 26% of cells had XY γH2AX staining that was indistinguishable from wild type cells (Two cells shown in Fig 3.6A). In all examined pachynema cells from *Atr -/-, Ngn3-Cre* males, γH2AX was undetectable in 100% of cells (n=30; Fig 3.6.B). In summary, I conclude that based on γH2AX staining associated with the sex chromosomes, MSCI is significantly impaired without ATR. This is more severe in *Atr -/-, Ngn3-Cre* than in *Atr -/-, Stra8-Cre* males and may account for differences observed by histology (Section 3.1).

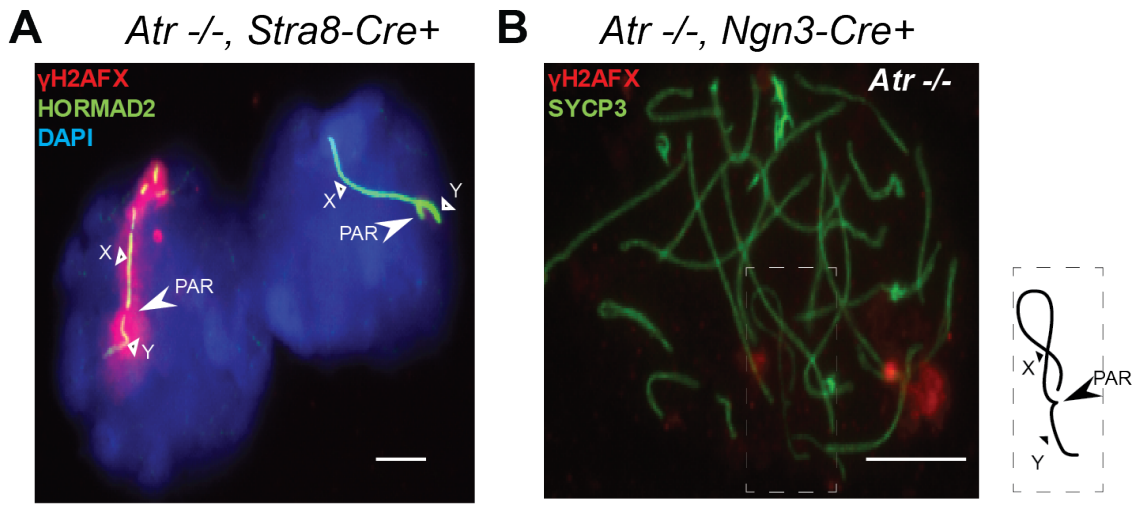

Figure 3.6 The loss of γH2AX in *Atr -/-* supports the failure to silence the X and Y

During early pachynema, after the majority of autosomes have synapsed and the sex chromosomes begin to move towards the periphery of the cell, prior to forming a distinct sex body in midpachynema. These data and images are from two separate experiments, to identify the sex chromosomes in (A) Anti-HORMAD2 was used which marks the non-homologous sex bivalents. In the representative image, the extent of γH2AX seen in the left cell is comparable to a *wt* cell. In contrast the right cell is devoid of γH2AX, except for a residual staining at the PAR (white chevron arrowhead). One would not expect the PAR to recruit γH2AX since it is homologous and synapsed. The X and Y indicated with white arrowheads. I did not stain with Anti-HORMAD2 in the experiment used to generate (B). Therefore to identify the sex chromosomes here one is reliant on the thickness of SYCP3 stained axes; synapsed axes are twice as thick as univalent axes. In the representative A*tr -/-, Ngn3-Cre* cell there is no specific γH2AX (A schematic representation of the sex bivalent is shown in the inset and labelled). Any remaining γH2AX signal is likely to be unspecific background staining. Scale bar, 10 μm

To examine if X-linked RNAs are being transcribed during meiosis in *Atr -/-, Ngn3-Cre* males, I first performed RNA-FISH in *Atr wt* zygotene and pachytene cells . I chose the X-gene *Scml2*, since it is robustly expressed in zygonema and early pachynema cells, but silenced after MSCI is established (Wojtasz et al., 2012). I used anti-HORMAD2 to identify cells as being in zygonema or pachynema. During zygonema, HORMAD2 marks pre-synaptic axes; whilst later during early pachynema it marks unsynapsed regions of the X and Y chromosomes. In validation of the approach, *Scml2* expression could be seen in zygotene cells from *Atr wt* (Fig 3.7A). Due to the repressive conditions imposed by MSCI later in pachynema, *Atr wt* cells lack *Scml2* RNA foci (Fig 3.7B). Like controls, in zygotene *Atr -/-* cells, *Scml2* expression could be seen (Fig 3.7C). Importantly, in early pachynema, *Atr -/-* cells contained *Scml2* foci, indicating that MSCI had failed (Fig 3.7D).

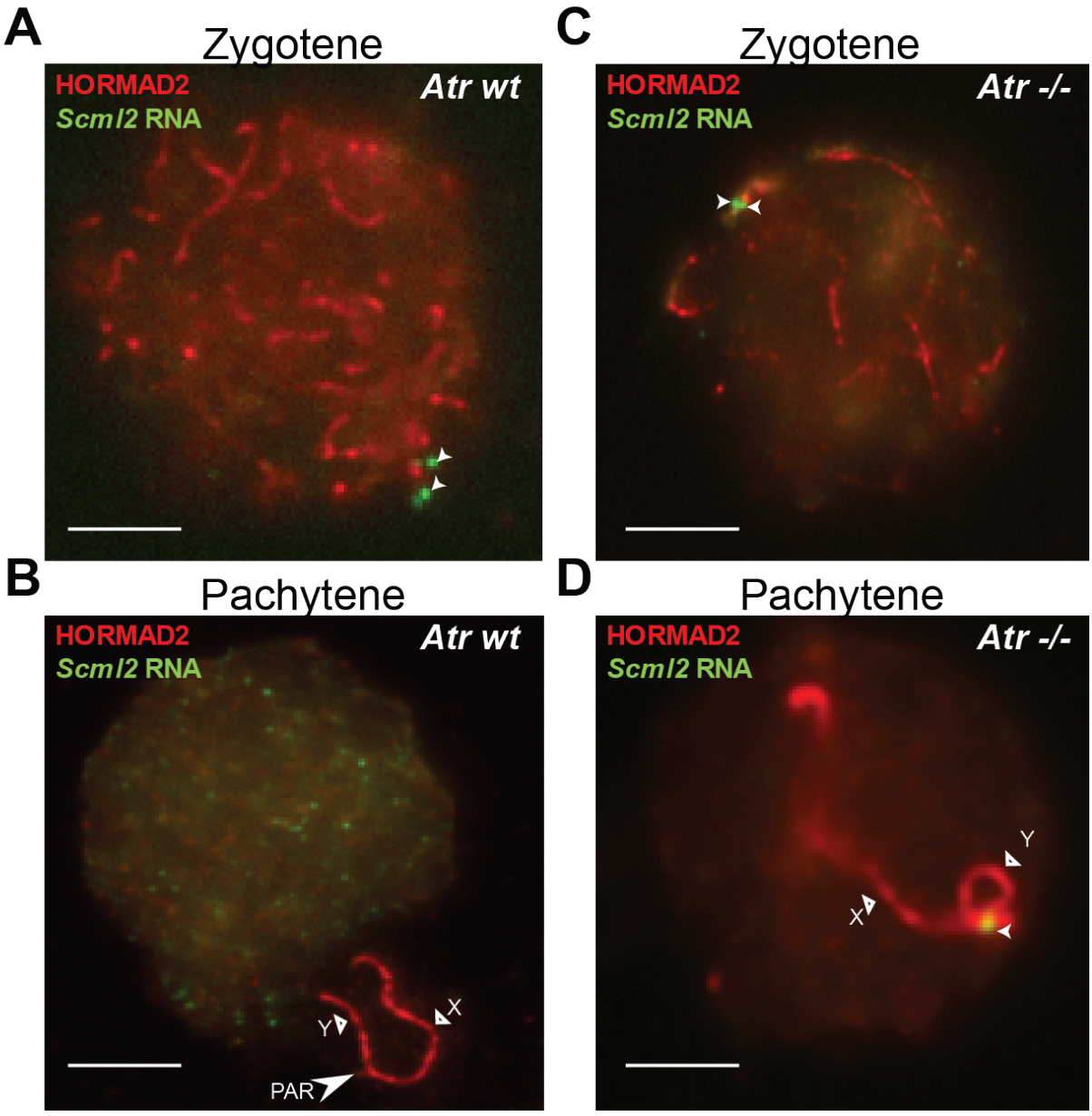

Figure 3.7 The loss of ATR causes MSCI-failure and inappropriate expression of *Scml2* in pachynema

The transcription of *Scml2* early in meiotic prophase is unaffected by the loss of ATR. Consequently in (**A and C**) zygotene cells that are from *Atr wt* and *Atr -/-* animals have focal *Scml2* signal (small arrowheads) that residue on the chromosome axes (positive for anti-HORMAD2) However due to the repression conditions imposed by MSCI in wildtype cells no *Scml2* should be expressed. It has been established that ATR is required for MSCI; therefore consistent with these assumptions and findings: respectively, I observed that (**B**) *Atr wt* pachytene cells did not express *Scml2; in* (**D**) In *Atr -/-* cells, *Scml2* RNA foci can be seen, indicative of depression of MSCI-caused conditions (open arrowheads). PAR = pseudoautosomal region. Scale bar ,10µm.

3.5 Discussion

The aim of this chapter was to evaluate three different *Cre*-driver lines for their suitability to conditionally deplete ATR in the testis. The data presented demonstrate that the three *Cre*-driver lines are active in the male germline. In contrast to previous work (Royo et al., 2013), this allowed the investigation of *Atr*-dependent phenotypes without the administration of tamoxifen. Germ cells from the three *Atr -/-* strains arrested either prior to meiosis or during meiotic prophase I.

Deletion of ATR using *Ddx4-Cre* revealed that ATR is required to permit meiotic entry. This suggests that ATR is likely required for S phase in mitotically dividing spermatogonia, as it is in other rapidly dividing cells (Brown and Baltimore, 2003, Ruzankina et al., 2007). Consequently, *Ddx4-Cre* cannot be used to uncover the role of ATR in meiosis.

Crucially, meiotic cells were present in the *Atr -/-, Stra8-Cre* and *Atr -/-, Ngn3-Cre* strains. Further observations were able to account for phenotypic differences between *Atr -/-, Stra8-Cre* and *Atr -/-, Ngn3-Cre* males. Other studies have found that *Stra8-Cre* is not completely efficient at excising floxed alleles of essential genes for meiotic recombination, including *Rad9a* (Vasileva et al., 2013) and *Hus1* (Lyndaker et al., 2013). In contrast, a previous study found *Ngn3-Cre* to be a highly effective meiotic *Cre*-driver (Zheng and Wang, 2012). Consistent with these findings, using western blots I found that ATR protein levels were lower in testes from *Atr -/-, Ngn3-Cre* than *Atr -/-, Stra8-Cre* males. Also, using IF and RNA-FISH, I found that the MSCI phenotypes in *Atr -/-, Stra8-Cre* males were not as penetrant as those in *Atr -/-, Ngn3-Cre* males. *Atr -/-, Ngn3-Cre* males had a comparable MSCI phenotype to *Atr -/-, Cre-ERT*^{2} mice (Royo et al., 2013). However, *Atr -/-, Ngn3-Cre* males are probably superior to the *Cre-ERT*^{2} model because in *Atr -/-, Ngn3-Cre* males I found that ATR was absent throughout meiotic prophase by IF. In conclusion, I will use the *Atr -/-, Ngn3-Cre* model for my later meiotic analysis.

Chapter 4. The roles of ATR in meiotic chromosome dynamics

In the previous chapter, I demonstrated that *Atr -/-, Ngn3-Cre* (hereafter referred to as *Atr -/-*) is a suitable model to elucidate the meiotic roles of ATR in mice. In this chapter, I determine whether ATR is required for the essential chromosomal dynamics in meiosis that enable meiotic recombination and accurate chromosome segregation.

The repair of meiotic DNA DSBs requires the maternal and paternal homologs to interact, enabling a homology search to identify suitable templates for repair (Baudat et al., 2000). Stable interactions between homologs result in deposition of the SC in a process known as synapsis (Zickler and Kleckner, 2015). As well as the SC, it is known that many other protein complexes, including cohesins, contribute to the highly complex and dynamic structure of meiotic chromosomes (Page and Hawley, 2004). Analysis of the architecture of meiotic chromosomes in different model organisms has found that the chromatin is organised into linear arrays of loops with evolutionarily conserved spacing (Kleckner, 2006). Due to the interdependent relationship between meiotic chromosome dynamics and meiotic recombination, genetic disruption of components of meiotic chromosomes can result in multiple meiotic phenotypes (Zickler and Kleckner, 2015). A comprehensive understanding of structure and function of meiotic chromosome dynamics is still missing, despite more than six decades of research (Fawcett, 1956).

Previous studies of *Atr*-orthologs do not describe whether ATR has an important role in meiotic chromosome dynamics. Therefore, my first objective is to determine whether meiotic chromosome structure is normal in *Atr -/-* cells and whether the loss of ATR impacts homologous synapsis. In mice, recombination and synapsis are interdependent. My second objective is to determine whether any effect on synapsis is altered in the absence of meiotic recombination. Finally, I investigate the localisation of important SC proteins and the phosphorylation of cohesin component SMC3.

4.1 ATR regulates homologous chromosome synapsis

In both mice and budding yeast, DNA DSB formation occurs in leptotene cells before synapsis (Mahadevaiah et al., 2001). SC proteins SYCP2 and SYCP3 are initially recruited to the base of meiotic chromosomal loops; their co-dependent recruitment is required to form the lateral element of the SC (Yang et al., 2006). Chromosomes begin to synapse with their homologous partner in zygonema and this proceeds until all homomorphic chromosomes have synapsed by early pachynema. On the synapsed bivalents, at least five additional components of the SC: SYCP1, SYCE1-3 and TEX12, can then be seen (Zickler and Kleckner, 2015).

It was shown previously that both SYCP3 and HORMAD2 recruitment was unaffected by ATR depletion (Royo et al., 2013). Therefore, using anti-SYCP3 immunostaining, I identified comparable meiotic sub-staged cells in both *Atr wt* and *Atr-/-;* co-staining with an antibody against HORMAD2 allowed the identification of univalent chromosomes (Wojtasz et al., 2009). Due to the cellular degradation associated with the activation of the midpachytene checkpoint at stage IV in *Atr -/-* cells, the last comparable time-point between *Atr -/-* and *Atr wt* is early pachynema.

First I analysed homologous synapsis in *Atr wt* cells at early pachynema. I found that synapsis occurred normally in 91.3% of cells (n=103; Fig 4.1A and C). In these cells only the non-homologous region of the XY bivalent recruited HORMAD2. The remaining 8.7% of cells had multiple HORMAD2 positive axes, indicating abnormal synapsis.

In *Atr -/-* cells, axis morphology appeared normal. However, in contrast to *Atr wt*, fewer than 14.0% of *Atr -/-* cells achieved homologous synapsis (n=172). The majority, i.e. 86.0% of cells, had multiple HORMAD2 positive asynapsed axes (n=172; Fig 4.1B). Therefore, the loss of ATR profoundly impaired homologous synapsis.

Previous studies have shown that the XY pair is preferentially affected in mutants with asynapsis, e.g. *Sycp1 -/-* males (de Vries et al., 2005). To determine whether

this was the case in *Atr -/-* males, I categorised cells into three classes of synapsis based on SYCP3 and HORMAD2 staining (Fig 4.1D):

- Class I: “normal synapsis”: HORMAD2 stains only the non-homologous region of the XY chromosomes and the pseudo-autosomal region (PAR) of the XY chromosome pair are synapsed.
- Class II: “XY asynapsis”: HORMAD2 stains the entire length of the unsynapsed XY.
- Class III: “XY and autosomal asynapsis”: HORMAD2 stains the unsynapsed autosomes and unsynapsed sex chromosomes.

As previously defined, Class I or “normal synapsis” occurred in the majority of *Atr wt* cells (91.3%), but the minority of *Atr -/-* cells (14.0%). Accordingly, Class II synapsis where the XY are unsynapsed and the autosomes are synapsed was rarely seen in *Atr wt* cells (3.9%), but was frequent in *Atr -/-* (19.2%) cells. The almost five-fold increase in the incidence of Class II synapsis from *Atr wt to Atr -/-* suggests that the XY bivalent is prone to asynapsis in the absence of ATR. Finally, Class III, or multiple HORMAD2 stained axes, was rarely seen in the remaining 4.9% of *Atr -/-* cells, whilst more than two-thirds of *Atr -/-* cells (66.9%) had this severe class of asynapsis.

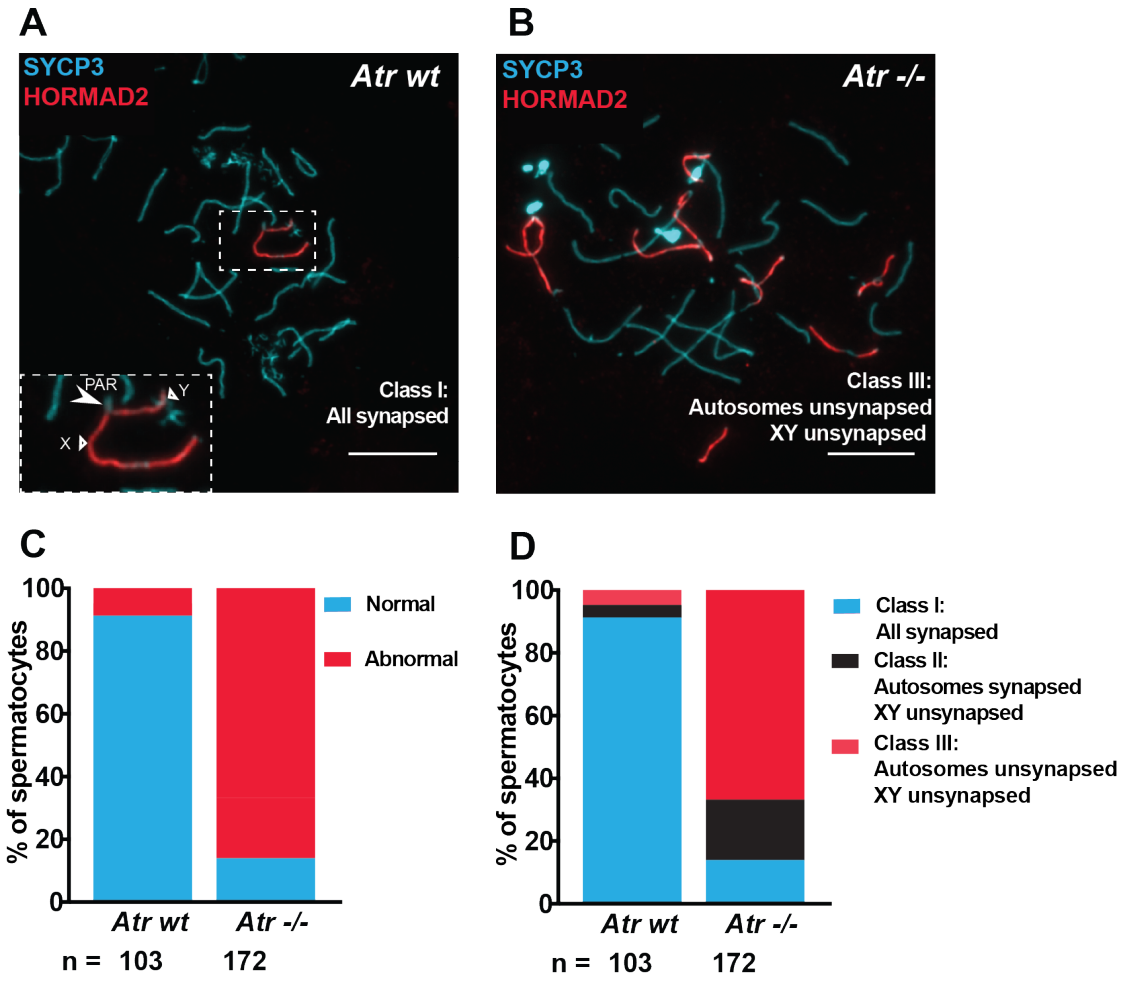

Figure 4.1 ATR regulates homologous synapsis

By early pachynema homologous chromosomes should have achieved synapsis. Representative of this in (**A**) >90% of *Atr wt* cells (n=103) all homologs have synapsed (Class I). Note that HORMAD2 should only be present on the non-homologous regions of the XY bivalent, although it does mark any asynapsed region. The dotted white rectangle indicates a 2x magnified inset: the X and Y are indicated by triangle-shaped arrowheads; the pseudo-autosomal region (PAR) by a chevron arrowhead. Since as in (**B**) >85% of *Atr -/-* cells are asynaptic there is abundant HORMAD2 stained axes: including XY asynapsis (Class II) and autosomal and XY asynapsis (Class III). Scale bar 10μm. (**C**) Simple quantification of the normal and abnormal synapsis in both genotypes. (**D**) Quantification after separating cells into three classes in preliminary investigations of incidence of X-Y asynapsis.

4.2 Asynapsis disproportionally affects XY PAR synapsis

My data suggested that the XY pair is preferentially unsynapsed in *Atr -/-* cells. To confirm this, I repeated the previous experiment with additional staining using an [auto]antibody that specifically recognises epitopes present at centromeres and kinetochores. This antibody is produced as a result of molecular pathology of patients with a limited form of systemic sclerosis. Formerly known as the acronym CREST referring to five ways it affects the skin: calcinosis, Raynaud's phenomenon, esophageal dysmotility, sclerodactyly, and telangiectasia.

Using unique characteristics, it is possible to discriminate the sex chromosomes from autosomes and therefore to determine whether the X and Y chromosomes have synapsed (shown schematically overleaf). This is because most mouse chromosomes are acrocentric, i.e. centromeres are terminal. However, the Y chromosome has a short arm (Yp) and long arm (Yq), which can be seen either side of an ACA focus (Fig 4.2.C). In addition, the X chromosome is a relatively large mouse chromosome that has a brighter DAPI positive heterochromatic centromere than similar sized autosomes. I used this criteria to determine how frequently sex chromosome pairing failure occurred in *Atr wt* and *Atr -/-* early pachytene cells.

I found that normal XY synapsis occurred in 95.7% of *Atr wt* cells (n=47; Fig 4.2A). In contrast, just 2.9% of *Atr -/-* cells achieved sex chromosome synapsis (n=37; Fig 4.2B). For both *Atr wt* and *Atr -/-* cells, I also determined the proportion of cells with unsynapsed sex chromosomes as a percentage of the total number of unsynapsed chromosomes. In *Atr wt* males, 3.8% (n=47) of HORMAD2 positive chromosomes were the X or Y; whereas in *Atr -/-* males this percentage was 22.7% (n=37; Fig 4.3C). In light of the approximate six-fold increase, I conclude that that the X and Y chromosomes are prone to asynapsis in the absence of ATR.

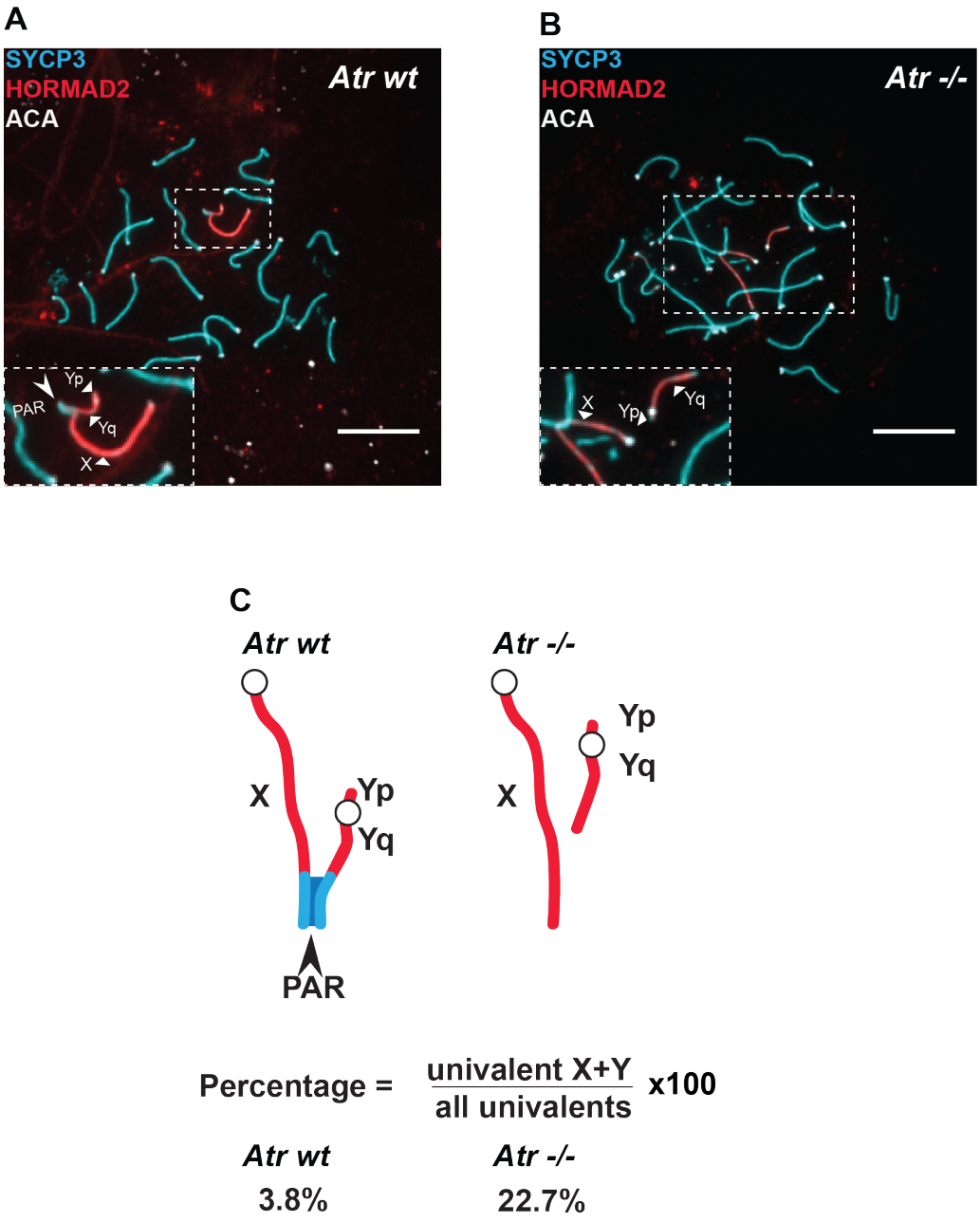

Figure 4.2 Sex chromosomes in *Atr -/-* cells are prone to asynapsis

(**A**) An *Atr wt* cell with normal synapsis and XY PAR pairing. The dotted white rectangle indicates a 2x magnified inset: the X and Y (Yp = Y short arm, Yq = Y long arm) are indicated by triangle-shaped arrowheads; the pseudoautosomal region (PAR) by a chevron arrowhead. (**B**) An *Atr -/-* cell with normal autosomal synapsis but XY asynapsis. Scale bars 10μm. (**C**) Schematic representation of the typical XY bivalent configurations in *Atr wt* and *Atr -/-* and the percentage of unsynapsed X and Y chromosomes, as the number of univalent sex chromosomes observed divided by the sum of all observed univalent.

4.3 ATR promotes synapsis without meiotic recombination

The data thus far established that ATR is required for successful homologous synapsis. I next wanted to determine how the synapsis defect might arise. It could conceivably originate from defective SC formation, defective meiotic recombination, or a combination of the two. If the deletion of ATR impeded SC formation in *Spo11-/-*, then ATR must have a role in SC formation. We therefore compared synapsis between *Spo11-/-* and *Atr -/- Spo11-/-* males. Previously type of genetic inference demonstrated that HORMAD1 had a direct role in SC formation that is independent of initiation of meiotic recombination (Daniel et al., 2011); i.e. the asynapsis phenotype of *Spo11 -/-* (Romanienko and Camerini-Otero, 2000, Baudat et al., 2000), is more//; severe without HORMAD1, *in Hormad1 -/- Spo11 -/-* mice.

Therefore, using a similar strategy, I used an antibody raised against SYCE2 as a marker of synapsed axes (Bolcun-Filas et al., 2007). I classified the extent of central element (CE) polymerisation into three classes (Fig 4.3a and b):

- Class I: “Complete SC”: SYCE2 continuous along an entire axis length
- Class II: “Incomplete SC”: Elongation of SYCE2 along part of an axis length
- Class III:“SC foci”: discrete punctate dots of SYCE2

The proportion of cells exhibiting “Complete SC” and “Incomplete SC” (Classes I and II) was significantly lower in *Atr -/- Spo11 -/-* than in *Atr wt Spo11 -/-* males. The mean ± SEM values for “Complete SC” were 1.5 ± 0.2038 for *Atr wt Spo11 -/-* and were 0.7813 ± 0.1422 (n=88) for *Atr -/- Spo11 -/-* (n=96). The mean ± SEM values for “Incomplete SC” were 16.07 ± 1.01 for *Atr wt Spo11 -/-* (n=88) and 11.84 ± 0.9155 for *Atr -/- Spo11 -/-* (n=96). These differences corresponded to a highly significant difference (p-values 0.0038 and 0.0022 respectively; unpaired t-tests).

However, the number of “SC foci” (Class III) was significantly increased at 17.96 ± 0.9178 (mean ± SEM; n=96) in *Atr -/- Spo11 -/-* cells compared with 12.90 ± 1.046 (mean ± SEM; n=88) in *Atr wt Spo11 -/-* cells (p= 0.003; unpaired t-test). In summary, I observed significantly fewer extended regions of SC and significantly

more SC foci in *Atr -/- Spo11 -/-* males. I conclude that ATR has a role in SC formation that is independent of meiotic recombination.

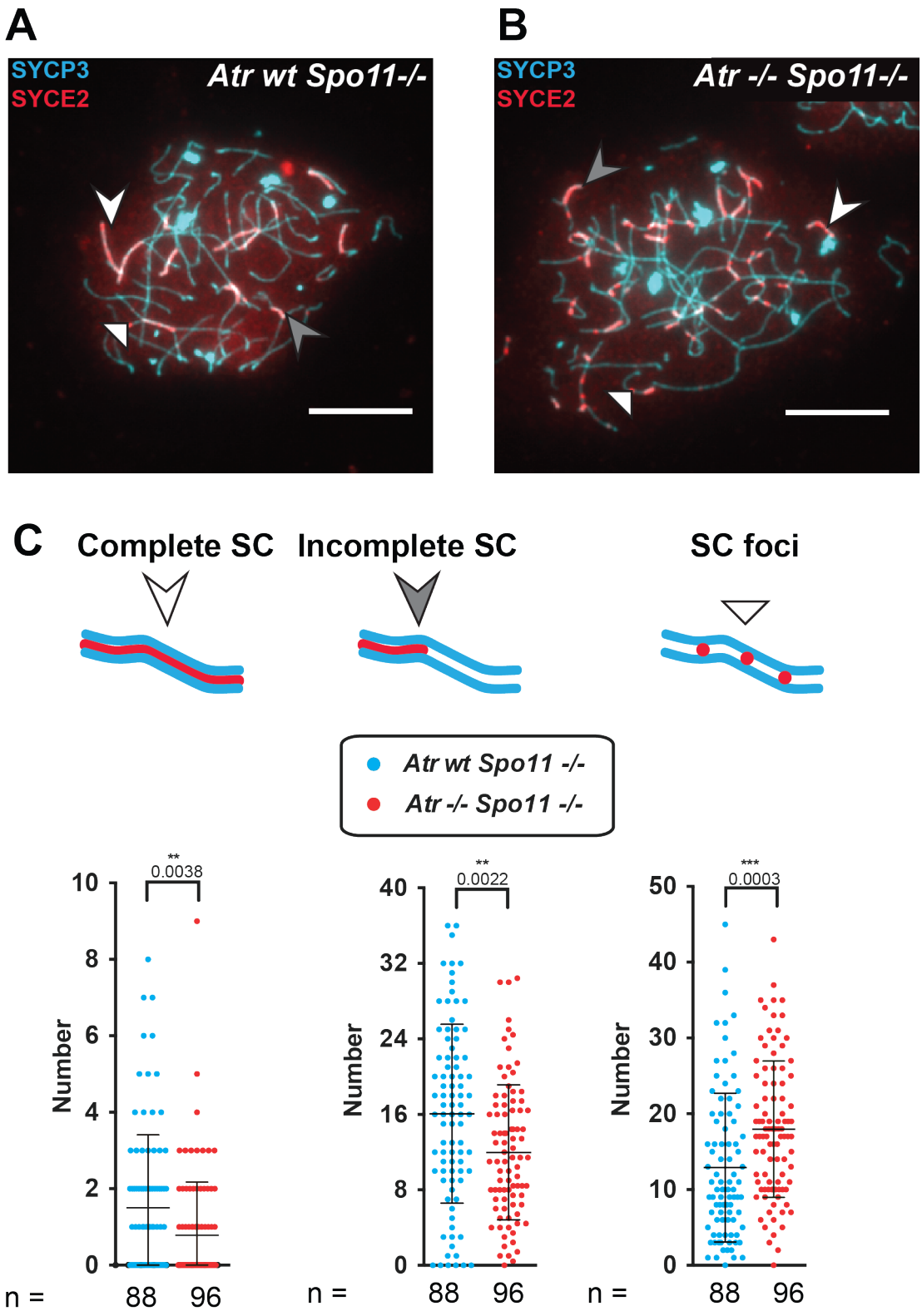

Figure 4.3 ATR regulates SC formation independently of SPO11

To determine whether ATR regulates SC formation early pachytene cells were selected on the basis of DAPI staining and the presence of nucleoli. Counts of 88 *Atr wt Spo11 -/-* and 96 *Atr -/- Spo11 -/-* cells found: (**A**) A typical *Atr wt Spo11 -/-* cell has more regions of complete SC (white chevron arrowhead) and incomplete SC (grey chevron arrowhead), whilst it has fewer SC foci (white triangular arrowhead). In contrast (**B**) *Atr -/- Spo11 -/-* cells have significantly fewer regions of complete SC and incomplete SC and slightly greater numbers of SC foci. Scale bar 10 μm. (**C**) Schematic and quantification of each genotype, p-values and (**/***) significance from unpaired t-tests.

4.4 Different requirements for ATR in SC protein localisation and SMC3-S1083 phosphorylation

Having established that ATR positively regulates meiotic chromosome synapsis in the presence and absence of meiotic recombination, the next aim was to investigate whether the loss of ATR altered the recruitment of some important meiotic chromosome associated proteins. Having established and confirmed that SYCP3 and HORMAD2 staining was unaffected in *Atr -/-, CreERT*^{2} mice (Royo et al., 2013), I next wanted to investigate the localisation of two other components of the SC: SYCE1 and SYCE2, as well as the localisation of a phosphorylated form of cohesin component SMC3.

I first examined SYCE1 and SYCE2 staining in early pachytene cells. In *Atr wt* samples, I found that SYCE1 was successfully recruited to synapsed axes (Fig 4.4A). Performing the same analysis using SYCE2, I found that 100% of cells (n=50) had SYCE2 on the synapsed autosomes and the PAR, as shown by a staining pattern indiscernible from SYCE1 (Fig 4.4 D).

In the absence of ATR, I found that despite obviously impaired homologous synapsis, SYCE1 and SYCE2 were present in 100% of cells on regions of homologous and non-homologous synapsis (n=49 and 50 respectively; Fig 4.4 B, C, E and F). In summary, I have found that the ability to recruit SYCP3, SYCE1 and SYCE2 to meiotic chromosomes is unaffected in *Atr -/-* cells.

SMC3 and SMC1 are the two heteromeric structural maintenance of chromosome (SMC) proteins in the cohesin complex. In mitosis, SMC3 is phosphorylated at serine-1083 (pSMC3-S1083) in response to DNA damage (Luo et al., 2008). In meiosis, SMC3 forms a linear structure coating chromosomal axes (Eijpe et al., 2000). In addition, pSMC3-S1083 is seen on asynapsed chromosomes, including the XY pair, and this occurs independently of ATM (Fukuda et al., 2012). Cohesin loading during meiosis is not affected by absence of SC proteins SYCP1 and SYCP3 (Kouznetsova et al., 2011). I therefore wanted to assess whether pSMC3-S1083 localisation still occurs in *Atr -/-* spermatocytes. To evaluate the functionally

importance of SMC3 phosphorylation a phosphor-deficient allele must be generated.

I found that in *Atr wt* males, pSMC3-S1083 was present on regions of asynapsis from zygonema onwards. At early pachynema the staining was restricted to the XY bivalent, as previously shown (Fukuda et al., 2012). In total, 96.0% of early pachytene cells had pSMC3-S1083 on the XY pair (n=50; Fig4.4G). To determine whether pSMC3-S1083 was ATR-dependent, I then analysed *Atr -/-* cells. I found that only 7.0% of *Atr -/-* cells had detectable pSMC3-S1083 on the X and Y chromosome (n=72; Fig4. I-J). Serine-1083 SMC3 phosphorylation is therefore ATR-dependent.

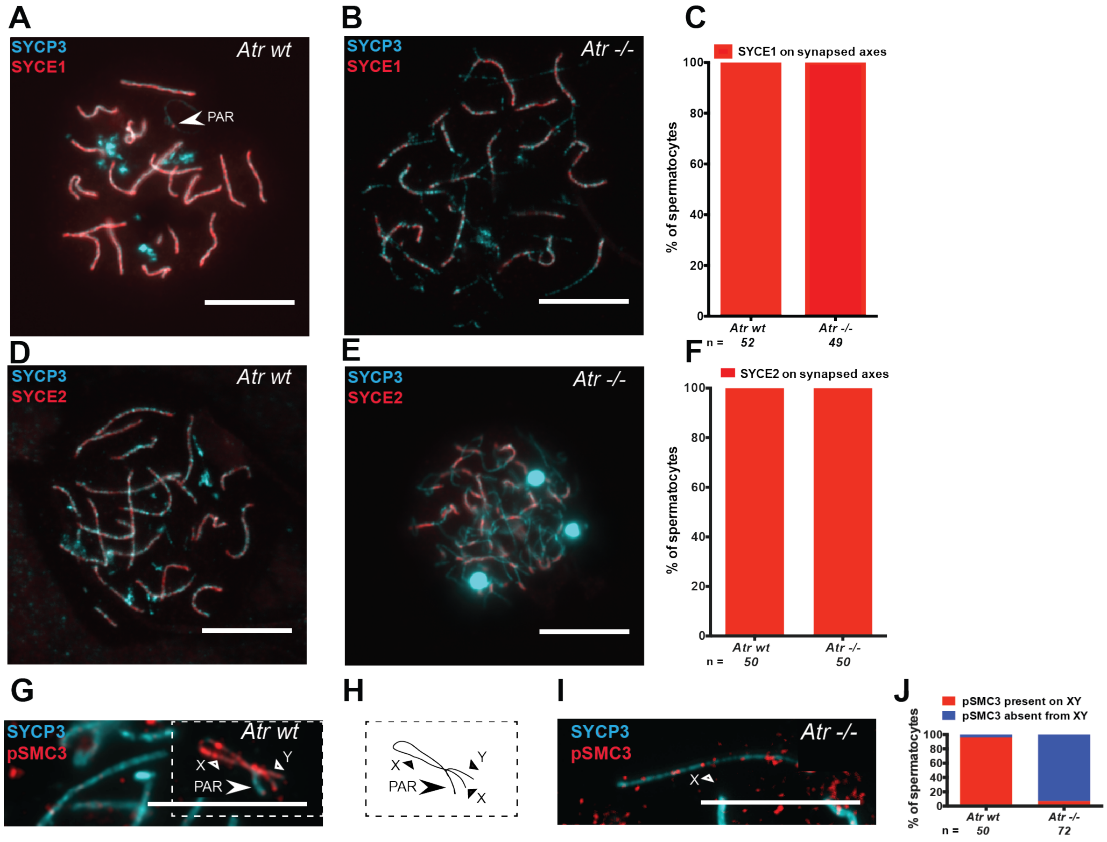

Figure 4.4 Different requirements for ATR in SC protein localisation and SMC3-S1083 phosphorylation

(**A-C**) SYCE1 is successfully recruited in *Atr wt* and *Atr -/-* to synapsed axes. Notably, SYCE1 is present at the synapsed PAR of the XY (white chevron arrowhead). (**D-F**). SYCE2 is successfully recruited in *Atr wt* and *Atr -/-*. (**G-J**) Recruitment of pSMC3-S1083 is ATR-dependent. The morphology of the XY bivalent in *Atr wt*, in the white dotted rectangle region is shown schematically in (**I**) with X, Y and PAR labelled. Scale bars, 10 μm.

4.5 Discussion

The aim of this chapter was to investigate whether ATR loss affects homologous chromosome synapsis. I found that most *Atr -/-* cells were unable to achieve homologous synapsis. Therefore, ATR promotes synapsis between homologous chromosomes. This function is at least partially independent of recombination.

Interestingly, even within highly asynaptic nuclei, some chromosomes achieved homologous synapsis. Residual expression of ATR might explain this observation, but this would seem to contradict the data in the previous chapter in which ATR levels were undetectable in *Atr -/-, Ngn3-Cre* testes. Perhaps there is remaining functional ATR protein that cannot be seen by western blotting or immunofluorescence.

I also found that the XY bivalent is prone to asynapsis in *Atr -/-* cells. In the future, it could prove fruitful to investigate whether specific autosomes are also sensitive to asynapsis. This could be achieved by whole genome painting of meiotic cells (Lightfoot et al., 2006). Focusing on the PAR, it could be useful to determine whether the small size of this chromosome region makes the XY pair prone to asynapsis (Perry et al., 2001); this could be achieved by characterising how a genetically engineered larger PAR would affect XY synapsis. Perhaps independent of chromosomal features, the XY asynapsis observed might be explained by a specific role for ATR at the PAR. In support of this suggestion, residual ATR is found at the PAR of tamoxifen-depleted *Atr -/-, Cre-ERT*^{2} males (Royo et al., 2013) and there is precedent for DNA damage kinases to have such specialized meiotic roles. For example, the related kinase ATM was shown to be required for generating the obligate crossover in the PAR of the XY bivalent (Barchi et al., 2008).

Finally, I also established that the recruitment of important SC components SYCP3, SYCE1 and SYCE2 was comparable in early pachytene cells from *Atr -/-* and *Atr wt* males. These data demonstrate that the affinity of these SC components to synapsed regions is not ATR-dependent. I was able to demonstrate that phosphorylation of SMC3-S1083 was absent in early pachytene *Atr -/-* cells. SMC3

would become an experimentally validated meiotic ATR-phosphotarget like HORMAD1 and HORMAD2 (Royo et al., 2013, Fukuda et al., 2012), provided non-phosphorylated SMC3 localisation is normal in *Atr -/-* cells. The lack of ATR, the lack of ATR kinase activity (or both) must explain the phenotypes observed. In the future it might prove useful to investigate the functional significance of particular phospho-deficient and phospho-mimetic alleles of HORMAD1, HORMAD2 and SMC3 to determine whether it is a direct relationship between these proteins that causes any of the asynapsis phenotypes I have observed. A conditional *Smc3* allele has been made recently, the meiotic roles of SMC3 and potential SMC3-ATR interactions could now be elucidated using an *Smc3 -/-, Ngn3-Cre* strain to overcome the embryonic lethality of previous murine *Smc3* models (Viny et al., 2015). Finally it would also be fruitful long-term objective to obtain a meiotic kinome of ATR activities using mass spectroscopic approaches.

Chapter 5. The roles of ATR in meiotic recombination

In this chapter I set out to determine whether ATR has fundamental roles in meiotic DSB formation and repair. Having established that synapsis was defective in early pachytene spermatocytes in *Atr -/-* mice (See Chapter 4), it was essential I determined whether different aspects of meiotic recombination occurred normally; since defective synapsis can arise from problems in meiotic DSB formation and/or repair.

Many proteins are essential for meiotic recombination, some of which are also required in response to mitotic DSBs; others however are meiosis-specific (Marcon and Moens, 2005). Baudat et al. (2013) recently categorised meiotic recombination proteins based on their function within the chronological steps of meiotic DSB formation and repair. These five groups are (i) DSB formation, (ii) DSB end resectioning, (iii) Strand invasion, (iv) Intermediate processing and (v) CO resolution (Baudat et al., 2013). Determining whether ATR belongs within any of these groups is therefore the key question in this chapter.

Correspondingly, the first objective of this chapter is to determine if meiotic DSBs form normally in the absence of ATR. Several publications have shown that the related kinase ATM negatively regulates DSB formation in different model organisms, including mice (Lange et al., 2011), flies (Joyce et al., 2011) and budding yeast (Blitzblau and Hochwagen, 2013). The study in mice quantified the levels of an early intermediate in meiotic recombination that consists of protein covalently bound to ssDNA, called a Spo11-oligo. In the absence of ATM, Spo11-oligo levels increased significantly. This phenomenon was not observed in other mutants with early and late meiotic recombination phenotypes, like strand-invasion deficient *Dmc1 -/-* and CO-defective *Mlh1 -/-* mice (Lange et al., 2011). It is plausible that ATR could regulate DSB formation in a similar manner to ATM.

Indeed, two studies in budding yeast have suggested a link between the *Atr*-ortholog MEC1 and DSB levels. The first study found using a hypomorphic spo11

allele in combination with recombination defective strains like dmc1Δ that meiotic DSB formation decreased in the *mec1* mutants (Gray et al., 2013). The study therefore suggested that ATR might act as an antagonist of ATM in DSB regulation. The second study, using an indirect approach, identified REC114 an ATM/ATR phosphotarget (Carballo JA, 2013). Rec114, a component of the pre-DSB complex that licenses Spo11 to create meiotic DSBs (see introduction 1.3.1), contains eight clustered S/T-Q amino acid motifs within approximately two hundred amino acids. Such arrangements constitute a serine/threonine cluster domain (SCD) (Traven and Heierhorst, 2005). These domains are thought to be functionally important to modulate protein function. Indeed, phosphor-mutant alleles that mimicked constitutive phosphorylation or prevented phosphorylation led to elevated DSB levels, reduced/delayed DSB formation, respectively (Carballo et al., 2008).

My second objective is to determine whether meiotic DSBs can be repaired normally, or if there are problems with DSB end-processing or strand invasion activities. Typically, the inactivation of important repair genes leads to unresolvable damage in pachynema. These persistent DSBs then trigger a meiotic checkpoint and germ cell elimination. *Atr*-orthologs have defective meiotic repair, suggesting that ATR is likely to have important roles in meiotic recombination. For example, it was found that the *Atr*-ortholog *Mei-41* is required to repair DSBs in *Drosophila* oocytes (Joyce et al., 2011). While *Arabidopsis thaliana Atr* mutants are fertile, studies of ATM and ATR orthologs found that the phenotypes of semi-sterile *Atm* and completely sterile *Atr, Atm* double mutants were alleviated by removing meiotic recombination using a *Spo11* mutation (Culligan and Britt, 2008). More recently it was discovered that *Atr* mutations are able to repress the defective DMC1 recruitment of *rad51* mutants (Kurzbauer et al., 2012).

My third objective is to monitor whether ATR regulates the types of repair. In mammalian somatic cells, the choice of DSB repair pathway depends on the stage in the cell cycle. In G2, homologous recombination (HR) is preferred, whilst in G1 non-homologous end-joining (NHEJ) is more frequently used (Mimitou and Symington, 2009). Consistent with the suggestion that prophase I is analogous to a G_2/M transition, in meiotic prophase the majority of DSBs are repaired by HR (Burgoyne et al., 2007). HR requires one of the three intact homologous donor

sequences, either the intact sister chromatid or the homologous chromatid, which are termed inter-sister (IS) and inter-chromatid (IC) repair respectively. In meiosis the majority of HR is carried out using the IH template; this is called IH-bias (Schwacha and Kleckner, 1994). In budding yeast, IH-bias is generated at least partially through the phosphorylation of meiotic chromosomal axes protein Hop1 by Mec1/Tel1. Hop1 also contains a SCD domain. Two studies have found that when three *HOP1* serines and threonines (S298, S311 and T318) were converted to alanines, the IH-bias was lost. This mutant allele enabled IS repair in a *hop1*^{SCD}*dmc1*Δ strain whereas *dmc1*Δ normally has persistent DSBs (Penedos et al., 2015, Carballo et al., 2008). Similarly, mouse studies have suggested that the formation of the synaptonemal complex is important for achieving an IH bias (Li et al., 2011). Since the sex chromosomes are largely unsynapsed, the non-homologous regions of the X and Y chromosome must be regulated distinctly, or simply exempt from this regulation. In addition, work in budding yeast established that ATM and ATR orthologs prevent additional DSBs occurring on intact templates, therefore disrupting normal IH-bias establishment (Zhang et al., 2011).

There is less evidence connecting *Atr*-orthologs to the later stages of meiotic recombination. Almost 40 years ago, *Drosophila* ortholog mutant alleles of *Mei-41* were shown to disrupt CO formation (Carpenter, 1979). In contrast, a more recent study found that a mutant allele of *Caenorhabditis elegans Atr*-ortholog *atl-1* is dispensable for CO formation (Garcia-Muse and Boulton, 2005). In mice, deletion of ATM in *Spo11 +/-* spermatocytes increases CO numbers on some larger chromosomes (Barchi et al., 2008), but it is unclear whether ATR influences CO formation.

5.1 ATR does not regulate the abundance of meiotic DSBs

Meiotic DSBs are created by the transesterase enzyme SPO11 (Keeney et al., 1997). After creating a meiotic DSB, paired SPO11 molecules remain covalently attached to 5' ends. Endonucleases, including components of the MRE11-complex, are then required to create a downstream nick and liberate the Spo11-oligo (Garcia et al., 2011). Spo11-oligos are considered a quantitative by-product of meiotic DSB formation; hence they can be measured to quantify DSB formation.

In collaboration with the Keeney lab (Julian Lange), DSB formation was examined in testes from juvenile (13.5 d*pp*) as well as some adult (30 d*pp*) mice. At 13.5 d*pp,* the first wave of meiotic cells is yet to reach pachynema; hence no apoptotic cells would be present. In the testes of the adult samples there are multiple waves of meiotic cells present, however this would include apoptotic *Atr -/-* stage IV/mid pachytene cells. The gel electrophoresis (GE) of the SPO11-imumnoprecipitated radiolabelled Spo11-oligo and the western blots of free SPO11 (not bound to DNA) gave a Spo11-oligo complex signal at around ~50kDa (Fig 5.1A-B). The signal from each lane was quantified and normalised to testis weight. Normalised Spo11-oligo complex levels are shown (Fig 5.1C-D). Spo11-oligo complex levels and free SPO11 protein appeared comparable between wildtype*, Atr wt* and *Atr -/-* samples (Fig 5.1A). Spo11-oligo complex levels were determined to be as follows: 1.00 in wildtype (n=3); 0.910 (n=3) in *Atr wt*; and 1.28 (n=6) in *Atr -/-* (Fig 5.1C). Correspondingly the p-values comparisons of the three genotypes were non-significant. These data demonstrate that the abundance of meiotic DSBs is comparable in *Atr wt* and *Atr -/-* mice. This supports the conclusion that the loss of ATR does not alter Spo11-oligo levels. A preliminary result from the adult samples also has the same outcome: the Spo11-oligo complex levels were *Atr wt* (1.000, n= 1) and *Atr -/-* (0.880, n=1).

Next, I wanted to look at the functional interplay between ATR and ATM in DSB formation. To test this, SPO11-oligo levels were assayed in the combined absence of ATM and ATR i.e. in *Atr -/- Atm -/-* spermatocytes. Consistent with previous reports (Lange et al., 2011), *Atm -/-* testes (n=5) had elevated levels of DSB formation with median Spo11-oligo levels 14.1x higher than wildtype levels. Levels

of free SPO11 were also decreased in *Atm -/-* relative to wildtype testes (Fig 5.1B). Spo11-oligo complex levels in the *Atr -/- Atm -/-* samples (n=4) were not significantly different from those in *Atm -/-* testes (Fig. 5.1D, $p = 0.2857$). Overall the data demonstrates that ATR loss does not reduce the elevated meiotic DSB levels in *Atm -/-* spermatocytes.

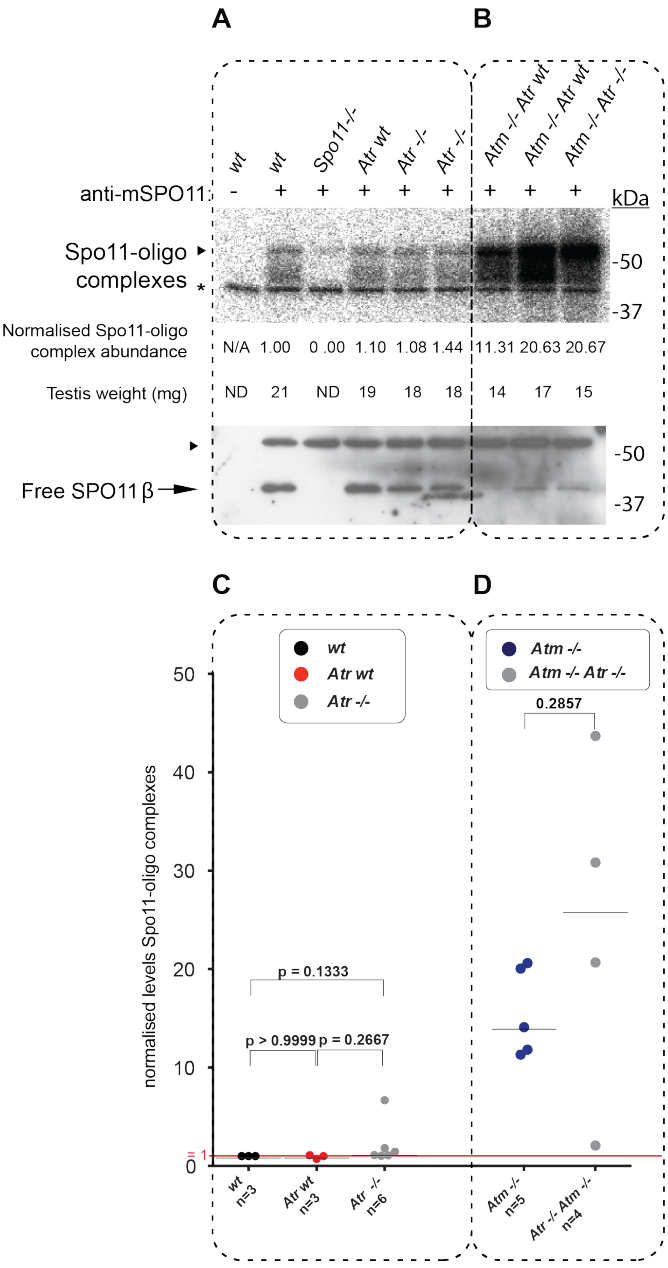

Figure 5.1 Spo11-oligo levels are regulated by ATM independently of ATR (blots performed by Julian Lange, Keeney lab)

(**A-B**) Top panel - radiolabelled plot of steady state Spo11-oligo complex levels from SPO11-IP of juvenile 13.5 days *post partum* (dpp) testes. Middle panel - quantified signal normalised to *wt* mice, testis weight indicated. Bottom panel - western blot of free SPO11. (**A**) Effect of ATR loss. (**B**) Effect of combined ATM and ATR loss. (**C-D**) Quantification of Spo11-oligo complex levels in (**A**) and (**B**) median levels are marked; and red line represents wildtype Spo11-oligo levels normalised to 1. Pair-wise Mann–Whitney tests were performed and p-values are indicated and support that Spo11-oligo levels across *wt, Atr wt* and *Atr-/-* mice are comparable, and that the loss of ATR in *Atm -/-* does not reduce Spo11-oligo levels. asterisk, non-specific terminal transferase, labelling; arrowheads, migration position of immunoglobulin heavy chain.

5.2 Altered nucleolytic processing in the absence of ATM and ATR

In wildtype samples Spo11-oligo complexes have a bimodal distribution, with a population at around 15-27 nucleotides (nt) and another at 31-35 nt (Lange et al., 2011). The loss of ATM also alters nucleolytic processing of Spo11-oligos complexes, changing the overall size distribution: fewer shorter oligos are present and larger oligos between 40-70 nt are prominent, as well as the occurrence of much larger oligos >400 nt (Lange et al., 2011). I observed a size distribution consistent with this previous report (Fig 5.2). However in *Atr -/- Atm -/-* samples, the Spo11-oligos had a different size to those in all other genotypes (Fig 5.2).

To investigate this effect more closely, Spo11-oligos were protease treated, ethanol precipitated and electrophoresed on polyacrylamide sequencing gels to improve resolution (Fig 5.4). The relative signal from each sample was then quantified as a percentage of the total signal per lane for size-separated nucleotides. As in the previous section, the effect of ATR loss on Spo11-oligo size was investigated (Fig 5.4 A,C). The comparable size distributions of Spo11-oligos across *wt, Atr wt* and *Atr -/-* samples demonstrate that the loss of ATR does not affect the nucleolytic processing of meiotic DSBs (Fig 5.4 C).

Next, the effect of combined loss of ATM and ATR on Spo11-oligo size was assessed (Fig 5.4 B,D). In the absence of both ATM and ATR, the populations of small (17-25 nt) and intermediate (~40-70 nt) oligos decreased relative to wildtype, and the occurrence of longer nucleotides increased. However, uniquely, Spo11-oligo in *Atr -/- Atm -/-* testes were far longer (>1kb) than in any other genotypes (Fig 5.3D). This data supports a model in which ATM is predominately responsible for nucleolytic processing of meiotic DSBs in wildtype mice, and that in the absence of ATM, ATR is able to play a compensatory role in meiotic DSB processing (Fig 5.3E).

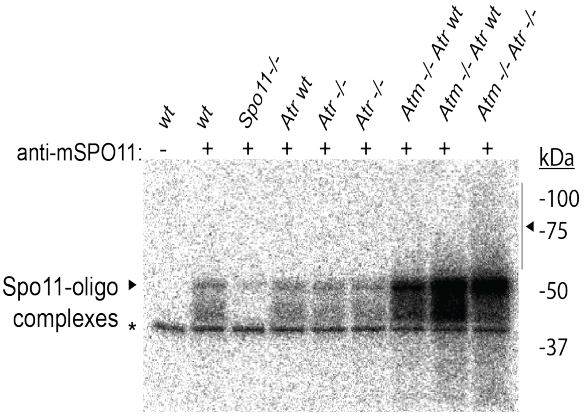

Figure 5.2 Novel larger spo11-oligos in *Atm -/- Atr -/-* (blots performed by Julian Lange, Keeney lab)

Spo11-oligo complex levels from *Atm -/-* are known to contain larger Spo11-oligos (Lange et al., 2011). Novel, even larger Spo11-oligos were consistently found in *Atm -/- Atr -/-* samples. Line and arrowhead to right of gel defines this region between 50-100 kDa. (N.B. Same gel as Fig 5.1, with less cropping).

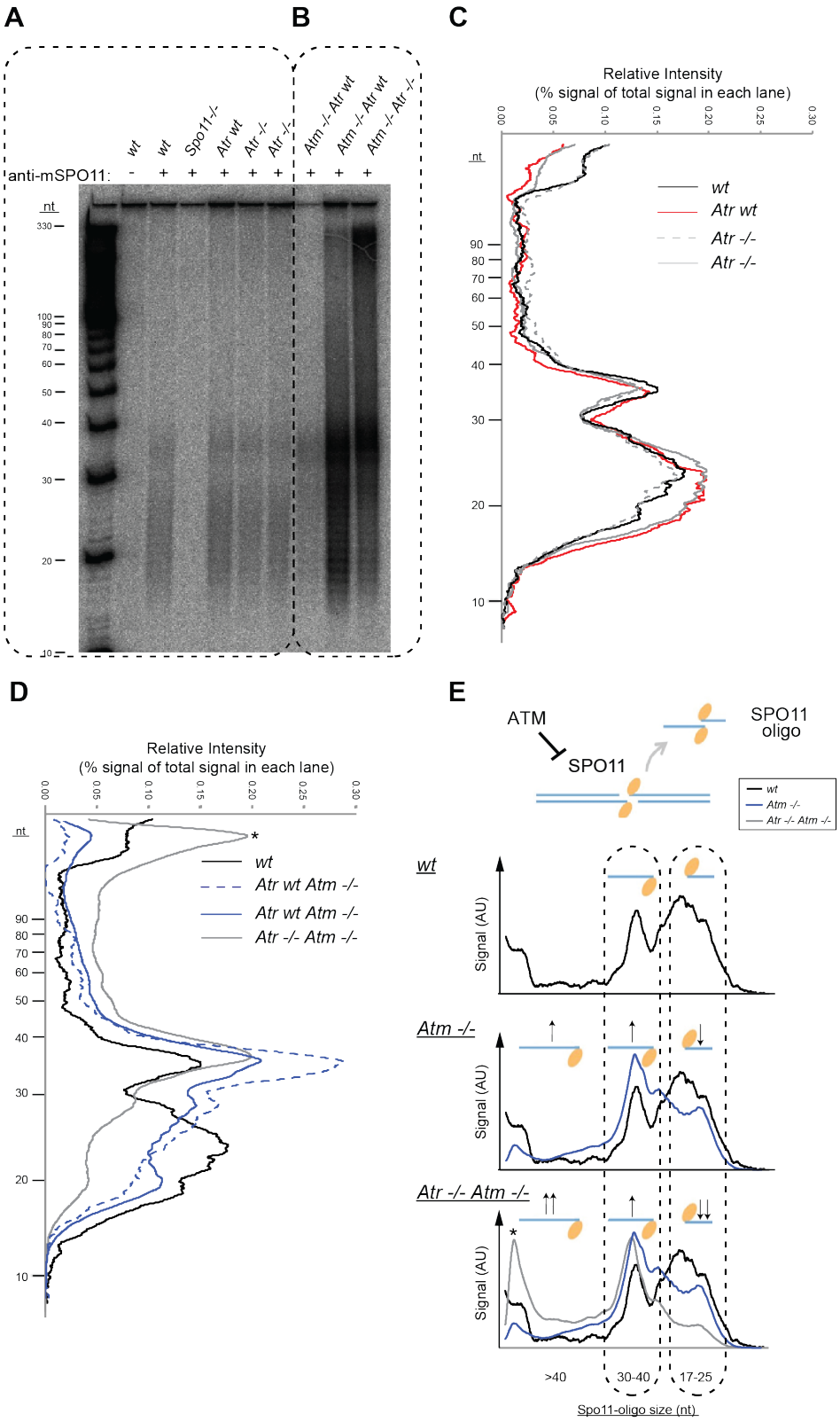

Figure 5.3. ATM and ATR cooperate to regulate nucleolytic processing (blots performed by Julian Lange, Keeney lab)
(**A-B**) Representative autoradiograph showing that SPO11–oligonucleotide distribution is not altered in (**A**) *Atr -/-*, but is altered in (**B**) *Atm -/-* and *Atr -/- Atm -/-* cells. (**C-D**) Lane traces for A and B respectively. Relative intensity is normalised against the total signal within each lane. Asterisk * denotes autoradiograph background. (**E**) Model demonstrating Spo11–oligonucleotide length variations in wildtype, *Atm -/-* and *Atr -/- Atm -/-* spermatocytes, indicating a role in nucleolytic processing of meiotic DSBs.

5.3 ATR regulates recombinase but not RPA recruitment to DSBs

The 3' ends of meiotic DSBs are resected, generating asymmetrical 3' single stranded DNA (ssDNA) tails (Burgoyne et al., 2007, Neale et al., 2005). These overhanging ends are utilised in the homology search and enable strain invasion. Initially, the RPA complex is recruited to the ssDNA tails before being replaced by the eukaryotic RECA-homolog RAD51 and the meiosis specific paralog DMC1 (Moens et al., 2002, Tarsounas et al., 1999). Recombinases RAD51 and DMC1 form nucleoprotein filaments that carry out the homology search at each DSB site (Kinebuchi et al., 2004, Short et al., 2016). This process can be observed cytologically using antibodies against RAD51, DMC1 and the 32kDa subunit of RPA2 (Moens et al., 2002, Tarsounas et al., 1999). Having established that meiotic DSB abundance was grossly unaffected by ATR loss, I wanted to determine whether ATR functioned in the subsequent steps of DSB repair. To aid comparisons with other recent studies of mouse meiosis, I used the same commercially available RAD51 and DMC1 antibodies as in a recent publication (Cole et al., 2012). I first investigated whether the number of foci per nuclei at late leptonema were similar in *Atr -/-* and *Atr wt*.

I observed that at late leptonema RAD51 focus counts in wildtype mice were similar to those previously published (Cole et al., 2012). In *Atr wt* males I found 199.6 ± 22.3 (median ± SD; n= 19) RAD51 foci. Cole et al. (2012) had found 219.2 ± 69.8 RAD51 foci. With DMC1, in *Atr wt* I observed 185.8 ± 31.3 (median ± SD; n= 22) foci, while Cole et al. (2012) found 225.5 ± 31.3 foci. Comparable to my RAD51 and DMC1 data, I found 227.4 ± 32.2 (n= 17) RPA foci in *Atr wt*. The similarity in total foci observed is likely to reflect the fact that at this stage RAD51, DMC1 and RPA are all recruited at 3' single stranded ends of the recently resected DSBs.

I then repeated these analyses in *Atr -/-* late leptotene cells. Interestingly reduced counts were observed both for RAD51 (105.2 ± 20.1; n=20; $p<0.0001$; Mann–Whitney test) and DMC1 (124.7 ± 32.0; n= 23; $p<0.0001$; Mann–Whitney test). These changes correspond to a 47% decrease in RAD51 and a similar 45% decrease for DMC1 focus counts relative to *Atr wt* males.

Surprisingly, in contrast to RAD51 and DMC1 counts, RPA counts were not reduced and were comparable between *Atr -/-* and *Atr wt* males. *Atr -/-* had 251 ± 35.7 foci (n= 22) whereas *Atr wt* had 228 ± 32.2 (n= 17; p=0.1054; Mann-Whitney test). Therefore at leptonema ATR is required for RAD51 and DMC1, but not RPA loading. Given these RPA data, together with the results of the Spo11-oligo analyses (Section 5.1), I surmise that ATR does not regulate meiotic DSB formation. However, ATR is required for an early step in meiotic recombination necessary for the correct recruitment of recombinases to meiotic DSBs.

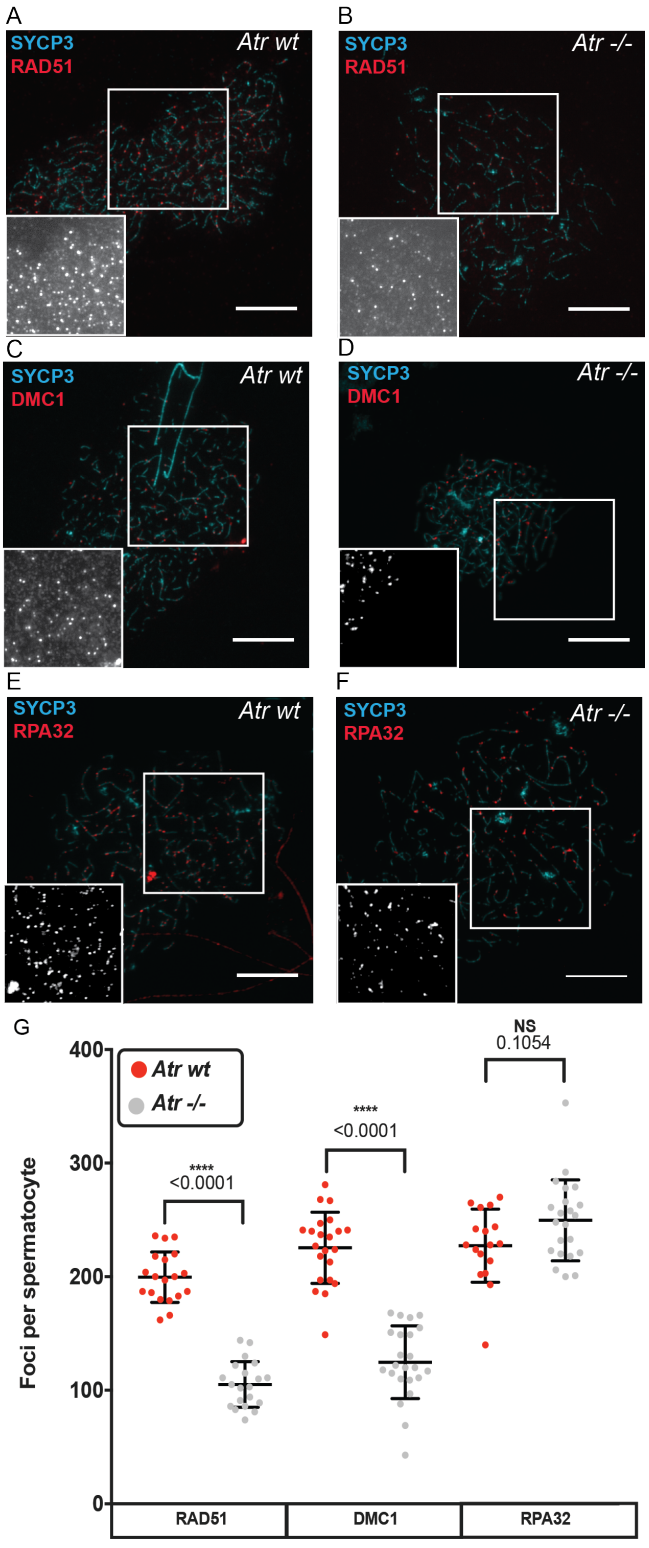

Figure 5.4 ATR is required for the correct localisation of meiotic recombinases

(**A-B**) *Atr -/-* cells have defective recruitment of RAD51 to meiotic DSBs. (**C-D**) DMC1 recruitment is also similarly defective in *Atr -/-*. (**E-F**) RPA32 recruitment is unaffected by ATR loss. Bars, 10 μm (**G**) Quantification of DSB foci in *Atr wt* and *Atr -/-*. Error bars are, SD, p-values from Mann-Whitney tests shown.

5.4 The RAD51 localisation defect in *Atr-/-* is independent of DMC1 and ATM

To confirm and develop my observations, I sought to determine whether defective RAD51 recruitment at late leptonema could be rescued by increasing the length of ssDNA tails or by increasing the number of DSBs in *Atr -/-* males.

In the absence of meiotic specific recombinase DMC1, meiotic DSBs are unable to be repaired, leading to asynapsis and persistent DNA damage (Pittman et al., 1998). Furthermore, in *dmc1*Δ budding yeast the length of the ssDNA tails is increased (Bishop et al., 1992); leading to a "hyper-resection" phenotype. This phenotype is likely to be conserved and present in mice. Indeed, a recent publication studying MEIOB, a ssDNA-binding protein, reported that MEIOB staining at meiotic DSBs is more intense in *Dmc1 -/-* than equivalent wildtype cells under identical imaging conditions (Souquet et al., 2013). Based on this information, I postulated that increasing the ssDNA length through *Dmc1* deletion might rescue the RAD51 defect in *Atr -/-* males. Furthermore, I hypothesised that increasing DSB number through *Atm* deletion might rescue RAD51 counts in *Atr -/-* mutants. To test these possibilities, I compared late leptotene RAD51 counts in *Atr -/-* mutants with those in *Atr -/- Dmc1 -/-* males and *Atr -/- Atm -/-* males.

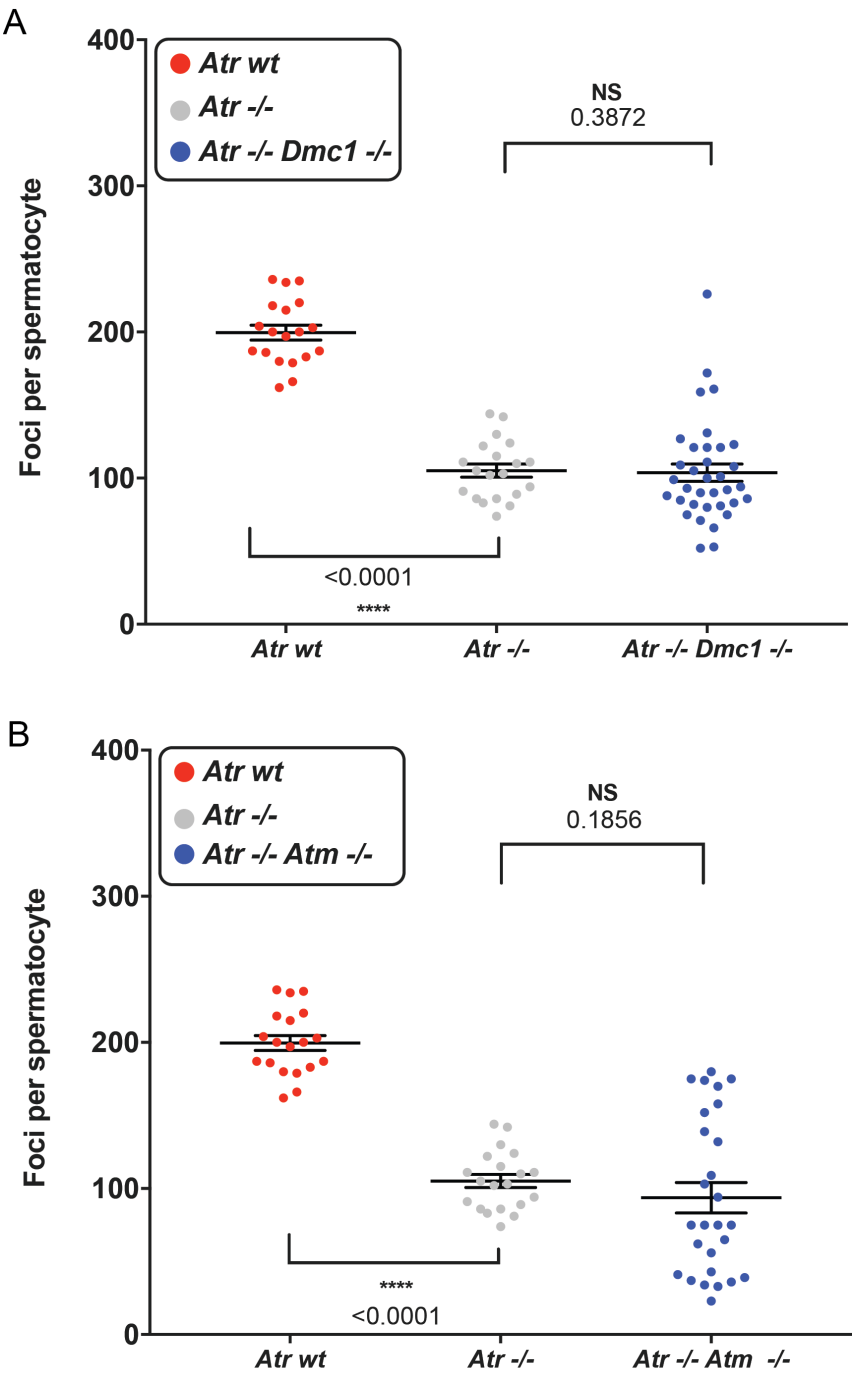

Figure 5.5 Defective leptotene RAD51 recruitment is independent of DMC1 and ATM

(**A**) RAD51 focus counts remain defective in *Atr -/-* cells independent of *Dmc1*. (**B**) Similar defective RAD51 recruitment in *Atr -/- Atm -/-* cells. P-values from Mann-Whitney tests indicated.

5.5 ATR regulates DSB repair kinetics in early pachynema

It has been shown that meiotic recombination is restricted on the sex chromosomes, so that during midpachynema CO formation only occurs within the PAR (Kauppi et al., 2011, Burgoyne, 1986). This is despite multiple DSBs, marked by RAD51, DMC1 and RPA, being present on the non-homologous regions of the X and Y during early pachynema (Tarsounas et al., 1999, Moens et al., 1999, Plug et al., 1998, Kauppi et al., 2012, Kauppi et al., 2011). These DSBs cannot be repaired via IH recombination due to the absence of a synaptic partner. It is therefore assumed that they are repaired later in pachynema, perhaps using the sister chromatid. I wished to use the non-homologous regions of the X as an experimental system to determine whether ATR is involved in the regulation of DSB repair on chromosomes that lack a synaptic partner.

To address this question I identified early pachytene cells where I could discriminate the X and Y chromosomes from the autosomes and examined recombination foci for RAD51, DMC1 and RPA on the X chromosome. In *Atr wt* males I found that the number of foci were similar for all three markers (Fig 5.6 A, C) : RAD51 14 ± 3.9 (Median ± SD; n= 77); DMC1 15 ± 3.2 (n= 73); and RPA 13 ± 5.3 (n= 70). In the absence of ATR, focus counts were significantly reduced for all three markers (Fig 5.6 A, C): RAD51 9 ± 3.5 (n= 68; p-value < 0.0001; Mann-Whitney test); DMC1 7 ± 3.7 (n= 81; p-value < 0.0001); and RPA 8.5 ± 4.5 (n= 76; p-value < 0.0001. The finding that RPA, which was unaffected in *Atr -/-* leptotene cells (See Section 5.2), was also reduced at pachynema suggested that ATR might regulate the timing and/or type of DSB repair on the asynapsed X chromosome.

Therefore, I next sought to determine whether ATR might also regulate the timing and/or type of DSB repair on synapsed autosomes. I found numerous DSB foci on synapsed autosomes from early pachytene *Atr wt* cells (Fig 5.4B-D): 41 ± 27.1 foci for RAD51 (n=19), 67 ± 37.1 foci for DMC1 (n=19), and 196 ± 26.9 (n=36) for RPA. Interestingly, the absence of ATR resulted in significantly fewer foci present on synapsed chromosomes. This a reduction does not prove that the DSBs are being repaired it does suggest they might be. Being a DSB on a synapsed chromosome it could have been repaired via either IH or IS recombination. For each DSB marker

the foci incidence was: 28 ± 13.8 for RAD51 (n=19; 0.0131), 21.5 ± 19.3 for DMC1 (n=20; p<0.0001) and 141 ± 29.3 for RPA (n=32; p<0.0001;Fig 5.4 D; Mann-Whitney test). This finding demonstrates that loss of ATR does not lead to increased numbers of persistent DSBs in early pachytene, in contrast to findings in other recombination mutants such as *Dmc1 -/-* and *Msh5 -/-* (Pittman et al., 1998, Edelmann et al., 1999). Instead, it suggests that ATR modulates the kinetics of DSB repair in early pachynema at both asynapsed and synapsed chromosome regions.

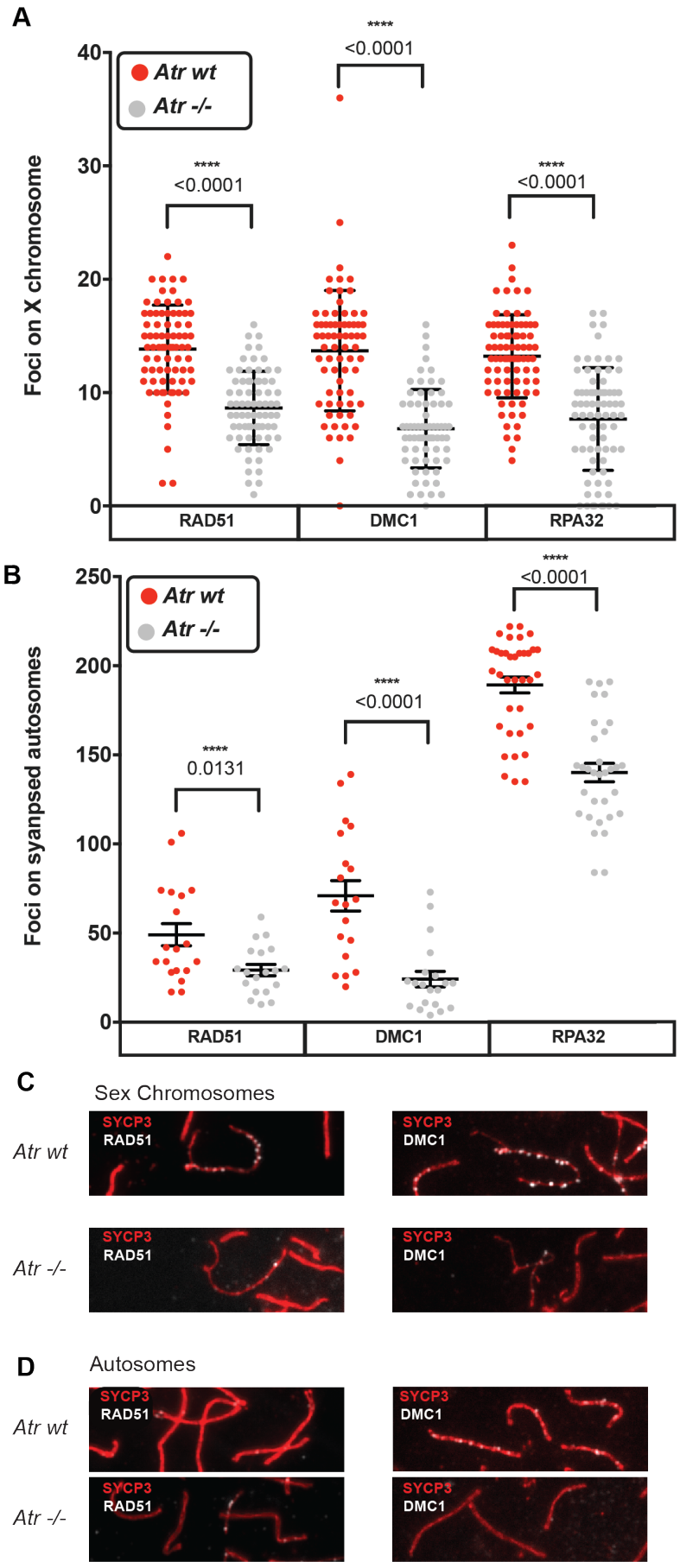

Figure 5.6 ATR regulates DSB kinetics on pachytene chromosomes

(**A**) The non-homologous regions of the large X chromosome (white arrowheads) have fewer RAD51, DMC1 and RPA32 foci in *Atr -/-* cells compared with *Atr wt*. (**B**) Homologous chromosomes also have fewer RAD51, DMC1 and RPA32 in *Atr -/-* cells compared with *Atr wt*. Bars, 10 μm. (**C-D**) Quantification of DSB foci in *Atr wt* and *Atr -/-* from (A-B); p-values from Mann-Whitney tests shown.

5.6 CO formation cannot be assessed in *Atr -/-* cells

In the remaining steps of meiotic recombination, RAD51, DMC1 and RPA are removed, and around 20-40 COs are formed per nucleus (Lipkin et al., 2002, Edelmann et al., 1996, Holloway et al., 2008). In mice the majority of CO formation is dependent on the MutLγ complex consisting of MLH3 and MLH1, antibodies against which can be used to visualize the MutLγ complex in wildtype late pachytene cells (Lipkin et al., 2002, Edelmann et al., 1996, Holloway et al., 2008). I therefore wished to determine whether ATR loss affected MLH3 focus formation.

In *Atr wt* males, I found that 71.8% (n=39) of early pachytene cells had at least one MLH3 focus (Fig 5.7A). By late pachynema, MLH3 foci were present in 95% (n=20) of cells, with at least one MLH3 focus present per chromosome pair (Fig 5.7B). Because meiosis in *Atr -/-* males arrests at mid pachynema (See Figure 3.3F), the latest cells that could be analysed in this model were in early pachynema. At this stage no MLH3 foci were seen in *Atr -/-* males (n=50; Fig 5.7C). These data support ATR having a role in CO maturation. However, given that MLH3 focus counts in wildtype males reach their peak after the point that *Atr -/-* spermatocytes arrest, a more detailed analysis was not possible.

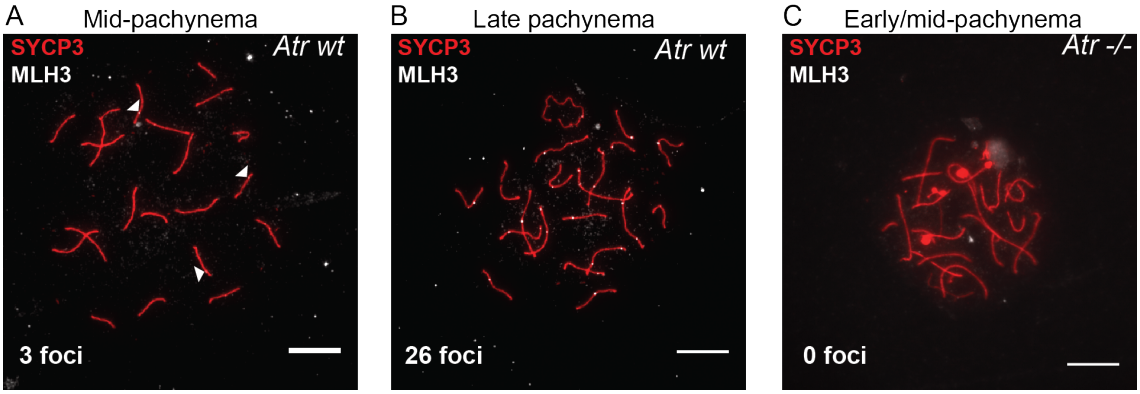

Figure 5.7 *Atr -/-* cells do not accumulate MLH3 by early/mid-pachynema

(**A**) *Atr wt* cells begin to recruit MLH3 foci (white arrowheads) in early to midpachynema. (**B**) The majority of *Atr wt* cells contain at least one MLH3 foci per chromosome by late pachynema. (**C**) In contrast MLH3 foci were absent from early/midpachytene *Atr -/-* cells. Focus counts indicated. Bars, 10 μm.

5.7 Discussion

The aim of this chapter was to determine whether ATR functions in meiotic recombination. I found that ATR is involved in three potentially distinct roles. Firstly, ATR regulates the length of SPO11-oligos in *Atm -/-* mice, suggesting an overlapping function for these kinases in an early stage of recombination. Secondly, while ATR is dispensable for normal DSB abundance, it is required for localisation of RAD51 and DMC1 at meiotic DSBs in late leptonema; a defect independent of recombination proteins DMC1 or ATM. Thirdly, meiotic ATR deficiency is distinct from many meiotic recombination mutants; e.g. *Dmc1 -/-* (Pittman et al., 1998) and *Msh5 -/-* (Edelmann et al., 1999), which have abundant unresolvable breaks during pachynema. In contrast, *Atr -/-* pachytene cells have fewer RAD51, DMC1 and RPA foci at early pachynema. Since all DSB markers are affected, this observation could indicate that ATR regulates the DSB repair process in pachytene cells.

My current data does not allow me to determine how loss of ATR causes these phenotypes. However, it does allow some conclusions to be drawn. Firstly, it appears that unlike ATM, ATR and its downstream substrates are dispensable for creation of normal numbers of meiotic DSBs. This possibility fits with recent data, which show that while ATM targets MRE11 and NBS1 are negative regulators of Spo11-oligo formation, the ATR target CHK2 is not required for normal Spo11-oligo complex levels (Pacheco et al., 2015). Furthermore, ATR can partially compensate for loss of ATM in generating Spo11-oligos of correct length. ATM/ATR could regulate the position where initial cleavage (nick) begins, or determine the extent of ssDNA resectioning, or both. In wildtype budding yeast it is known that nicking of ssDNA can occur up to 300 nucleotides away, approximately 100 nm away from the DSB (Garcia et al., 2011). Perhaps in *Atm -/-* cells the distance from the nick site to DSB increases, increasing further in *Atr -/- Atm -/-* cells. Alternatively, a reduction in the 3'-5' activity of nucleases would increase SPO11-oligo length and thus explain increased SPO11-oligo size(s). Multiple nucleases could act at this stage, some of which have candidate ATM/ATR phosphorylation motifs. The budding yeast nuclease, *SAE2*, is known to be phosphorylated by ATM/ATR to regulate meiotic resectioning (Cartagena-Lirola et al., 2006). Spo11-oligo nuclease activity might also be partially phosphorylation independent and partial

phosphorylation dependent, as shown by the differential meiotic DSB resection phenotypes of budding yeast *tel1*Δ and *tel1-kinase* dead alleles (Keeney et al., 2014).

The phenotype observed at leptonema in *Atr -/-* cells may indicate that ATR has a primary role in RAD51/DMC1 loading, alternatively, this may have been a secondary defect from the conversion of DSBs into resected single-stranded tails. In support of the former hypothesis, RAD51 loading was still impaired in the combined absence of ATR and ATM/DMC1. Evidence suggests that in response to DNA damage, RAD51 is capable of being phosphorylated by ATR and/or downstream checkpoint kinase CHK1 (Sorensen et al., 2005, Flott et al., 2011). It has also been shown that ATR phosphorylates CHK1 during meiosis (Fedoriw et al., 2015). It is tempting to postulate such a hypothetical phosphorylation cascade to explain this phenotype. However, I have two lines of argument against this. Firstly, the analysis of published RAD51 structure suggests access to the ATR-phosphorylation motif is not surface exposed (Conway et al., 2004) and thus phosphorylation is unlikely unless there are considerable conformational changes. Secondly, the CHK1-phosphorylation motif in RAD51 is not present in DMC1 (Sorensen et al., 2005) and, since both recombinases had similarly defective recruitment in late leptonema cells without ATR, describing a putative mechanism becomes significantly more complex. Finally, it would be useful for understanding ATR-dependent interactions between proteins associated with later steps in meiotic recombination like MSH4/5 (Kneitz et al., 2000, Edelmann et al., 1999) and CO markers MLH1/3 (Lipkin et al., 2002, Edelmann et al., 1996). This could be achieved by developing and characterising a model of *Atr -/-* in female meiosis, in which cells would likely progress beyond mid pachynema due to the absence of MSCI failure (Morelli and Cohen, 2005).

Chapter 6. The roles of ATR in meiotic checkpoints

Cell cycle checkpoints function as cellular quality control mechanisms that prevent cell cycle progression until key events have been achieved. The activation of meiotic checkpoints has been implicated in genetically derived infertility in mice and humans (Royo et al., 2010, de Vries et al., 2012). Thus, whilst activation of these checkpoints may confer infertility, disruption of the checkpoint can result in the survival of lower quality gametes and formation of aneuploid embryos.

Based upon function, checkpoint proteins are divided into sensors, mediators, transducers or effectors, which coordinate, delay and/or prevent cell-cycle progression. In somatic cells the PIKKs ATM, ATR and DNA-PK are the three sensor kinases that lead the response to DSBs, thereby signalling cell cycle arrest via phosphorylation of effector kinases CHK1 and CHK2 (Elledge, 1996).

Genetic experiments examining meiotic arrest phenotypes established that mice have two distinct prophase I checkpoints that cause arrest at stage IV, or midpachynema. The DNA damage dependent checkpoint operates in recombination mutants, e.g. *Dmc1*, *Msh5* and *Trip13*$^{mod/mod}$ mutants, responds to persistent meiotic DSBs, and causes arrest early in stage IV. ATM is involved in the DNA damage checkpoint, since removing this PIKK from recombination defective mutants like *Trip13*$^{mod/mod}$ males enabled spermatocytes to progress further than in single recombination mutants (Pacheco et al., 2015). The second, so-called DNA damage independent checkpoint operates in all models with asynapsis, including the recombination mutants listed above, as well as *Spo11* nulls (Barchi et al., 2005), F_1-hybrids (Turner, 2015, Bhattacharyya et al., 2014) and chromosomal translocation models (Odorisio et al., 1998, Turner et al., 2006). This checkpoint causes arrest later in stage IV. The trigger of the DNA damage independent checkpoint is less clear, but may be defective MSCI. MSCI is the transcriptional silencing of the heteromorphic sex chromosomes in male pachytene spermatocytes (Turner et al., 2004, Baarends et al., 2005). MSCI is mediated by serine-139 phosphorylation of histone H2AX (γH2AX) by ATR (Rogakou et al., 1998, Royo et al., 2013). Defective MSCI has been shown to be sufficient to cause stage IV arrest (Royo et al., 2010). Currently, this is hypothesised to occur because asynapsed

autosomes titrate ATR and other essential meiotic silencing proteins like BRCA1 from the sex chromosomes (Mahadevaiah et al., 2008, Pacheco et al., 2015).

In this chapter I will further investigate the relationship between ATR and meiotic checkpoints. I compare the requirements for ATR in the stage IV arrest of mutants that activate either the DNA damage dependent checkpoint or the DNA damage independent checkpoints and examine different compound PIKK mutant mice.

6.1 The checkpoint arrest persists in *Atr -/-* prophase I mutants

First I investigated the effect of deleting *Atr* in mutants with both asynapsis and persistent DNA damage (*Atm -/-, Dmc1-/-* and *Msh5 -/-*) and in mutants with asynapsis but no persistent DNA damage (*Spo11 -/-*). Although *Atr* could have a role in prophase I checkpoints, I predicted that stage IV arrest would remain in all these double mutants, because MSCI would not occur. I therefore compared the histology of *Atr wt Atm -/-*, *Atr wt Dmc1-/-*, *Atr wt Msh5 -/-* and *Atr wt Spo11 -/-* mice to littermates without ATR: *Atr -/- Atm -/-*, *Atr -/- Dmc1 -/-*, and *Atr -/- Msh5 -/-* and *Atr -/- Spo11 -/-* (Fig 6.2C-J). *Atr wt* and *Atr -/-* genotypes are also included to permit comparisons (Fig 6.2A,B).

In the *Atr wt,* there was no stage IV arrest, and post-meiotic cells were seen. However, in all of the other models, apoptosis at stage IV was seen (Fig 6.2C-J). This supports data that MSCI failure is a major cause for stage IV arrest in spermatocytes.

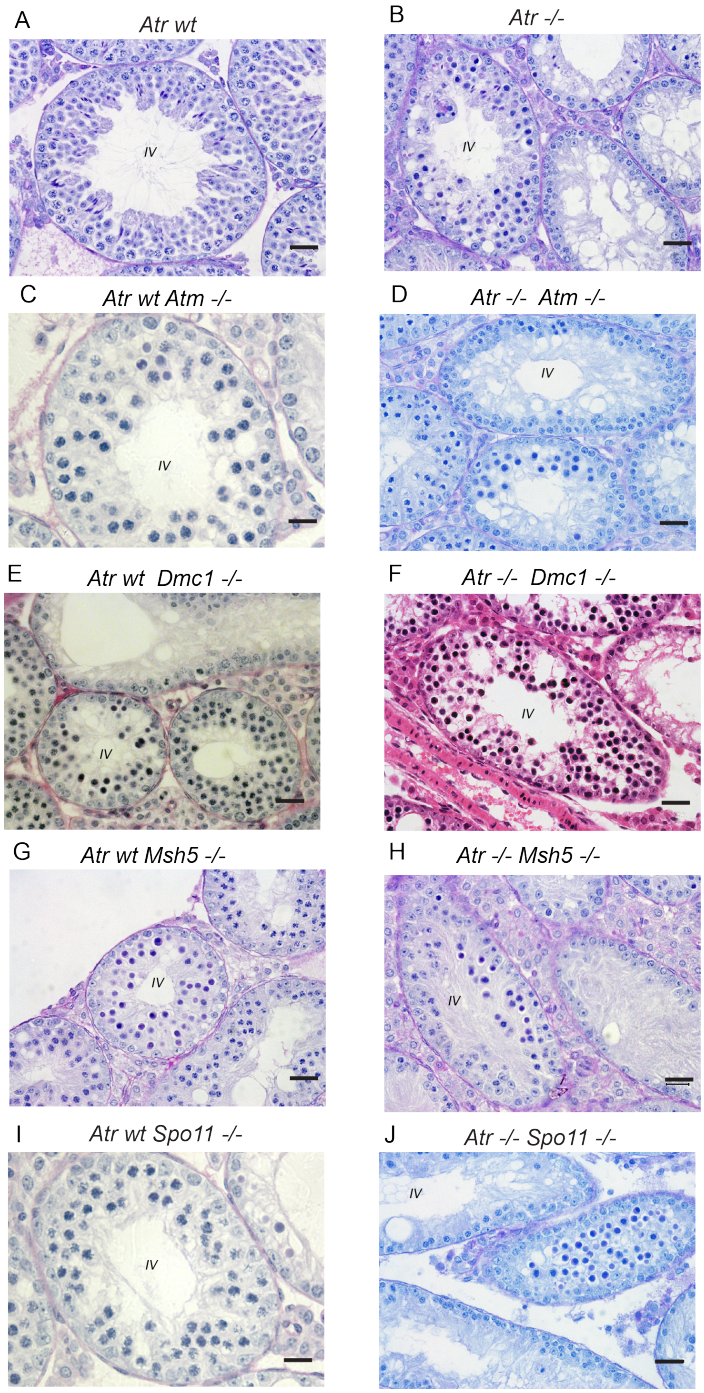

Figure 6.1 Loss of ATR does not rescue stage IV arrest of mutant mice

Testis sections were stained with Periodic-acid Schiff (P-AS)*: (**A**) spermatogenesis is normal in *Atr wt* and no apoptotic pachytene spermatocytes are present in the labelled stage IV tubule. In contrast apoptotic cells can be seen in all remaining panels (**B-J**). This is due to the stage IV block persisting in mutants with ATR (left column) and without ATR (right column). Scale bar, 50 µm. *Haematoxylin and eosin section used instead of low quality P-AS section.

6.2 The stage IV arrest persists in a *PIKK-null* model

An alternative hypothesis to MSCI defects causing arrest in these mutants, including *Atm -/- Atr -/-,* is that a checkpoint is still operating, and that it is dependent on the third PIKK, PRKDC. I therefore studied germ cell progress in mice deficient for all three PIKKs. I was unable to generate mice that were homozygous for both *Atm* and a hypomorphic mutant allele of *Prkdc,* termed *Prkdc*^{scid} (Bosma et al., 1983). This is due to a synthetic lethality between PRKDC and ATM in embryogenesis; mice deficient for both of these genes arrest as early embryos (Gurley and Kemp, 2001). To overcome this problem I replaced the *Atm* null mutation with an *Atm flox* conditional allele (Callen et al., 2009) and combined it with the *Ngn3-Cre* driver line to create a series of PIKK mutants.

I found that spermatogenesis was normal in *Prkdc*$^{scid/scid}$ males (Fig 6.2A). Consistent with earlier work, there was no histological defects (Bellani et al., 2005). The stage IV block also remained in *Atr -/- Prkdc*$^{scid/scid}$ compound mutants (Fig 6.2B). Finally, in mice deficient for all three DNA-damage checkpoint kinases, pachytene spermatocytes also arrested at stage IV (Fig 6.C). This demonstrated that genetically removing the PIKKs in combination does not prevent the stage IV arrest.

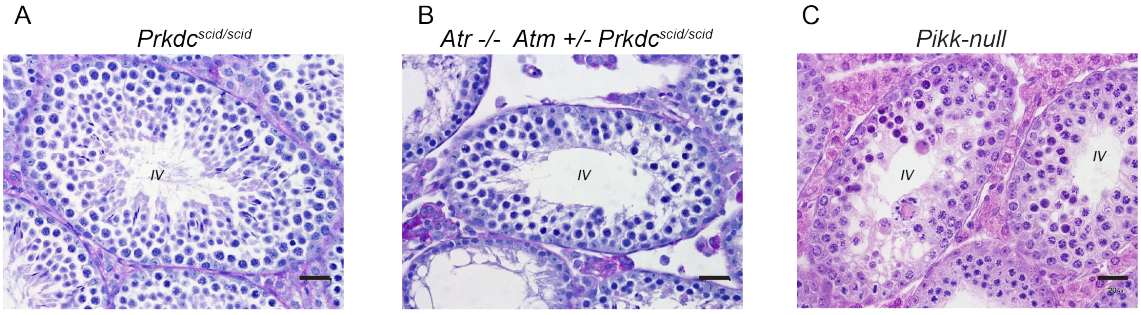

Figure 6.2 Persistent stage IV block in PIKK meiotic mutants

Testis sections were stained with P-AS sections: (**A**) despite defective PRKDC activity, no defects in spermatogenesis were present in *Dnapk*$^{scid/scid}$. (**B**) In the absence of ATR and PRKDC, the stage IV block remains. (**C**) Pachytene cells deficient for all three classic sensor DNA-damage checkpoint kinases also trigger the arrest at stage IV. Scale bar, 50 μm.

6.3 CHK2 phosphorylation staining in male meiosis is non-specific

In somatic cells, CHK2 is a critical effector kinase that functions downstream of ATM to bring about in cell cycle arrest following DNA damage (van Vugt et al., 2010). In somatic cells, ATM, phosphorylates CHK2 in response to DSBs (van Vugt et al., 2010). However, in meiosis ATR may function directly upstream of CHK2 given that: (a) it appears that ATM and ATR have specialized roles in meiosis (Barchi et al., 2008, Pacheco et al., 2015, Lange et al., 2011); (b) *Atm*-deficiency does not rescue *Dmc1 -/-* oocyte losses (Elias El Inati *pers comms*) and (c) *Chk2*-deficiency partially rescues the post-natal oocyte depletion in *Dmc1 -/-* and *Atm* -/- mice (Bolcun-Filas et al., 2014). These findings suggested ATR-dependent activation of CHK2 could be important for checkpoints in meiotic cells.

To test this hypothesis, I examined whether ATR was required for the phosphorylation of CHK2 in male meiosis at a well-characterised phosphorylation site, threonine 68 (van Vugt et al., 2010). I found that pCHK2-T68 staining was present in 96.7% of early pachytene cells in *Atr wt* males (n=60; Fig 6.3A). Within these cells, pCHK2-T68 was localised to the XY pair, which is consistent with CHK2 phosphorylation playing a role in monitoring MSCI and/or asynapsis. I then examined pCHK2-T68 staining on the XY bivalent in *Atr -/-* pachytene cells. I found that pCHK2-T68 was absent in 100% of cells (n=50; Fig 6.3B). This observation suggested that phosphorylation of CHK2-T68 during pachynema is dependent on ATR and it could potentially be a direct interaction.

To confirm this I needed a negative control experiment. To show that my staining was specific, I therefore repeated my immunostaining on testes from *Chk2 -/-* mice (Hirao et al., 2000). Surprisingly, the epitope recognised by the pCHK2-T68 antibody was preserved on the XY pair in early pachytene cells in this *Chk2 -/-* mutant (Fig 6.3C). This finding calls into question the specificity of the pCHK2-T68 antibody staining on the XY pair. Thus, the antibody was not suitable for assessing whether ATR regulates CHK2-T68 phosphorylation.

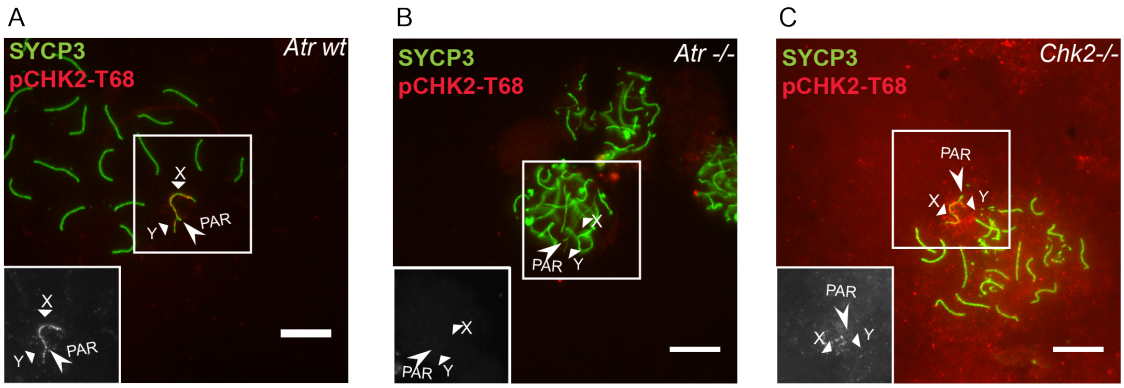

Figure 6.3 CHK2 phosphorylation appears ATR-dependent

(A) Consistent with roles in meiotic checkpoints pCHK2-T68 was present on the XY bivalent in *Atr wt;* (**B**) suggestive of ATR-dependency pCHK2 is lost in *Atr -/-;* (**C**) the absence of CHK2 prevents specific pCHK2-T68 binding, however equivalent staining as *Atr wt*, which is non-specific, is also present.

6.4 Pseudo-sex body formation is ATR-dependent

I previously generated *Atr -/- Spo11 -/-* mice to test the role of ATR in SC formation (Fig 4.3) and the DNA-damage independent checkpoint. However, these mutants also allowed me to determine whether formation of the pseudo-sex body (PSB) is ATR-dependent. The PSB, marked by γH2AX, could be seen in *Spo11 -/-* testis sections by immunohistochemistry (IHC) (Fig 6.4A). In equivalently staged IHC testis sections from *Atr -/- Spo11 -/-* males, there was a distinct lack of γH2AX signals in the SYCP3-containing meiotic cells. This finding suggested that PSB formation in *Spo11 -/-* males is ATR-dependent. To examine this phenotype more closely, I performed IF using the same antibodies. 96% (n=50; Fig 6.4C) of midpachytene cells from *Spo11 -/-* mice contained a PSB, whereas no PSB-like staining was seen in *Atr -/- Spo11 -/-* males (n=50; Fig 6.4D). This data demonstrates that PSB formation is indeed ATR-dependent.

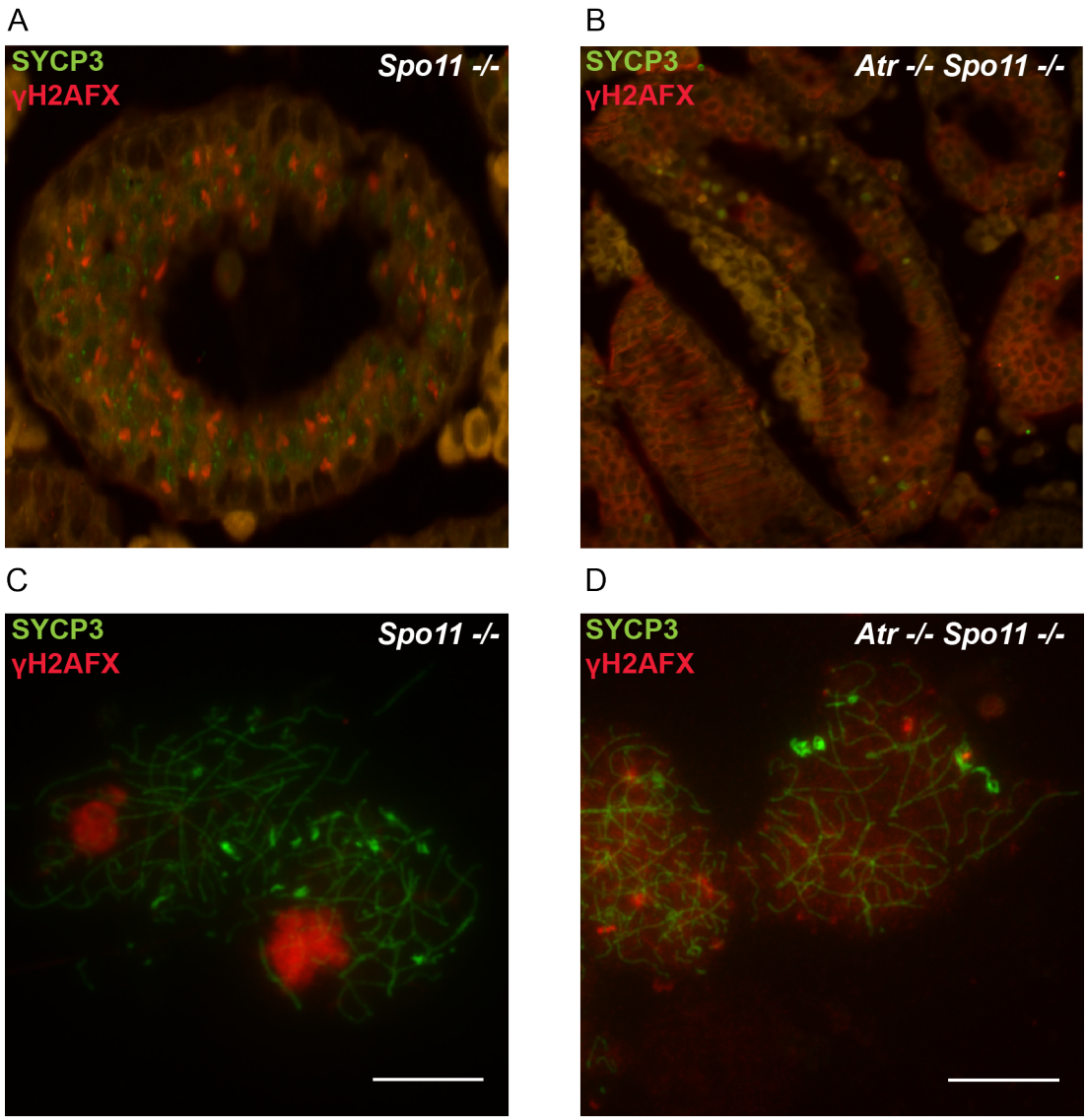

Figure 6.4 Pseudo-sex-body formation is ATR-dependent

(**A**) Distinct γH2AX domains within each pachytene cell denote the PSB in *Spo11 -/-*. (**B**) In *Atr -/- Spo11 -/-,* whilst the tubule shown has a significantly reduced number of germ cells (SYCP3 positive cells), in the remaining cells γH2AX is absent. Monitoring individual nuclei via IF in (**C**) two *Spo11 -/-* pachytene cells each with PSBs; whereas (**D**) *Atr -/- Spo11 -/-* does not contain a PSB. Scale bar, 10 μm.

6.5 The apoptotic wave of γH2AX is PRKDC dependent

No roles have been found for PRKDC in meiosis (Bellani et al., 2005). This may be because during meiosis NHEJ is down regulated (Goedecke et al., 1999). Using my series of PIKK mutants, I wanted to determine whether there was any genetic evidence that would argue for a role for PRKDC in meiosis, particularly in perturbed situations that would compromise normal meiotic recombination. It is known that in meiosis there are two separate waves of γH2AX: the first occurs in leptotene/zygotene cells (Mahadevaiah et al., 2001) and is dependent on ATM (Barchi et al., 2005) (Bellani et al., 2005, Turner et al., 2004, Celeste et al., 2002). The second wave occurs in pachytene cells and ATR is responsible (Royo et al., 2013, see also section 3.5). I assessed SYCP3 and γH2AX staining using IHC to monitor whether the absence of PRKDC altered γH2AX staining in meiotic sub-stages.

I first confirmed the specificity of the γH2AX antibody by performing IHC on testis sections from *H2AX -/-* males. γH2AX staining was absent in these testes, which confirmed that the antibody is specific (Fig 6.5A). Next, I performed IHC analysis for SYCP3 and γH2AX on PIKK mutants. I found that γH2AX staining in leptonema/zygonema and pachynema was normal in $Prkdc^{scid/scid}$ testis (Fig 6.5B) and hence is not dependent on PRKDC. In *Atm -/- Dnapk*$^{scid/scid}$ males, the first wave of γH2AX in lepotene/zygotene cells was absent, whilst the second wave of meiotic γH2AX in pachytene cells was present (Fig 6.5C). This pattern is consistent with γH2AX staining in *Atm -/-* males (Bellani et al., 2005). In *Atr -/- Atm -/-* $Prkdc^{+/scid}$ samples, the leptotene/zygotene and pachytene cells respectively lacked the first and second waves of γH2AX, as anticipated from analysis of *Atm -/-* males (Bellani et al., 2005) and *Atr -/-* males (Royo et al., 2013). However, γH2AX staining was seen in apoptotic pachytene cells at stage IV (Fig 6.5D). γH2AX is a known phosphotarget of kinases ATM, ATR and PRKDC (Marechal and Zou, 2013). This result suggested that γH2AX staining of apoptotic pachytene cells occurs independently of both ATM and ATR.

To confirm if apoptotic γH2AX staining in stage IV cells was dependent on PRKDC, I performed IHC on *Atr -/- Atm -/-* $Prkdc^{scid/scid}$ samples. No γH2AX could be seen in

any cells from all meiotic sub-stages (Fig 6.5E). This infers that PRKDC phosphorylates H2AX in apoptotic conditions and thus that PRKDC is able to function in meiosis. In conclusion, I present a model of γH2AX staining in male meiotic cells and suggest which kinase is primarily responsible for each wave (Fig 6.5F).

Figure 6.5 Apoptotic γH2AX is PRKDC dependent

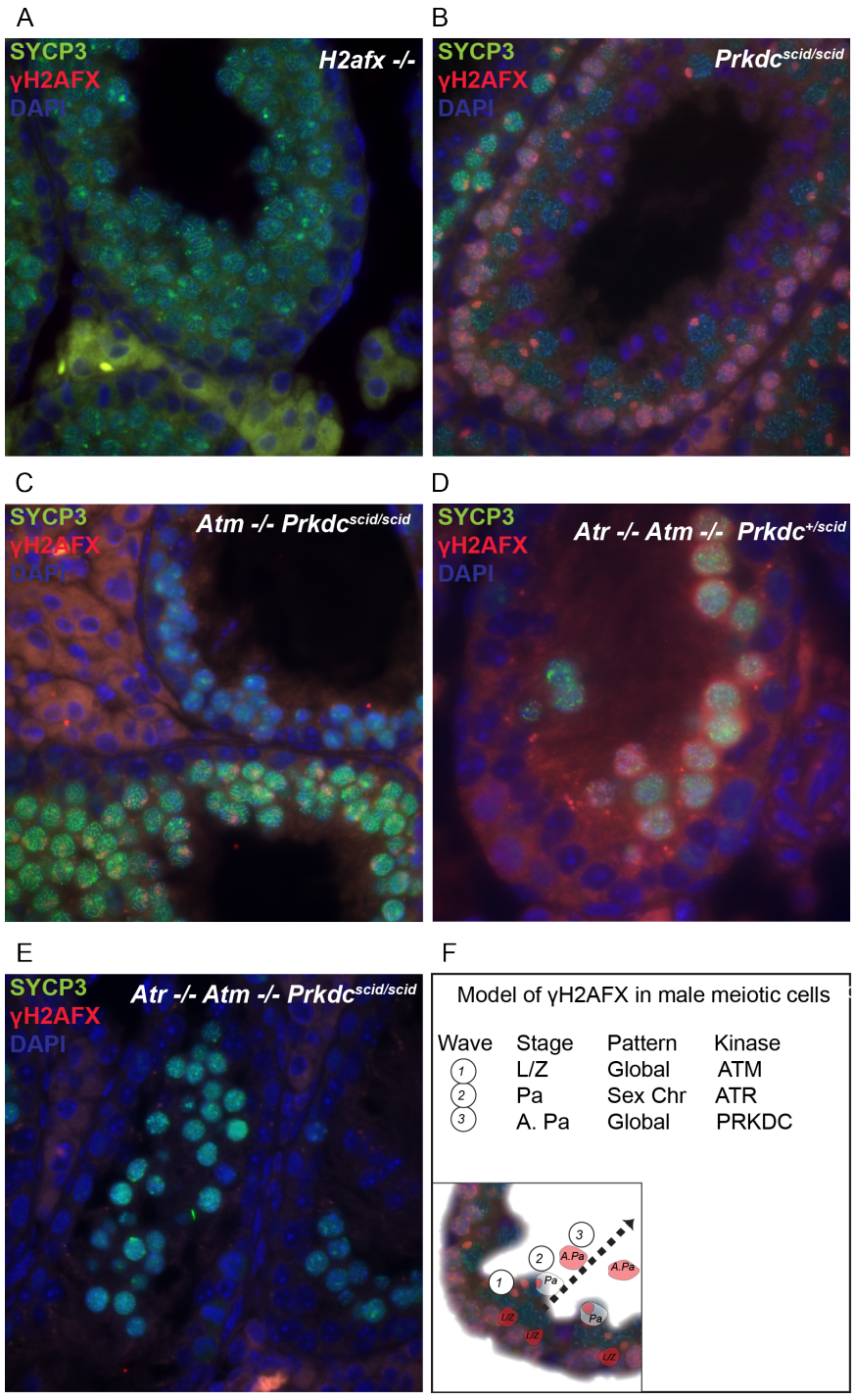

(**A**) Mice homozygous for *Prkdc*$^{scid/scid}$ have normal γH2AX staining and normal spermatogenesis: first wave (DSB-formation) and the second wave (MSCI) of γH2AX are preserved. (**B**) In *H2AX -/-*, γH2AX is prevented and no staining is present even in apoptotic pachytene cells. (**C**) In *Atm -/- Prkdc*$^{scid/scid}$ the first wave (DSB-formation) is lost and the second wave (MSCI) is preserved, as has been shown for *Atm -/-* previously (Bellani et al., 2005, Turner et al., 2005). (**D**) In *Atr -/- Atm -/- Prkdc*$^{+/scid}$, whilst the first wave (DSB-formation) and the second wave (MSCI) are lost, a third apoptotic wave of γH2AX cells is present and prominent in pachytene cells. (**E**) The third apoptotic wave of pachytene cells is lost in *Atr -/- Atm -/- Prkdc*$^{scid/scid,}$ suggesting that it is PRKDC dependent. (**F**) Model of γH2AX in male meiotic cells, for the first (DSB-formation), the second (MSCI) and third (apoptotic) waves with the predominately responsible kinases indicated.

6.6 Discussion

The aim of this chapter was to investigate the roles of ATR in meiotic prophase I checkpoints. I have been able to determine that *Atr*-deficiency does not rescue the checkpoint arrest seen in both DNA damage dependent and DNA damage independent mutant spermatocytes. Furthermore, mutant male mice deficient for all three DNA damage sensor kinases also arrest at stage IV. This latter finding suggests one of two possibilities: namely that the stage IV arrest is not mediated by the PIKKs, or that in the absence of the PIKKs other mechanisms, e.g. MSCI-failure, can cause stage IV arrest. Future analyses in females, in which MSCI does not occur and where there is a larger temporal difference between DNA damage dependent (perinatal loss) and DNA damage independent (post-natal) oocyte loss, will allow these possibilities to be discriminated.

A series of publications from the Schemti lab (Rinaldi et al., 2017a, Rinaldi et al., 2017b, Bolcun-Filas et al., 2014) have genetically demonstrated that the canonical cell-cycle effector kinase CHK2 is important the restoration preservation of fertile regulator of the oocyte DNA damage dependent checkpoint (Bolcun-Filas et al., 2014), I investigated the role of ATR in CHK2 phosphorylation. I found that the pCHK2-T68 antibody was non-specific; therefore I am unable to make any conclusion about the role of CHK2 phosphorylation in mediating the stage IV block observed in the mutant models. However, the finding does serve to illustrate the importance of appropriate controls when using antibodies. In the future, it will be essential to use specific reagents to determine the status of the PIKK effector kinases in the DNA damage dependent and DNA damage independent checkpoints. These findings will allow us to conclude whether these checkpoints trigger different downstream effector pathways.

In the remaining section, I analysed compound mutant mice and was able to demonstrate for the first time that ATR is responsible for the γH2AX associated with the formation of the PSB in *Spo11-/-* mice. Also, I was able to infer that PRKDC mediates a third wave of γH2AX within degenerating midpachytene cells. This finding implies that components of the NHEJ pathway may be active in

mammalian meiosis, contrary to previous suggestions (Goedecke et al., 1999). Further experimentation is required to determine whether this apoptotic γH2AX is present in both DNA damage dependent and DNA damage independent mutants, as well as in female meiosis, and whether alternative repair pathways like NHEJ are activated in conditions where canonical meiotic HR is disrupted.

Chapter 7. Discussion

7.1 General summary

How quality control in mammalian meiotic prophase is achieved remains unclear. Prophase I is an instrumental part of gametogenesis. It couples the repair of genotoxic meiotic DSBs to the accurate “reshuffling and dealing” of maternal and paternal chromatids required to generate euploid sperm and ova. For decades there has been interest in understanding how meiotic cells tolerate and coordinate genome-wide DDR. Generally, cell cycle progression is ensured by molecular mechanisms known as checkpoints. There are medical needs to understand whether canonical DDR-checkpoints are present in meiosis, or if there are non-canonical meiosis-specific adaptations of the core DDR-checkpoint machinery. Using murine models of conditional *Atr*-deficiency in male meiosis, in order to overcome the embryonic lethality of *Atr -/-* mice, my thesis supports the conclusion that ATR is fundamental to meiotic prophase and not exclusively a checkpoint response protein. The results herein demonstrate that ATR is required for chromosome synapsis and meiotic recombination. Analysis of compound *Atr*-deficient mutants permitted the molecular and genetic dissection of the synapsis and recombination defects I found in *Atr -/-* spermatocytes (See Chapter 3). My analysis of *Atr*-deficient DNA damage-dependent and DNA damage-independent compound mutants, as well as the *Pikk*-nulls (See Chapter 6), adds further evidence that the stage IV arrest of various male meiotic models can be explained by MSCI failure.

7.2 Fundamental roles of ATR in promoting chromosome synapsis

A major finding of this thesis is that ATR is required for meiotic chromosome synapsis and that this function is at least partially independent of meiotic recombination (see Chapter 4). Further analysis showed that SYCP3, SYCE1 and SYCE2 localisation were normal in the absence of ATR. Future experiments are required to tell how ATR regulates synapsis and whether its functions are phosphorylation-dependent or not. In addition to the known ATR phosphotargets HORMAD1 and HORMAD2 (Royo et al., 2013), I have presented data suggesting that SMC3 is an ATR phosphotarget.

Bioinformatics and literature studies, together with mass spectroscopy experiments, should help identify additional potential candidates from the components of meiotic chromosomal axes containing the ATM/ATR consensus motifs (Huttlin et al., 2010, Fukuda et al., 2012, Yang et al., 2006). A conditional *Smc3* mutant mouse model (Viny et al., 2015), could be combined with either a *Stra8-Cre* or *Ngn3-Cre* Cre-driver to facilitate the study of *Smc3* -/- spermatocytes. In terms of functional consequences, it would be necessary to validate the functional consequences of loss of phosphorylated residues relative to published phenotypes of complete genetic knockouts using genome editing like CRISPR/Cas9 (REF). Whilst this is yet to be done for HORMAD1-S375 or HORMAD2-S271, it would be an important step in determining the consequences of pSMC3 loss by characterising the phenotype of conditional *Smc3 -/-* spermatocytes.

7.3 Fundamental roles of ATR in DNA DSB repair

Next, I assayed the role of ATR in recombination. In *Atr*-deficient spermatocytes, levels of Spo11-oligo complexes, together with RPA foci counts, were unaffected in late leptotene cells, suggesting that ATR does not regulate DSB abundance, although this does not rule out perturbed DSB localisation However, I was able to find at least three important roles for ATR in subsequent steps in meiotic recombination (see chapter 5).

Firstly, ATR functions redundantly in the absence of ATM to regulate Spo11-oligo length. The influence of ATR on Spo11-oligo length could be at the level of DSB placement or subsequent resectioning. The sequencing and mapping of these longer Spo11-oligos, and comparisons between *Atr -/-* and *Atm -/-* mutants, might help tease apart these possibilities and better understand the overall functions of the PIKKs in early recombination. Encouraging steps have already been made in this regard in budding yeast (Mimitou et al., 2017).

Secondly, RAD51 and DMC1 recruitment was diminished by the absence of ATR. It is unclear whether these interactions between the recombinases and ATR are evolutionarily conserved. A study of the *A. thaliana* orthologs found that *atr* mutants do have significantly reduced RAD51 counts (Kurzbauer et al., 2012); however they also found that defective DMC1 recruitment in a *rad51* mutant strain was ATR-dependent and that the inactivation of *atr* restored DMC1 foci counts in *atr rad51* (Kurzbauer et al., 2012). Unfortunately, it was out of the scope of their study to investigate RAD51 counts in *atr dmc1* double mutant strains.

Thirdly, the kinetics of DSB repair during pachytene is significantly altered in the absence of ATR. This finding suggests that ATR regulates the timing and/or type of DSB repair that takes place. The next step in characterising the roles of ATR in meiotic recombination would be to examine intermediate recombination markers like MSH4 and MSH5 (Kneitz et al., 2000) (Edelmann et al., 1999).

Finally, it is important to determine whether ATR regulates CO formation in mice, in a manner similar to that first described in *D. melanogaster* (Carpenter, 1979). To

achieve this aim, it would be necessary to investigate the localisation of additional CO markers like MLH1 in *Atr -/-* spermatocytes. Any phenotype in CO localisation could be further investigated by analysing immunostaining for more recently identified murine CO-promoting factors RNF212, HEI10 and CNTD1 in *Atr* -/- cells, perhaps utilising the *Atr -/- Stra8-Cre* strain described in Chapter 3 (Hunter, 2015).

7.4 The roles of ATR and other kinases in prophase I checkpoint

Another important finding in this thesis was that the stage IV or midpachytene checkpoint in male meiosis is preserved in mice lacking all PIKK sensor kinases. The cause of arrest in these mice, and in other midpachytene arrest mutants, could be defective MSCI rather than activation of a checkpoint, as suggested previously (Royo et al., 2010). This possibility could be investigated by looking at female meiosis, in which MSCI does not occur. Meiotic checkpoints occur at different time points in female and males (See Chapter 6). Male germ cells with problems in meiotic recombination or synapsis arrest around two weeks after birth, at stage IV. In contrast, female germ cells with DNA damage defects arrest perinatally, while those with synaptic defects are eliminated weeks later (Di Giacomo et al., 2005), since oocytes enter meiosis prior to birth.

Analysing the functions of ATR in female mouse meiosis is difficult, because a germ cell specific CRE-driver that is active at this very early stage of oogenesis is not available. The establishment of such a CRE-driver would be important to determine whether the ATR-dependent meiotic phenotypes that I identified are male-specific. To determine whether ATR is involved in the DNA-damage dependent and independent checkpoints oocyte counts would have to be performed in recombination and synapsis mutants carrying an *Atr* deletion. A recent study demonstrated that CHK2 functions in the DNA-damage dependent checkpoint arrest of recombination defective mutant oocytes (Bolcun-Filas et al., 2014). It would be interesting to determine whether ATR acts upstream of CHK2 in this checkpoint pathway. Undoubtedly this is an exceptionally interesting and important area for future meiotic research.

Finally, in addition to CHK2 phosphorylation, CHK1 phosphorylation and degradation of cell cycle regulator CDC25A are key molecular steps in canonical checkpoint arrest (Marechal and Zou, 2013). It would be important to investigate the status of CHK1/2 and CDC25A, as well as pro-apoptotic factors p63, BAX, PUMA and NOXA in wildtype and recombination / synapsis defective mice. These factors have already been shown to have a role in either preserving oocyte loss

with ages, or preventing female germ cell losses in response to exogenous DNA damage (Suh et al., 2006, Perez et al., Kerr et al., 2012), and therefore are good candidates for mediating the DSB-dependent and independent checkpoint pathways.

Chapter 8. References

ABDU, U., BRODSKY, M. & SCHUPBACH, T. 2002. Activation of a meiotic checkpoint during Drosophila oogenesis regulates the translation of Gurken through Chk2/Mnk. *Curr Biol,* 12**,** 1645-51.

ADAMS, I. R. & MCLAREN, A. 2002. Sexually dimorphic development of mouse primordial germ cells: switching from oogenesis to spermatogenesis. *Development,* 129**,** 1155-64.

AHMED, E. A. & DE ROOIJ, D. G. 2009. Staging of mouse seminiferous tubule cross-sections. *Methods Mol Biol,* 558**,** 263-77.

ALLERS, T. & LICHTEN, M. 2001. Differential timing and control of noncrossover and crossover recombination during meiosis. *Cell,* 106**,** 47-57.

ASHLEY, T., GAETH, A. P., CREEMERS, L. B., HACK, A. M. & DE ROOIJ, D. G. 2004. Correlation of meiotic events in testis sections and microspreads of mouse spermatocytes relative to the mid-pachytene checkpoint. *Chromosoma,* 113**,** 126-36.

BAARENDS, W. M., WASSENAAR, E., VAN DER LAAN, R., HOOGERBRUGGE, J., SLEDDENS-LINKELS, E., HOEIJMAKERS, J. H., DE BOER, P. & GROOTEGOED, J. A. 2005. Silencing of unpaired chromatin and histone H2A ubiquitination in mammalian meiosis. *Mol Cell Biol,* 25**,** 1041-53.

BAKER, C. L., WALKER, M., KAJITA, S., PETKOV, P. M. & PAIGEN, K. 2014. PRDM9 binding organizes hotspot nucleosomes and limits Holliday junction migration. *Genome Res,* 24**,** 724-32.

BANNISTER, L. A., REINHOLDT, L. G., MUNROE, R. J. & SCHIMENTI, J. C. 2004. Positional cloning and characterization of mouse mei8, a disrupted allelle of the meiotic cohesin Rec8. *Genesis,* 40**,** 184-94.

BARCHI, M., MAHADEVAIAH, S., DI GIACOMO, M., BAUDAT, F., DE ROOIJ, D. G., BURGOYNE, P. S., JASIN, M. & KEENEY, S. 2005. Surveillance of different recombination defects in mouse spermatocytes yields distinct responses despite elimination at an identical developmental stage. *Mol Cell Biol,* 25**,** 7203-15.

BARCHI, M., ROIG, I., DI GIACOMO, M., DE ROOIJ, D. G., KEENEY, S. & JASIN, M. 2008. ATM promotes the obligate XY crossover and both crossover control and chromosome axis integrity on autosomes. *PLoS Genet,* 4**,** e1000076.

BARLOW, A. L., BENSON, F. E., WEST, S. C. & HULTEN, M. A. 1997. Distribution of the Rad51 recombinase in human and mouse spermatocytes. *EMBO J,* 16**,** 5207-15.

BARLOW, C., LIYANAGE, M., MOENS, P. B., TARSOUNAS, M., NAGASHIMA, K., BROWN, K., ROTTINGHAUS, S., JACKSON, S. P., TAGLE, D., RIED, T. & WYNSHAW-BORIS, A. 1998. Atm deficiency results in severe meiotic disruption as early as leptonema of prophase I. *Development,* 125**,** 4007-17.

BAUDAT, F., BUARD, J., GREY, C., FLEDEL-ALON, A., OBER, C., PRZEWORSKI, M., COOP, G. & DE MASSY, B. 2010. PRDM9 is a major determinant of meiotic recombination hotspots in humans and mice. *Science,* 327**,** 836-40.

BAUDAT, F., IMAI, Y. & DE MASSY, B. 2013. Meiotic recombination in mammals: localization and regulation. *Nat Rev Genet,* 14**,** 794-806.

BAUDAT, F., MANOVA, K., YUEN, J. P., JASIN, M. & KEENEY, S. 2000. Chromosome synapsis defects and sexually dimorphic meiotic progression in mice lacking Spo11. *Mol Cell,* 6**,** 989-98.

BEAN, C. J., SCHANER, C. E. & KELLY, W. G. 2004. Meiotic pairing and imprinted X chromatin assembly in Caenorhabditis elegans. *Nat Genet,* 36**,** 100-5.

BELLANI, M. A., ROMANIENKO, P. J., CAIRATTI, D. A. & CAMERINI-OTERO, R. D. 2005. SPO11 is required for sex-body formation, and Spo11 heterozygosity rescues the prophase arrest of Atm-/- spermatocytes. *J Cell Sci,* 118**,** 3233-45.

BELLVE, A. R., CAVICCHIA, J. C., MILLETTE, C. F., O'BRIEN, D. A., BHATNAGAR, Y. M. & DYM, M. 1977. Spermatogenic cells of the prepuberal mouse. Isolation and morphological characterization. *J Cell Biol,* 74**,** 68-85.

BERGERAT, A., DE MASSY, B., GADELLE, D., VAROUTAS, P. C., NICOLAS, A. & FORTERRE, P. 1997. An atypical topoisomerase II from Archaea with implications for meiotic recombination. *Nature,* 386**,** 414-7.

BERKOWITZ, K. M., SOWASH, A. R., KOENIG, L. R., URCUYO, D., KHAN, F., YANG, F., WANG, P. J., JONGENS, T. A. & KAESTNER, K. H. 2012. Disruption of CHTF18 causes defective meiotic recombination in male mice. *PLoS Genet,* 8**,** e1002996.

BHALLA, N. & DERNBURG, A. F. 2005. A conserved checkpoint monitors meiotic chromosome synapsis in Caenorhabditis elegans. *Science,* 310**,** 1683-6.

BHATTACHARYYA, T., REIFOVA, R., GREGOROVA, S., SIMECEK, P., GERGELITS, V., MISTRIK, M., MARTINCOVA, I., PIALEK, J. & FOREJT, J. 2014. X chromosome control of meiotic chromosome synapsis in mouse inter-subspecific hybrids. *PLoS Genet,* 10**,** e1004088.

BISHOP, D. K., PARK, D., XU, L. & KLECKNER, N. 1992. DMC1: a meiosis-specific yeast homolog of E. coli recA required for recombination, synaptonemal complex formation, and cell cycle progression. *Cell,* 69**,** 439-56.

BISIG, C. G., GUIRALDELLI, M. F., KOUZNETSOVA, A., SCHERTHAN, H., HOOG, C., DAWSON, D. S. & PEZZA, R. J. 2012. Synaptonemal complex components persist at centromeres and are required for homologous centromere pairing in mouse spermatocytes. *PLoS Genet,* 8**,** e1002701.

BISWAS, U., WETZKER, C., LANGE, J., CHRISTODOULOU, E. G., SEIFERT, M., BEYER, A. & JESSBERGER, R. 2013. Meiotic cohesin SMC1beta provides prophase I centromeric cohesion and is required for multiple synapsis-associated functions. *PLoS Genet,* 9**,** e1003985.

BLITZBLAU, H. G. & HOCHWAGEN, A. 2013. ATR/Mec1 prevents lethal meiotic recombination initiation on partially replicated chromosomes in budding yeast. *Elife,* 2**,** e00844.

BOLCUN-FILAS, E., COSTA, Y., SPEED, R., TAGGART, M., BENAVENTE, R., DE ROOIJ, D. G. & COOKE, H. J. 2007. SYCE2 is required for synaptonemal complex assembly, double strand break repair, and homologous recombination. *J Cell Biol,* 176**,** 741-7.

BOLCUN-FILAS, E., HALL, E., SPEED, R., TAGGART, M., GREY, C., DE MASSY, B., BENAVENTE, R. & COOKE, H. J. 2009. Mutation of the mouse Syce1 gene disrupts synapsis and suggests a link between synaptonemal complex structural components and DNA repair. *PLoS Genet,* 5**,** e1000393.

BOLCUN-FILAS, E., RINALDI, V. D., WHITE, M. E. & SCHIMENTI, J. C. 2014. Reversal of female infertility by Chk2 ablation reveals the oocyte DNA damage checkpoint pathway. *Science,* 343**,** 533-6.

BORDE, V. 2007. The multiple roles of the Mre11 complex for meiotic recombination. *Chromosome Res,* 15**,** 551-63.

BOSMA, G. C., CUSTER, R. P. & BOSMA, M. J. 1983. A severe combined immunodeficiency mutation in the mouse. *Nature,* 301**,** 527-30.

BRICK, K., SMAGULOVA, F., KHIL, P., CAMERINI-OTERO, R. D. & PETUKHOVA, G. V. 2012. Genetic recombination is directed away from functional genomic elements in mice. *Nature,* 485**,** 642-5.

BROOKER, A. S. & BERKOWITZ, K. M. 2014. The roles of cohesins in mitosis, meiosis, and human health and disease. *Methods Mol Biol,* 1170**,** 229-66.

BROWN, E. J. & BALTIMORE, D. 2000. ATR disruption leads to chromosomal fragmentation and early embryonic lethality. *Genes Dev,* 14**,** 397-402.

BROWN, E. J. & BALTIMORE, D. 2003. Essential and dispensable roles of ATR in cell cycle arrest and genome maintenance. *Genes Dev,* 17**,** 615-28.

BROWN, M. S., GRUBB, J., ZHANG, A., RUST, M. J. & BISHOP, D. K. 2015. Small Rad51 and Dmc1 Complexes Often Co-occupy Both Ends of a Meiotic DNA Double Strand Break. *PLoS Genet,* 11**,** e1005653.

BRUSH, G. S., CLIFFORD, D. M., MARINCO, S. M. & BARTRAND, A. J. 2001. Replication protein A is sequentially phosphorylated during meiosis. *Nucleic Acids Res,* 29**,** 4808-17.

BURGOYNE, P. S. 1986. Mammalian X and Y crossover. *Nature,* 319**,** 258-9.

BURGOYNE, P. S., MAHADEVAIAH, S. K. & TURNER, J. M. 2007. The management of DNA double-strand breaks in mitotic G2, and in mammalian meiosis viewed from a mitotic G2 perspective. *Bioessays,* 29**,** 974-86.

BURGOYNE, P. S., MAHADEVAIAH, S. K. & TURNER, J. M. 2009. The consequences of asynapsis for mammalian meiosis. *Nat Rev Genet,* 10**,** 207-16.

BYERS, S. L., WILES, M. V., DUNN, S. L. & TAFT, R. A. 2012. Mouse estrous cycle identification tool and images. *PLoS One,* 7**,** e35538.

CALLEN, E., JANKOVIC, M., WONG, N., ZHA, S., CHEN, H. T., DIFILIPPANTONIO, S., DI VIRGILIO, M., HEIDKAMP, G., ALT, F. W., NUSSENZWEIG, A. & NUSSENZWEIG, M. 2009. Essential role for DNA-PKcs in DNA double-strand break repair and apoptosis in ATM-deficient lymphocytes. *Mol Cell,* 34**,** 285-97.

CARBALLO, J. A. & CHA, R. S. 2007. Meiotic roles of Mec1, a budding yeast homolog of mammalian ATR/ATM. *Chromosome Res,* 15**,** 539-50.

CARBALLO, J. A., JOHNSON, A. L., SEDGWICK, S. G. & CHA, R. S. 2008. Phosphorylation of the axial element protein Hop1 by Mec1/Tel1 ensures meiotic interhomolog recombination. *Cell,* 132**,** 758-70.

CARBALLO JA, P. S., SERRENTINO ME, JOHNSON AL, GEYMONAT M, BORDE V, KLEIN F, CHA RS 2013. Budding yeast ATM/ATR control meiotic double-strand break (DSB) levels by down-regulating Rec114, an essential component of the DSB-machinery. 9**,** e1003545.

CAROFIGLIO, F., INAGAKI, A., DE VRIES, S., WASSENAAR, E., SCHOENMAKERS, S., VERMEULEN, C., VAN CAPPELLEN, W. A., SLEDDENS-LINKELS, E., GROOTEGOED, J. A., TE RIELE, H. P., DE MASSY, B. & BAARENDS, W. M. 2013. SPO11-independent DNA repair foci and their role in meiotic silencing. *PLoS Genet,* 9**,** e1003538.

CARPENTER, A. T. 1979. Recombination nodules and synaptonemal complex in recombination-defective females of Drosophila melanogaster. *Chromosoma,* 75**,** 259-92.

CARTAGENA-LIROLA, H., GUERINI, I., VISCARDI, V., LUCCHINI, G. & LONGHESE, M. P. 2006. Budding Yeast Sae2 is an In Vivo Target of the Mec1 and Tel1 Checkpoint Kinases During Meiosis. *Cell Cycle,* 5**,** 1549-59.

CELESTE, A., PETERSEN, S., ROMANIENKO, P. J., FERNANDEZ-CAPETILLO, O., CHEN, H. T., SEDELNIKOVA, O. A., REINA-SAN-MARTIN, B., COPPOLA, V., MEFFRE, E., DIFILIPPANTONIO, M. J., REDON, C., PILCH, D. R., OLARU, A., ECKHAUS, M., CAMERINI-OTERO, R. D., TESSAROLLO, L., LIVAK, F., MANOVA, K., BONNER, W. M., NUSSENZWEIG, M. C. & NUSSENZWEIG, A. 2002. Genomic instability in mice lacking histone H2AX. *Science,* 296**,** 922-7.

CHENG, Y. H., CHUANG, C. N., SHEN, H. J., LIN, F. M. & WANG, T. F. 2013. Three distinct modes of Mec1/ATR and Tel1/ATM activation illustrate differential checkpoint targeting during budding yeast early meiosis. *Mol Cell Biol,* 33**,** 3365-76.

CHOI, K. & HENDERSON, I. R. 2015. Meiotic recombination hotspots - a comparative view. *Plant J,* 83**,** 52-61.

CLOUTIER, J. M., MAHADEVAIAH, S. K., ELINATI, E., TOTH, A. & TURNER, J. 2016. Mammalian meiotic silencing exhibits sexually dimorphic features. *Chromosoma,* 125**,** 215-26.

CLOUTIER, J. M. & TURNER, J. M. 2010. Meiotic sex chromosome inactivation. *Curr Biol,* 20**,** R962-3.

COLE, F., KAUPPI, L., LANGE, J., ROIG, I., WANG, R., KEENEY, S. & JASIN, M. 2012. Homeostatic control of recombination is implemented progressively in mouse meiosis. *Nat Cell Biol,* 14**,** 424-30.

CONWAY, A. B., LYNCH, T. W., ZHANG, Y., FORTIN, G. S., FUNG, C. W., SYMINGTON, L. S. & RICE, P. A. 2004. Crystal structure of a Rad51 filament. *Nat Struct Mol Biol,* 11**,** 791-6.

COOKE, H. J. & SAUNDERS, P. T. 2002. Mouse models of male infertility. *Nat Rev Genet,* 3**,** 790-801.

COOPER, T. J., GARCIA, V. & NEALE, M. J. 2016. Meiotic DSB patterning: A multifaceted process. *Cell Cycle,* 15**,** 13-21.

CORTEZ, D., GUNTUKU, S., QIN, J. & ELLEDGE, S. J. 2001. ATR and ATRIP: partners in checkpoint signaling. *Science,* 294**,** 1713-6.

COUTEAU, F. & ZETKA, M. 2011. DNA damage during meiosis induces chromatin remodeling and synaptonemal complex disassembly. *Dev Cell,* 20**,** 353-63.

CULLIGAN, K. M. & BRITT, A. B. 2008. Both ATM and ATR promote the efficient and accurate processing of programmed meiotic double-strand breaks. *Plant J,* 55**,** 629-38.

DAISH, T. J., CASEY, A. E. & GRUTZNER, F. 2015. Lack of sex chromosome specific meiotic silencing in platypus reveals origin of MSCI in therian mammals. *BMC Biol,* 13**,** 106.

DANIEL, K., LANGE, J., HACHED, K., FU, J., ANASTASSIADIS, K., ROIG, I., COOKE, H. J., STEWART, A. F., WASSMANN, K., JASIN, M., KEENEY, S. & TOTH, A. 2011. Meiotic homologue alignment and its quality surveillance are controlled by mouse HORMAD1. *Nat Cell Biol,* 13**,** 599-610.

DAVIS, A. J., CHEN, B. P. & CHEN, D. J. 2014. DNA-PK: a dynamic enzyme in a versatile DSB repair pathway. *DNA Repair (Amst),* 17**,** 21-9.

DE BOER, E., JASIN, M. & KEENEY, S. 2015. Local and sex-specific biases in crossover vs. noncrossover outcomes at meiotic recombination hot spots in mice. *Genes Dev,* 29**,** 1721-33.

DE ROOIJ, D. G. 1973. Spermatogonial stem cell renewal in the mouse. I. Normal situation. *Cell Tissue Kinet,* 6**,** 281-7.

DE ROOIJ, D. G. 2001. Proliferation and differentiation of spermatogonial stem cells. *Reproduction,* 121**,** 347-54.

DE VRIES, F. A., DE BOER, E., VAN DEN BOSCH, M., BAARENDS, W. M., OOMS, M., YUAN, L., LIU, J. G., VAN ZEELAND, A. A., HEYTING, C. & PASTINK, A. 2005. Mouse Sycp1 functions in synaptonemal complex assembly, meiotic recombination, and XY body formation. *Genes Dev,* 19**,** 1376-89.

DE VRIES, M., VOSTERS, S., MERKX, G., D'HAUWERS, K., WANSINK, D. G., RAMOS, L. & DE BOER, P. 2012. Human male meiotic sex chromosome inactivation. *PLoS One,* 7**,** e31485.

DI GIACOMO, M., BARCHI, M., BAUDAT, F., EDELMANN, W., KEENEY, S. & JASIN, M. 2005. Distinct DNA-damage-dependent and -independent responses drive the loss of oocytes in recombination-defective mouse mutants. *Proc Natl Acad Sci U S A,* 102**,** 737-42.

DION, V., KALCK, V., HORIGOME, C., TOWBIN, B. D. & GASSER, S. M. 2012. Increased mobility of double-strand breaks requires Mec1, Rad9 and the homologous recombination machinery. *Nat Cell Biol,* 14**,** 502-9.

DUROCHER, D. & JACKSON, S. P. 2001. DNA-PK, ATM and ATR as sensors of DNA damage: variations on a theme? *Curr Opin Cell Biol,* 13**,** 225-31.

EDELMANN, W., COHEN, P. E., KANE, M., LAU, K., MORROW, B., BENNETT, S., UMAR, A., KUNKEL, T., CATTORETTI, G., CHAGANTI, R., POLLARD, J. W., KOLODNER, R. D. & KUCHERLAPATI, R. 1996. Meiotic pachytene arrest in MLH1-deficient mice. *Cell,* 85**,** 1125-34.

EDELMANN, W., COHEN, P. E., KNEITZ, B., WINAND, N., LIA, M., HEYER, J., KOLODNER, R., POLLARD, J. W. & KUCHERLAPATI, R. 1999. Mammalian MutS homologue 5 is required for chromosome pairing in meiosis. *Nat Genet,* 21**,** 123-7.

EIJPE, M., HEYTING, C., GROSS, B. & JESSBERGER, R. 2000. Association of mammalian SMC1 and SMC3 proteins with meiotic chromosomes and synaptonemal complexes. *J Cell Sci,* 113 (Pt 4)**,** 673-82.

ELLEDGE, S. J. 1996. Cell cycle checkpoints: preventing an identity crisis. *Science,* 274**,** 1664-72.

ELSON, A., WANG, Y., DAUGHERTY, C. J., MORTON, C. C., ZHOU, F., CAMPOS-TORRES, J. & LEDER, P. 1996. Pleiotropic defects in ataxia-telangiectasia protein-deficient mice. *Proc Natl Acad Sci U S A,* 93**,** 13084-9.

FALK, J. E., CHAN, A. C., HOFFMANN, E. & HOCHWAGEN, A. 2010. A Mec1- and PP4-dependent checkpoint couples centromere pairing to meiotic recombination. *Dev Cell,* 19**,** 599-611.

FAWCETT, D. W. 1956. The fine structure of chromosomes in the meiotic prophase of vertebrate spermatocytes. *J Biophys Biochem Cytol,* 2**,** 403-6.

FEDORIW, A. M., MENON, D., KIM, Y., MU, W. & MAGNUSON, T. 2015. Key mediators of somatic ATR signaling localize to unpaired chromosomes in spermatocytes. *Development,* 142**,** 2972-80.

FERNANDEZ-CAPETILLO, O., MAHADEVAIAH, S. K., CELESTE, A., ROMANIENKO, P. J., CAMERINI-OTERO, R. D., BONNER, W. M., MANOVA, K., BURGOYNE, P. & NUSSENZWEIG, A. 2003. H2AX is required for chromatin remodeling and inactivation of sex chromosomes in male mouse meiosis. *Dev Cell,* 4**,** 497-508.

FLOTT, S., KWON, Y., PIGLI, Y. Z., RICE, P. A., SUNG, P. & JACKSON, S. P. 2011. Regulation of Rad51 function by phosphorylation. *EMBO Rep,* 12**,** 833-9.

FOREJT, J. & IVANYI, P. 1974. Genetic studies on male sterility of hybrids between laboratory and wild mice (Mus musculus L.). *Genet Res,* 24**,** 189-206.

FUKUDA, T., FUKUDA, N., AGOSTINHO, A., HERNANDEZ-HERNANDEZ, A., KOUZNETSOVA, A. & HOOG, C. 2014. STAG3-mediated stabilization of REC8 cohesin complexes promotes chromosome synapsis during meiosis. *EMBO J,* 33**,** 1243-55.

FUKUDA, T., PRATTO, F., SCHIMENTI, J. C., TURNER, J. M., CAMERINI-OTERO, R. D. & HOOG, C. 2012. Phosphorylation of chromosome core components may serve as axis marks for the status of chromosomal events during mammalian meiosis. *PLoS Genet,* 8**,** e1002485.

GALLARDO, T., SHIRLEY, L., JOHN, G. B. & CASTRILLON, D. H. 2007. Generation of a germ cell-specific mouse transgenic Cre line, Vasa-Cre. *Genesis,* 45**,** 413-7.

GARCIA, V., BRUCHET, H., CAMESCASSE, D., GRANIER, F., BOUCHEZ, D. & TISSIER, A. 2003. AtATM is essential for meiosis and the somatic response to DNA damage in plants. *Plant Cell,* 15**,** 119-32.

GARCIA, V., GRAY, S., ALLISON, R. M., COOPER, T. J. & NEALE, M. J. 2015. Tel1(ATM)-mediated interference suppresses clustered meiotic double-strand-break formation. *Nature,* 520**,** 114-8.

GARCIA, V., PHELPS, S. E., GRAY, S. & NEALE, M. J. 2011. Bidirectional resection of DNA double-strand breaks by Mre11 and Exo1. *Nature,* 479**,** 241-4.

GARCIA-MUSE, T. & BOULTON, S. J. 2005. Distinct modes of ATR activation after replication stress and DNA double-strand breaks in Caenorhabditis elegans. *EMBO J,* 24**,** 4345-55.

GRAY, S., ALLISON, R. M., GARCIA, V., GOLDMAN, A. S. & NEALE, M. J. 2013. Positive regulation of meiotic DNA double-strand break formation by activation of the DNA damage checkpoint kinase Mec1(ATR). *Open Biol,* 3**,** 130019.

GREENE, E. C. 2016. DNA Sequence Alignment during Homologous Recombination. *J Biol Chem,* 291**,** 11572-80.

GRUHN, J. R., AL-ASMAR, N., FASNACHT, R., MAYLOR-HAGEN, H., PEINADO, V., RUBIO, C., BROMAN, K. W., HUNT, P. A. & HASSOLD, T. 2016. Correlations between Synaptic Initiation and Meiotic Recombination: A Study of Humans and Mice. *Am J Hum Genet,* 98**,** 102-15.

GRUSHCOW, J. M., HOLZEN, T. M., PARK, K. J., WEINERT, T., LICHTEN, M. & BISHOP, D. K. 1999. Saccharomyces cerevisiae checkpoint genes MEC1, RAD17 and RAD24 are required for normal meiotic recombination partner choice. *Genetics,* 153**,** 607-20.

GUIOLI, S., LOVELL-BADGE, R. & TURNER, J. M. 2012. Error-prone ZW pairing and no evidence for meiotic sex chromosome inactivation in the chicken germ line. *PLoS Genet,* 8**,** e1002560.

HACKETT, J. A. & SURANI, M. A. 2013. DNA methylation dynamics during the mammalian life cycle. *Philos Trans R Soc Lond B Biol Sci,* 368**,** 20110328.

HAMER, G., WANG, H., BOLCUN-FILAS, E., COOKE, H. J., BENAVENTE, R. & HOOG, C. 2008. Progression of meiotic recombination requires structural maturation of the central element of the synaptonemal complex. *J Cell Sci,* 121**,** 2445-51.

HANDEL, M. A. & SCHIMENTI, J. C. 2010. Genetics of mammalian meiosis: regulation, dynamics and impact on fertility. *Nat Rev Genet,* 11**,** 124-36.

HARTWELL, L. H. & WEINERT, T. A. 1989. Checkpoints: controls that ensure the order of cell cycle events. *Science,* 246**,** 629-34.

HENDERSON, S. A. 1963. Differential Ribonucleic Acid Synthesis of X and Autosomes during Meiosis. *Nature,* 200**,** 1235.

HERRAN, Y., GUTIERREZ-CABALLERO, C., SANCHEZ-MARTIN, M., HERNANDEZ, T., VIERA, A., BARBERO, J. L., DE ALAVA, E., DE ROOIJ, D. G., SUJA, J. A., LLANO, E. & PENDAS, A. M. 2011. The cohesin subunit RAD21L functions in meiotic synapsis and exhibits sexual dimorphism in fertility. *EMBO J,* 30**,** 3091-105.

HESS, R. A. 1990. Quantitative and qualitative characteristics of the stages and transitions in the cycle of the rat seminiferous epithelium: light microscopic observations of perfusion-fixed and plastic-embedded testes. *Biol Reprod,* 43**,** 525-42.

HIRAO, A., KONG, Y. Y., MATSUOKA, S., WAKEHAM, A., RULAND, J., YOSHIDA, H., LIU, D., ELLEDGE, S. J. & MAK, T. W. 2000. DNA damage-induced activation of p53 by the checkpoint kinase Chk2. *Science,* 287**,** 1824-7.

HO, H. C. & BURGESS, S. M. 2011. Pch2 acts through Xrs2 and Tel1/ATM to modulate interhomolog bias and checkpoint function during meiosis. *PLoS Genet,* 7**,** e1002351.

HOLLOWAY, J. K., BOOTH, J., EDELMANN, W., MCGOWAN, C. H. & COHEN, P. E. 2008. MUS81 generates a subset of MLH1-MLH3-independent crossovers in mammalian meiosis. *PLoS Genet,* 4**,** e1000186.

HOLLOWAY, J. K., SUN, X., YOKOO, R., VILLENEUVE, A. M. & COHEN, P. E. 2014. Mammalian CNTD1 is critical for meiotic crossover maturation and deselection of excess precrossover sites. *J Cell Biol,* 205**,** 633-41.

HOLLOWAY, K., ROBERSON, E. C., CORBETT, K. L., KOLAS, N. K., NIEVES, E. & COHEN, P. E. 2011. NEK1 Facilitates Cohesin Removal during Mammalian Spermatogenesis. *Genes (Basel),* 2**,** 260-79.

HOPKINS, J., HWANG, G., JACOB, J., SAPP, N., BEDIGIAN, R., OKA, K., OVERBEEK, P., MURRAY, S. & JORDAN, P. W. 2014. Meiosis-specific cohesin component, Stag3 is essential for maintaining centromere chromatid cohesion, and required for DNA repair and synapsis between homologous chromosomes. *PLoS Genet,* 10**,** e1004413.

HUNTER, N. 2015. Meiotic Recombination: The Essence of Heredity. *Cold Spring Harb Perspect Biol,* 7.

HUTTLIN, E. L., JEDRYCHOWSKI, M. P., ELIAS, J. E., GOSWAMI, T., RAD, R., BEAUSOLEIL, S. A., VILLEN, J., HAAS, W., SOWA, M. E. & GYGI, S. P. 2010. A tissue-specific atlas of mouse protein phosphorylation and expression. *Cell,* 143**,** 1174-89.

ICHIJIMA, Y., ICHIJIMA, M., LOU, Z., NUSSENZWEIG, A., CAMERINI-OTERO, R. D., CHEN, J., ANDREASSEN, P. R. & NAMEKAWA, S. H. 2011. MDC1 directs chromosome-wide silencing of the sex chromosomes in male germ cells. *Genes Dev,* 25**,** 959-71.

JACKSON, S. P. & BARTEK, J. 2009. The DNA-damage response in human biology and disease. *Nature,* 461**,** 1071-8.

JEFFREYS, A. J., HOLLOWAY, J. K., KAUPPI, L., MAY, C. A., NEUMANN, R., SLINGSBY, M. T. & WEBB, A. J. 2004. Meiotic recombination hot spots and human DNA diversity. *Philos Trans R Soc Lond B Biol Sci,* 359**,** 141-52.

JOSHI, N., BROWN, M. S., BISHOP, D. K. & BORNER, G. V. 2015. Gradual implementation of the meiotic recombination program via checkpoint pathways controlled by global DSB levels. *Mol Cell,* 57**,** 797-811.

JOYCE, E. F., PEDERSEN, M., TIONG, S., WHITE-BROWN, S. K., PAUL, A., CAMPBELL, S. D. & MCKIM, K. S. 2011. Drosophila ATM and ATR have distinct activities in the regulation of meiotic DNA damage and repair. *J Cell Biol,* 195**,** 359-67.

KAUPPI, L., BARCHI, M., BAUDAT, F., ROMANIENKO, P. J., KEENEY, S. & JASIN, M. 2011. Distinct properties of the XY pseudoautosomal region crucial for male meiosis. *Science,* 331**,** 916-20.

KAUPPI, L., BARCHI, M., LANGE, J., BAUDAT, F., JASIN, M. & KEENEY, S. 2013. Numerical constraints and feedback control of double-strand breaks in mouse meiosis. *Genes Dev,* 27**,** 873-86.

KAUPPI, L., JASIN, M. & KEENEY, S. 2012. The tricky path to recombining X and Y chromosomes in meiosis. *Ann N Y Acad Sci,* 1267**,** 18-23.

KEEGAN, K. S., HOLTZMAN, D. A., PLUG, A. W., CHRISTENSON, E. R., BRAINERD, E. E., FLAGGS, G., BENTLEY, N. J., TAYLOR, E. M., MEYN, M. S., MOSS, S. B., CARR, A. M., ASHLEY, T. & HOEKSTRA, M. F. 1996. The Atr and Atm protein kinases associate with different sites along meiotically pairing chromosomes. *Genes Dev,* 10**,** 2423-37.

KEENEY, S. 2001. Mechanism and control of meiotic recombination initiation. *Curr Top Dev Biol,* 52**,** 1-53.

KEENEY, S., GIROUX, C. N. & KLECKNER, N. 1997. Meiosis-specific DNA double-strand breaks are catalyzed by Spo11, a member of a widely conserved protein family. *Cell,* 88**,** 375-84.

KEENEY, S., LANGE, J. & MOHIBULLAH, N. 2014. Self-organization of meiotic recombination initiation: general principles and molecular pathways. *Annu Rev Genet,* 48**,** 187-214.

KERR, J. B., HUTT, K. J., MICHALAK, E. M., COOK, M., VANDENBERG, C. J., LIEW, S. H., BOUILLET, P., MILLS, A., SCOTT, C. L., FINDLAY, J. K. & STRASSER, A. 2012. DNA damage-induced primordial follicle oocyte apoptosis and loss of fertility require TAp63-mediated induction of Puma and Noxa. *Mol Cell,* 48**,** 343-52.

KIERSZENBAUM, A. L. & TRES, L. L. 1974. Nucleolar and perichromosomal RNA synthesis during meiotic prophase in the mouse testis. *J Cell Biol,* 60**,** 39-53.

KIM, S., PETERSON, S. E., JASIN, M. & KEENEY, S. 2016. Mechanisms of germ line genome instability. *Semin Cell Dev Biol,* 54**,** 177-87.

KINEBUCHI, T., KAGAWA, W., ENOMOTO, R., TANAKA, K., MIYAGAWA, K., SHIBATA, T., KURUMIZAKA, H. & YOKOYAMA, S. 2004. Structural basis for octameric ring formation and DNA interaction of the human homologous-pairing protein Dmc1. *Mol Cell,* 14**,** 363-74.

KLECKNER, N. 2006. Chiasma formation: chromatin/axis interplay and the role(s) of the synaptonemal complex. *Chromosoma,* 115**,** 175-94.

KNEITZ, B., COHEN, P. E., AVDIEVICH, E., ZHU, L., KANE, M. F., HOU, H., JR., KOLODNER, R. D., KUCHERLAPATI, R., POLLARD, J. W. & EDELMANN, W. 2000. MutS homolog 4 localization to meiotic chromosomes is required for chromosome pairing during meiosis in male and female mice. *Genes Dev,* 14**,** 1085-97.

KOGO, H., TSUTSUMI, M., INAGAKI, H., OHYE, T., KIYONARI, H. & KURAHASHI, H. 2012a. HORMAD2 is essential for synapsis surveillance during meiotic prophase via the recruitment of ATR activity. *Genes Cells,* 17**,** 897-912.

KOGO, H., TSUTSUMI, M., OHYE, T., INAGAKI, H., ABE, T. & KURAHASHI, H. 2012b. HORMAD1-dependent checkpoint/surveillance mechanism eliminates asynaptic oocytes. *Genes Cells,* 17**,** 439-54.

KONG, A., THORLEIFSSON, G., GUDBJARTSSON, D. F., MASSON, G., SIGURDSSON, A., JONASDOTTIR, A., WALTERS, G. B., JONASDOTTIR, A., GYLFASON, A., KRISTINSSON, K. T., GUDJONSSON, S. A., FRIGGE, M. L., HELGASON, A., THORSTEINSDOTTIR, U. & STEFANSSON, K. 2010. Fine-scale recombination rate differences between sexes, populations and individuals. *Nature,* 467**,** 1099-103.

KOUZNETSOVA, A., BENAVENTE, R., PASTINK, A. & HOOG, C. 2011. Meiosis in mice without a synaptonemal complex. *PLoS One,* 6**,** e28255.

KUMAR, R., BOURBON, H. M. & DE MASSY, B. 2010. Functional conservation of Mei4 for meiotic DNA double-strand break formation from yeasts to mice. *Genes Dev,* 24**,** 1266-80.

KURZBAUER, M. T., UANSCHOU, C., CHEN, D. & SCHLOGELHOFER, P. 2012. The recombinases DMC1 and RAD51 are functionally and spatially separated during meiosis in Arabidopsis. *Plant Cell,* 24**,** 2058-70.

LAEMMLI, U. K. 1970. Cleavage of structural proteins during the assembly of the head of bacteriophage T4. *Nature,* 227**,** 680-5.

LANGE, J., PAN, J., COLE, F., THELEN, M. P., JASIN, M. & KEENEY, S. 2011. ATM controls meiotic double-strand-break formation. *Nature,* 479**,** 237-40.

LI, X. C., BOLCUN-FILAS, E. & SCHIMENTI, J. C. 2011. Genetic evidence that synaptonemal complex axial elements govern recombination pathway choice in mice. *Genetics,* 189**,** 71-82.

LI, X. C. & SCHIMENTI, J. C. 2007. Mouse pachytene checkpoint 2 (trip13) is required for completing meiotic recombination but not synapsis. *PLoS Genet,* 3**,** e130.

LIBBY, B. J., REINHOLDT, L. G. & SCHIMENTI, J. C. 2003. Positional cloning and characterization of Mei1, a vertebrate-specific gene required for normal meiotic chromosome synapsis in mice. *Proc Natl Acad Sci U S A,* 100**,** 15706-11.

LIFSCHYTZ, E. & LINDSLEY, D. L. 1972. The role of X-chromosome inactivation during spermatogenesis (Drosophila-allocycly-chromosome evolution-male sterility-dosage compensation). *Proc Natl Acad Sci U S A,* 69**,** 182-6.

LIGHTFOOT, D. A., KOUZNETSOVA, A., MAHDY, E., WILBERTZ, J. & HOOG, C. 2006. The fate of mosaic aneuploid embryos during mouse development. *Dev Biol,* 289**,** 384-94.

LINDEGREN, C. C. 1955. Non-Mendelian Segregation in a Single Tetrad of Saccharomyces Ascribed to Gene Conversion. *Science,* 121**,** 605-7.

LIPKIN, S. M., MOENS, P. B., WANG, V., LENZI, M., SHANMUGARAJAH, D., GILGEOUS, A., THOMAS, J., CHENG, J., TOUCHMAN, J. W., GREEN, E. D., SCHWARTZBERG, P., COLLINS, F. S. & COHEN, P. E. 2002. Meiotic arrest and aneuploidy in MLH3-deficient mice. *Nat Genet,* 31**,** 385-90.

LIU, J., WU, T. C. & LICHTEN, M. 1995. The location and structure of double-strand DNA breaks induced during yeast meiosis: evidence for a covalently linked DNA-protein intermediate. *EMBO J,* 14**,** 4599-608.

LIU, J. G., YUAN, L., BRUNDELL, E., BJORKROTH, B., DANEHOLT, B. & HOOG, C. 1996. Localization of the N-terminus of SCP1 to the central element of the synaptonemal complex and evidence for direct interactions between the N-termini of SCP1 molecules organized head-to-head. *Exp Cell Res,* 226**,** 11-9.

LIU, Q., GUNTUKU, S., CUI, X. S., MATSUOKA, S., CORTEZ, D., TAMAI, K., LUO, G., CARATTINI-RIVERA, S., DEMAYO, F., BRADLEY, A., DONEHOWER, L. A. & ELLEDGE, S. J. 2000. Chk1 is an essential kinase that is regulated by Atr and required for the G(2)/M DNA damage checkpoint. *Genes Dev,* 14**,** 1448-59.

LLANO, E., HERRAN, Y., GARCIA-TUNON, I., GUTIERREZ-CABALLERO, C., DE ALAVA, E., BARBERO, J. L., SCHIMENTI, J., DE ROOIJ, D. G., SANCHEZ-MARTIN, M. & PENDAS, A. M. 2012. Meiotic cohesin complexes are essential for the formation of the axial element in mice. *J Cell Biol,* 197**,** 877-85.

LOVELL-BADGE, R. & ROBERTSON, E. 1990. XY female mice resulting from a heritable mutation in the primary testis-determining gene, Tdy. *Development,* 109**,** 635-46.

LUO, H., LI, Y., MU, J. J., ZHANG, J., TONAKA, T., HAMAMORI, Y., JUNG, S. Y., WANG, Y. & QIN, J. 2008. Regulation of intra-S phase checkpoint by ionizing radiation (IR)-dependent and IR-independent phosphorylation of SMC3. *J Biol Chem,* 283**,** 19176-83.

LYDALL, D., NIKOLSKY, Y., BISHOP, D. K. & WEINERT, T. 1996. A meiotic recombination checkpoint controlled by mitotic checkpoint genes. *Nature,* 383**,** 840-3.

LYNDAKER, A. M., LIM, P. X., MLECZKO, J. M., DIGGINS, C. E., HOLLOWAY, J. K., HOLMES, R. J., KAN, R., SCHLAFER, D. H., FREIRE, R., COHEN, P. E. & WEISS, R. S. 2013. Conditional inactivation of the DNA damage response gene Hus1 in mouse testis reveals separable roles for components of the RAD9-RAD1-HUS1 complex in meiotic chromosome maintenance. *PLoS Genet,* 9**,** e1003320.

LYNN, A., SOUCEK, R. & BORNER, G. V. 2007. ZMM proteins during meiosis: crossover artists at work. *Chromosome Res,* 15**,** 591-605.

MACQUEEN, A. J. & HOCHWAGEN, A. 2011. Checkpoint mechanisms: the puppet masters of meiotic prophase. *Trends Cell Biol,* 21**,** 393-400.

MAHADEVAIAH, S. K., BOURC'HIS, D., DE ROOIJ, D. G., BESTOR, T. H., TURNER, J. M. & BURGOYNE, P. S. 2008. Extensive meiotic asynapsis in mice antagonises meiotic silencing of unsynapsed chromatin and consequently disrupts meiotic sex chromosome inactivation. *J Cell Biol,* 182**,** 263-76.

MAHADEVAIAH, S. K., ROYO, H., VANDEBERG, J. L., MCCARREY, J. R., MACKAY, S. & TURNER, J. M. 2009. Key features of the X inactivation process are conserved between marsupials and eutherians. *Curr Biol,* 19**,** 1478-84.

MAHADEVAIAH, S. K., TURNER, J. M., BAUDAT, F., ROGAKOU, E. P., DE BOER, P., BLANCO-RODRIGUEZ, J., JASIN, M., KEENEY, S., BONNER, W. M. & BURGOYNE, P. S. 2001. Recombinational DNA double-strand breaks in mice precede synapsis. *Nat Genet,* 27**,** 271-6.

MARCON, E. & MOENS, P. B. 2005. The evolution of meiosis: recruitment and modification of somatic DNA-repair proteins. *Bioessays,* 27**,** 795-808.

MARECHAL, A. & ZOU, L. 2013. DNA damage sensing by the ATM and ATR kinases. *Cold Spring Harb Perspect Biol,* 5.

MATSUDA, T. & CEPKO, C. L. 2007. Controlled expression of transgenes introduced by in vivo electroporation. *Proc Natl Acad Sci U S A,* 104**,** 1027-32.

MATSUOKA, S., BALLIF, B. A., SMOGORZEWSKA, A., MCDONALD, E. R., 3RD, HUROV, K. E., LUO, J., BAKALARSKI, C. E., ZHAO, Z., SOLIMINI, N., LERENTHAL, Y., SHILOH, Y., GYGI, S. P. & ELLEDGE, S. J. 2007. ATM and ATR substrate analysis reveals extensive protein networks responsive to DNA damage. *Science,* 316**,** 1160-6.

MATSUOKA, S., HUANG, M. & ELLEDGE, S. J. 1998. Linkage of ATM to cell cycle regulation by the Chk2 protein kinase. *Science,* 282**,** 1893-7.

MCCARREY, J. R., DILWORTH, D. D. & SHARP, R. M. 1992. Semiquantitative analysis of X-linked gene expression during spermatogenesis in the mouse: ethidium-bromide staining of RT-PCR products. *Genet Anal Tech Appl,* 9**,** 117-23.

MCKEE, B. D. & HANDEL, M. A. 1993. Sex chromosomes, recombination, and chromatin conformation. *Chromosoma,* 102**,** 71-80.

MEISTRICH, M. L. & HESS, R. A. 2013. Assessment of spermatogenesis through staging of seminiferous tubules. *Methods Mol Biol,* 927**,** 299-307.

MIMITOU, E. P. & SYMINGTON, L. S. 2009. DNA end resection: many nucleases make light work. *DNA Repair (Amst),* 8**,** 983-95.

MIMITOU, E. P., YAMADA, S. & KEENEY, S. 2017. A global view of meiotic double-strand break end resection. *Science,* 355**,** 40-45.

MINE-HATTAB, J. & ROTHSTEIN, R. 2012. Increased chromosome mobility facilitates homology search during recombination. *Nat Cell Biol,* 14**,** 510-7.

MOENS, P. B., KOLAS, N. K., TARSOUNAS, M., MARCON, E., COHEN, P. E. & SPYROPOULOS, B. 2002. The time course and chromosomal localization of recombination-related proteins at meiosis in the mouse are compatible with models that can resolve the early DNA-DNA interactions without reciprocal recombination. *J Cell Sci,* 115**,** 1611-22.

MOENS, P. B., TARSOUNAS, M., MORITA, T., HABU, T., ROTTINGHAUS, S. T., FREIRE, R., JACKSON, S. P., BARLOW, C. & WYNSHAW-BORIS, A. 1999. The association of ATR protein with mouse meiotic chromosome cores. *Chromosoma,* 108**,** 95-102.

MONESI, V. 1965a. Differential rate of ribonucleic acid synthesis in the autosomes and sex chromosomes during male meiosis in the mouse. *Chromosoma,* 17**,** 11-21.

MONESI, V. 1965b. Synthetic activities during spermatogenesis in the mouse RNA and protein. *Exp Cell Res,* 39**,** 197-224.

MORELLI, M. A. & COHEN, P. E. 2005. Not all germ cells are created equal: aspects of sexual dimorphism in mammalian meiosis. *Reproduction,* 130**,** 761-81.

MURAKAMI, H. & KEENEY, S. 2008. Regulating the formation of DNA double-strand breaks in meiosis. *Genes Dev,* 22**,** 286-92.

MURGA, M., BUNTING, S., MONTANA, M. F., SORIA, R., MULERO, F., CANAMERO, M., LEE, Y., MCKINNON, P. J., NUSSENZWEIG, A. & FERNANDEZ-CAPETILLO, O. 2009. A mouse model of ATR-Seckel shows embryonic replicative stress and accelerated aging. *Nat Genet,* 41**,** 891-8.

NAGAOKA, S. I., HASSOLD, T. J. & HUNT, P. A. 2012. Human aneuploidy: mechanisms and new insights into an age-old problem. *Nat Rev Genet,* 13**,** 493-504.

NEALE, M. J. & KEENEY, S. 2006. Clarifying the mechanics of DNA strand exchange in meiotic recombination. *Nature,* 442**,** 153-8.

NEALE, M. J., PAN, J. & KEENEY, S. 2005. Endonucleolytic processing of covalent protein-linked DNA double-strand breaks. *Nature,* 436**,** 1053-7.

OAKBERG, E. F. 1956. A description of spermiogenesis in the mouse and its use in analysis of the cycle of the seminiferous epithelium and germ cell renewal. *Am J Anat,* 99**,** 391-413.

ODORISIO, T., RODRIGUEZ, T. A., EVANS, E. P., CLARKE, A. R. & BURGOYNE, P. S. 1998. The meiotic checkpoint monitoring synapsis eliminates spermatocytes via p53-independent apoptosis. *Nat Genet,* 18**,** 257-61.

OLSEN, J. V., VERMEULEN, M., SANTAMARIA, A., KUMAR, C., MILLER, M. L., JENSEN, L. J., GNAD, F., COX, J., JENSEN, T. S., NIGG, E. A., BRUNAK, S. & MANN, M. 2010. Quantitative phosphoproteomics reveals widespread full phosphorylation site occupancy during mitosis. *Sci Signal,* 3**,** ra3.

PACHECO, S., MARCET-ORTEGA, M., LANGE, J., JASIN, M., KEENEY, S. & ROIG, I. 2015. The ATM signaling cascade promotes recombination-dependent pachytene arrest in mouse spermatocytes. *PLoS Genet,* 11**,** e1005017.

PAGE, S. L. & HAWLEY, R. S. 2004. The genetics and molecular biology of the synaptonemal complex. *Annu Rev Cell Dev Biol,* 20**,** 525-58.

PAN, J. & KEENEY, S. 2009. Detection of SPO11-oligonucleotide complexes from mouse testes. *Methods Mol Biol,* 557**,** 197-207.

PARVANOV, E. D., PETKOV, P. M. & PAIGEN, K. 2010. Prdm9 controls activation of mammalian recombination hotspots. *Science,* 327**,** 835.

PENEDOS, A., JOHNSON, A. L., STRONG, E., GOLDMAN, A. S., CARBALLO, J. A. & CHA, R. S. 2015. Essential and Checkpoint Functions of Budding Yeast ATM and ATR during Meiotic Prophase Are Facilitated by Differential Phosphorylation of a Meiotic Adaptor Protein, Hop1. *PLoS One,* 10**,** e0134297.

PEREZ, G. I., ROBLES R FAU - KNUDSON, C. M., KNUDSON CM FAU - FLAWS, J. A., FLAWS JA FAU - KORSMEYER, S. J., KORSMEYER SJ FAU - TILLY, J. L. & TILLY, J. L. Prolongation of ovarian lifespan into advanced chronological age by Bax-deficiency.

PERRY, J. & KLECKNER, N. 2003. The ATRs, ATMs, and TORs are giant HEAT repeat proteins. *Cell,* 112**,** 151-5.

PERRY, J., PALMER, S., GABRIEL, A. & ASHWORTH, A. 2001. A short pseudoautosomal region in laboratory mice. *Genome Res,* 11**,** 1826-32.

PHADNIS, N., HYPPA, R. W. & SMITH, G. R. 2011. New and old ways to control meiotic recombination. *Trends Genet,* 27**,** 411-21.

PHILLIPS, R. J., HAWKER, S. G. & MOSELEY, H. J. 1973. Bare-patches, a new sex-linked gene in the mouse, associated with a high production of XO females. I. A preliminary report of breeding experiments. *Genet Res,* 22**,** 91-9.

PITTMAN, D. L., COBB, J., SCHIMENTI, K. J., WILSON, L. A., COOPER, D. M., BRIGNULL, E., HANDEL, M. A. & SCHIMENTI, J. C. 1998. Meiotic prophase arrest with failure of chromosome synapsis in mice deficient for Dmc1, a germline-specific RecA homolog. *Mol Cell,* 1**,** 697-705.

PLUG, A. W., PETERS, A. H., KEEGAN, K. S., HOEKSTRA, M. F., DE BOER, P. & ASHLEY, T. 1998. Changes in protein composition of meiotic nodules during mammalian meiosis. *J Cell Sci,* 111 (Pt 4)**,** 413-23.

POON, R. Y. 2016. Cell Cycle Control: A System of Interlinking Oscillators. *Methods Mol Biol,* 1342**,** 3-19.

POWERS, N. R., PARVANOV, E. D., BAKER, C. L., WALKER, M., PETKOV, P. M. & PAIGEN, K. 2016. The Meiotic Recombination Activator PRDM9 Trimethylates Both H3K36 and H3K4 at Recombination Hotspots In Vivo. *PLoS Genet,* 12**,** e1006146.

QIAO, H., PRASADA RAO, H. B., YANG, Y., FONG, J. H., CLOUTIER, J. M., DEACON, D. C., NAGEL, K. E., SWARTZ, R. K., STRONG, E., HOLLOWAY, J. K., COHEN, P. E., SCHIMENTI, J., WARD, J. & HUNTER, N. 2014. Antagonistic roles of ubiquitin ligase HEI10 and SUMO ligase RNF212 regulate meiotic recombination. *Nat Genet,* 46**,** 194-9.

REBOURCET, D., O'SHAUGHNESSY, P. J., MONTEIRO, A., MILNE, L., CRUICKSHANKS, L., JEFFREY, N., GUILLOU, F., FREEMAN, T. C., MITCHELL, R. T. & SMITH, L. B. 2014. Sertoli cells maintain Leydig cell number and peritubular myoid cell activity in the adult mouse testis. *PLoS One,* 9**,** e105687.

REYNOLDS, A., QIAO, H., YANG, Y., CHEN, J. K., JACKSON, N., BISWAS, K., HOLLOWAY, J. K., BAUDAT, F., DE MASSY, B., WANG, J., HOOG, C., COHEN, P. E. & HUNTER, N. 2013. RNF212 is a dosage-sensitive regulator of crossing-over during mammalian meiosis. *Nat Genet,* 45**,** 269-78.

RINALDI, V. D., BOLCUN-FILAS, E., KOGO, H., KURAHASHI, H. & SCHIMENTI, J. C. 2017a. The DNA Damage Checkpoint Eliminates Mouse Oocytes with Chromosome Synapsis Failure. *Mol Cell,* 67**,** 1026-1036 e2.

RINALDI, V. D., HSIEH, K., MUNROE, R., BOLCUN-FILAS, E. & SCHIMENTI, J. C. 2017b. Pharmacological Inhibition of the DNA Damage Checkpoint Prevents Radiation-Induced Oocyte Death. *Genetics,* 206**,** 1823-1828.

RISAL, S., ADHIKARI, D. & LIU, K. 2016. Animal Models for Studying the In Vivo Functions of Cell Cycle CDKs. *Methods Mol Biol,* 1336**,** 155-66.

ROBERT, T., NORE, A., BRUN, C., MAFFRE, C., CRIMI, B., BOURBON, H. M. & DE MASSY, B. 2016. The TopoVIB-Like protein family is required for meiotic DNA double-strand break formation. *Science,* 351**,** 943-9.

RODRIGUEZ, T. A. & BURGOYNE, P. S. 2001. Spermatogenic failure in male mice with four sex chromosomes. *Chromosoma,* 110**,** 124-9.

ROIG, I., DOWDLE, J. A., TOTH, A., DE ROOIJ, D. G., JASIN, M. & KEENEY, S. 2010. Mouse TRIP13/PCH2 is required for recombination and normal higher-order chromosome structure during meiosis. *PLoS Genet,* 6.

ROMANIENKO, P. J. & CAMERINI-OTERO, R. D. 2000. The mouse Spo11 gene is required for meiotic chromosome synapsis. *Mol Cell,* 6**,** 975-87.

ROSET, R., INAGAKI, A., HOHL, M., BRENET, F., LAFRANCE-VANASSE, J., LANGE, J., SCANDURA, J. M., TAINER, J. A., KEENEY, S. & PETRINI, J. H. 2014. The Rad50 hook domain regulates DNA damage signaling and tumorigenesis. *Genes Dev,* 28**,** 451-62.

ROYO, H., POLIKIEWICZ, G., MAHADEVAIAH, S. K., PROSSER, H., MITCHELL, M., BRADLEY, A., DE ROOIJ, D. G., BURGOYNE, P. S. & TURNER, J. M. 2010. Evidence that meiotic sex chromosome inactivation is essential for male fertility. *Curr Biol,* 20**,** 2117-23.

ROYO, H., PROSSER, H., RUZANKINA, Y., MAHADEVAIAH, S. K., CLOUTIER, J. M., BAUMANN, M., FUKUDA, T., HOOG, C., TOTH, A., DE ROOIJ, D. G., BRADLEY, A., BROWN, E. J. & TURNER, J. M. 2013. ATR acts stage

specifically to regulate multiple aspects of mammalian meiotic silencing. *Genes Dev,* 27**,** 1484-94.

ROYO, H., SEITZ, H., ELINATI, E., PETERS, A. H., STADLER, M. B. & TURNER, J. M. 2015. Silencing of X-Linked MicroRNAs by Meiotic Sex Chromosome Inactivation. *PLoS Genet,* 11**,** e1005461.

RUZANKINA, Y., PINZON-GUZMAN, C., ASARE, A., ONG, T., PONTANO, L., COTSARELIS, G., ZEDIAK, V. P., VELEZ, M., BHANDOOLA, A. & BROWN, E. J. 2007. Deletion of the developmentally essential gene ATR in adult mice leads to age-related phenotypes and stem cell loss. *Cell Stem Cell,* 1**,** 113-26.

SADATE-NGATCHOU, P. I., PAYNE, C. J., DEARTH, A. T. & BRAUN, R. E. 2008. Cre recombinase activity specific to postnatal, premeiotic male germ cells in transgenic mice. *Genesis,* 46**,** 738-42.

SCHONHOFF, S. E., GIEL-MOLONEY, M. & LEITER, A. B. 2004. Neurogenin 3-expressing progenitor cells in the gastrointestinal tract differentiate into both endocrine and non-endocrine cell types. *Dev Biol,* 270**,** 443-54.

SCHRAMM, S., FRAUNE, J., NAUMANN, R., HERNANDEZ-HERNANDEZ, A., HOOG, C., COOKE, H. J., ALSHEIMER, M. & BENAVENTE, R. 2011. A novel mouse synaptonemal complex protein is essential for loading of central element proteins, recombination, and fertility. *PLoS Genet,* 7**,** e1002088.

SCHWACHA, A. & KLECKNER, N. 1994. Identification of joint molecules that form frequently between homologs but rarely between sister chromatids during yeast meiosis. *Cell,* 76**,** 51-63.

SEEBER, A., DION, V. & GASSER, S. M. 2013. Checkpoint kinases and the INO80 nucleosome remodeling complex enhance global chromatin mobility in response to DNA damage. *Genes Dev,* 27**,** 1999-2008.

SEKIDO, R. & LOVELL-BADGE, R. 2009. Sex determination and SRY: down to a wink and a nudge? *Trends in Genetics,* 25**,** 19-29.

SHALTIEL, I. A., KRENNING, L., BRUINSMA, W. & MEDEMA, R. H. 2015. The same, only different - DNA damage checkpoints and their reversal throughout the cell cycle. *J Cell Sci,* 128**,** 607-20.

SHANBHAG, N. M., RAFALSKA-METCALF, I. U., BALANE-BOLIVAR, C., JANICKI, S. M. & GREENBERG, R. A. 2010. ATM-dependent chromatin changes silence transcription in cis to DNA double-strand breaks. *Cell,* 141**,** 970-81.

SHILOH, Y. 2001. ATM and ATR: networking cellular responses to DNA damage. *Curr Opin Genet Dev,* 11**,** 71-7.

SHIN, Y. H., CHOI, Y., ERDIN, S. U., YATSENKO, S. A., KLOC, M., YANG, F., WANG, P. J., MEISTRICH, M. L. & RAJKOVIC, A. 2010. Hormad1 mutation disrupts synaptonemal complex formation, recombination, and chromosome segregation in mammalian meiosis. *PLoS Genet,* 6**,** e1001190.

SHIU, P. K. & METZENBERG, R. L. 2002. Meiotic silencing by unpaired DNA: properties, regulation and suppression. *Genetics,* 161**,** 1483-95.

SHIU, P. K., RAJU, N. B., ZICKLER, D. & METZENBERG, R. L. 2001. Meiotic silencing by unpaired DNA. *Cell,* 107**,** 905-16.

SHORT, J. M., LIU, Y., CHEN, S., SONI, N., MADHUSUDHAN, M. S., SHIVJI, M. K. & VENKITARAMAN, A. R. 2016. High-resolution structure of the presynaptic RAD51 filament on single-stranded DNA by electron cryo-microscopy. *Nucleic Acids Res*.

SINCLAIR, A. H., BERTA, P., PALMER, M. S., HAWKINS, J. R., GRIFFITHS, B. L., SMITH, M. J., FOSTER, J. W., FRISCHAUF, A. M., LOVELL-BADGE, R. & GOODFELLOW, P. N. 1990. A gene from the human sex-determining region encodes a protein with homology to a conserved DNA-binding motif. *Nature,* 346**,** 240-4.

SLAMA, R., HANSEN, O. K., DUCOT, B., BOHET, A., SORENSEN, D., GIORGIS ALLEMAND, L., EIJKEMANS, M. J., ROSETTA, L., THALABARD, J. C., KEIDING, N. & BOUYER, J. 2012. Estimation of the frequency of involuntary infertility on a nation-wide basis. *Hum Reprod,* 27**,** 1489-98.

SMITH, L. 2011. Good planning and serendipity: exploiting the Cre/Lox system in the testis. *Reproduction,* 141**,** 151-61.

SOLARI, A. J. 1964. The Morphology and Ultrastructure of the Sex Vesicle in the Mouse. *Exp Cell Res,* 36**,** 160-8.

SOLARI, A. J. 1974. The behavior of the XY pair in mammals. *Int Rev Cytol,* 38**,** 273-317.

SORENSEN, C. S., HANSEN, L. T., DZIEGIELEWSKI, J., SYLJUASEN, R. G., LUNDIN, C., BARTEK, J. & HELLEDAY, T. 2005. The cell-cycle checkpoint kinase Chk1 is required for mammalian homologous recombination repair. *Nat Cell Biol,* 7**,** 195-201.

SOUQUET, B., ABBY, E., HERVE, R., FINSTERBUSCH, F., TOURPIN, S., LE BOUFFANT, R., DUQUENNE, C., MESSIAEN, S., MARTINI, E., BERNARDINO-SGHERRI, J., TOTH, A., HABERT, R. & LIVERA, G. 2013. MEIOB targets single-strand DNA and is necessary for meiotic recombination. *PLoS Genet,* 9**,** e1003784.

STANZIONE, M., BAUMANN, M., PAPANIKOS, F., DERELI, I., LANGE, J., RAMLAL, A., TRANKNER, D., SHIBUYA, H., DE MASSY, B., WATANABE, Y., JASIN, M., KEENEY, S. & TOTH, A. 2016. Meiotic DNA break formation requires the unsynapsed chromosome axis-binding protein IHO1 (CCDC36) in mice. *Nat Cell Biol,* 18**,** 1208-1220.

SUH, E. K., YANG, A., KETTENBACH, A., BAMBERGER, C., MICHAELIS, A. H., ZHU, Z., ELVIN, J. A., BRONSON, R. T., CRUM, C. P. & MCKEON, F. 2006. p63 protects the female germ line during meiotic arrest. *Nature,* 444**,** 624-8.

TAKETO, T. & NAUMOVA, A. K. 2013. Oocyte heterogeneity with respect to the meiotic silencing of unsynapsed X chromosomes in the XY female mouse. *Chromosoma,* 122**,** 337-49.

TARSOUNAS, M., MORITA, T., PEARLMAN, R. E. & MOENS, P. B. 1999. RAD51 and DMC1 form mixed complexes associated with mouse meiotic chromosome cores and synaptonemal complexes. *J Cell Biol,* 147**,** 207-20.

TERASAWA, M., SHINOHARA, A., HOTTA, Y., OGAWA, H. & OGAWA, T. 1995. Localization of RecA-like recombination proteins on chromosomes of the lily at various meiotic stages. *Genes Dev,* 9**,** 925-34.

THOMA, M. E., MCLAIN, A. C., LOUIS, J. F., KING, R. B., TRUMBLE, A. C., SUNDARAM, R. & BUCK LOUIS, G. M. 2013. Prevalence of infertility in the United States as estimated by the current duration approach and a traditional constructed approach. *Fertil Steril,* 99**,** 1324-1331 e1.

TOMIMATSU, N., MUKHERJEE, B. & BURMA, S. 2009. Distinct roles of ATR and DNA-PKcs in triggering DNA damage responses in ATM-deficient cells. *EMBO Rep,* 10**,** 629-35.

TRAVEN, A. & HEIERHORST, J. 2005. SQ/TQ cluster domains: concentrated ATM/ATR kinase phosphorylation site regions in DNA-damage-response proteins. *Bioessays,* 27**,** 397-407.

TURNER, J. M. 2015. Meiotic Silencing in Mammals. *Annu Rev Genet,* 49**,** 395-412.

TURNER, J. M., APRELIKOVA, O., XU, X., WANG, R., KIM, S., CHANDRAMOULI, G. V., BARRETT, J. C., BURGOYNE, P. S. & DENG, C. X. 2004. BRCA1, histone H2AX phosphorylation, and male meiotic sex chromosome inactivation. *Curr Biol,* 14**,** 2135-42.

TURNER, J. M., MAHADEVAIAH, S. K., ELLIS, P. J., MITCHELL, M. J. & BURGOYNE, P. S. 2006. Pachytene asynapsis drives meiotic sex chromosome inactivation

and leads to substantial postmeiotic repression in spermatids. *Dev Cell,* 10**,** 521-9.

TURNER, J. M., MAHADEVAIAH, S. K., FERNANDEZ-CAPETILLO, O., NUSSENZWEIG, A., XU, X., DENG, C. X. & BURGOYNE, P. S. 2005. Silencing of unsynapsed meiotic chromosomes in the mouse. *Nat Genet,* 37**,** 41-7.

VASILEVA, A., HOPKINS, K. M., WANG, X., WEISBACH, M. M., FRIEDMAN, R. A., WOLGEMUTH, D. J. & LIEBERMAN, H. B. 2013. The DNA damage checkpoint protein RAD9A is essential for male meiosis in the mouse. *J Cell Sci,* 126**,** 3927-38.

VERGOUWEN, R. P., JACOBS, S. G., HUISKAMP, R., DAVIDS, J. A. & DE ROOIJ, D. G. 1991. Proliferative activity of gonocytes, Sertoli cells and interstitial cells during testicular development in mice. *J Reprod Fertil,* 93**,** 233-43.

VILLA, M., CASSANI, C., GOBBINI, E., BONETTI, D. & LONGHESE, M. P. 2016. Coupling end resection with the checkpoint response at DNA double-strand breaks. *Cell Mol Life Sci,* 73**,** 3655-63.

VINY, A. D., OTT, C. J., SPITZER, B., RIVAS, M., MEYDAN, C., PAPALEXI, E., YELIN, D., SHANK, K., REYES, J., CHIU, A., ROMIN, Y., BOYKO, V., THOTA, S., MACIEJEWSKI, J. P., MELNICK, A., BRADNER, J. E. & LEVINE, R. L. 2015. Dose-dependent role of the cohesin complex in normal and malignant hematopoiesis. *The Journal of Experimental Medicine,* 212**,** 1819-1832.

VRIELYNCK, N., CHAMBON, A., VEZON, D., PEREIRA, L., CHELYSHEVA, L., DE MUYT, A., MEZARD, C., MAYER, C. & GRELON, M. 2016. A DNA topoisomerase VI-like complex initiates meiotic recombination. *Science,* 351**,** 939-43.

WARD, A., HOPKINS, J., MCKAY, M., MURRAY, S. & JORDAN, P. W. 2016. Genetic Interactions Between the Meiosis-Specific Cohesin Components, STAG3, REC8, and RAD21L. *G3 (Bethesda),* 6**,** 1713-24.

WEINERT, T. A., KISER, G. L. & HARTWELL, L. H. 1994. Mitotic checkpoint genes in budding yeast and the dependence of mitosis on DNA replication and repair. *Genes Dev,* 8**,** 652-65.

WINTERS, T., MCNICOLL, F. & JESSBERGER, R. 2014. Meiotic cohesin STAG3 is required for chromosome axis formation and sister chromatid cohesion. *EMBO J,* 33**,** 1256-70.

WOJTASZ, L., CLOUTIER, J. M., BAUMANN, M., DANIEL, K., VARGA, J., FU, J., ANASTASSIADIS, K., STEWART, A. F., REMENYI, A., TURNER, J. M. & TOTH, A. 2012. Meiotic DNA double-strand breaks and chromosome asynapsis in mice are monitored by distinct HORMAD2-independent and -dependent mechanisms. *Genes Dev,* 26**,** 958-73.

WOJTASZ, L., DANIEL, K., ROIG, I., BOLCUN-FILAS, E., XU, H., BOONSANAY, V., ECKMANN, C. R., COOKE, H. J., JASIN, M., KEENEY, S., MCKAY, M. J. & TOTH, A. 2009. Mouse HORMAD1 and HORMAD2, two conserved meiotic chromosomal proteins, are depleted from synapsed chromosome axes with the help of TRIP13 AAA-ATPase. *PLoS Genet,* 5**,** e1000702.

XU, H., BEASLEY, M. D., WARREN, W. D., VAN DER HORST, G. T. & MCKAY, M. J. 2005. Absence of mouse REC8 cohesin promotes synapsis of sister chromatids in meiosis. *Dev Cell,* 8**,** 949-61.

XU, Y., ASHLEY, T., BRAINERD, E. E., BRONSON, R. T., MEYN, M. S. & BALTIMORE, D. 1996. Targeted disruption of ATM leads to growth retardation, chromosomal fragmentation during meiosis, immune defects, and thymic lymphoma. *Genes Dev,* 10**,** 2411-22.

YANG, F., DE LA FUENTE, R., LEU, N. A., BAUMANN, C., MCLAUGHLIN, K. J. & WANG, P. J. 2006. Mouse SYCP2 is required for synaptonemal complex

assembly and chromosomal synapsis during male meiosis. *J Cell Biol,* 173**,** 497-507.

YUAN, L., LIU, J. G., HOJA, M. R., WILBERTZ, J., NORDQVIST, K. & HOOG, C. 2002. Female germ cell aneuploidy and embryo death in mice lacking the meiosis-specific protein SCP3. *Science,* 296**,** 1115-8.

YUAN, L., LIU, J. G., ZHAO, J., BRUNDELL, E., DANEHOLT, B. & HOOG, C. 2000. The murine SCP3 gene is required for synaptonemal complex assembly, chromosome synapsis, and male fertility. *Mol Cell,* 5**,** 73-83.

ZANDERS, S., SONNTAG BROWN, M., CHEN, C. & ALANI, E. 2011. Pch2 modulates chromatid partner choice during meiotic double-strand break repair in Saccharomyces cerevisiae. *Genetics,* 188**,** 511-21.

ZHANG, L., KIM, K. P., KLECKNER, N. E. & STORLAZZI, A. 2011. Meiotic double-strand breaks occur once per pair of (sister) chromatids and, via Mec1/ATR and Tel1/ATM, once per quartet of chromatids. *Proc Natl Acad Sci U S A,* 108**,** 20036-41.

ZHENG, K. & WANG, P. J. 2012. Blockade of pachytene piRNA biogenesis reveals a novel requirement for maintaining post-meiotic germline genome integrity. *PLoS Genet,* 8**,** e1003038.

ZICKLER, D. & KLECKNER, N. 1999. Meiotic chromosomes: integrating structure and function. *Annu Rev Genet,* 33**,** 603-754.

ZICKLER, D. & KLECKNER, N. 2015. Recombination, Pairing, and Synapsis of Homologs during Meiosis. *Cold Spring Harb Perspect Biol,* 7.